

AFNAL-TR-84-4031

A REVIEW OF CRACK CLOSURE

AD-A142 273

S. Banerjee

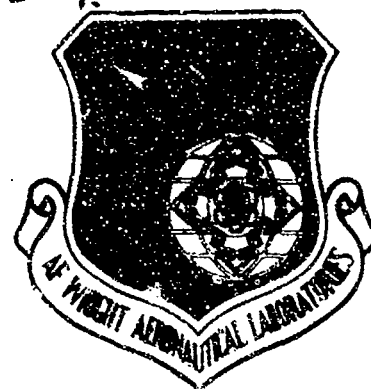
University of Dayton
Research Institute
300 College Park Drive
Dayton, Ohio 45469

April 1984

Interim Report for Period August 1983 Through December 1983

Approved for public release; distribution unlimited

MATERIALS LABORATORY
AIR FORCE WRIGHT AERONAUTICAL LABORATORIES
AIR FORCE SYSTEMS COMMAND
WRIGHT-PATTERSON AIR FORCE BASE, OHIO 45433



DTIC FILE COPY

DTIC
JUN 20 1984


84 06 18 061'


NOTICE

When Government drawings, specifications, or other data are used for any purpose other than in connection with a definitely related Government procurement operation, the United States Government thereby incurs no responsibility nor any obligation whatsoever; and the fact that the government may have formulated, furnished, or in any way supplied the said drawings, specifications, or other data, is not to be regarded by implication or otherwise as in any manner licensing the holder or any other person or corporation, or conveying any rights or permission to manufacture use, or sell any patented invention that may in any way be related thereto.

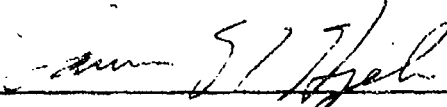
This report has been reviewed by the Office of Public Affairs (ASD/PA) and is releasable to the National Technical Information Service (NTIS). At NTIS, it will be available to the general public, including foreign nations.

This technical report has been reviewed and is approved for publication.


THEODORE NICHOLAS, Project Engineer
Metals Behavior Branch
Metals and Ceramics Division


JOHN P. HENDERSON, Chief
Metals Behavior Branch
Metals and Ceramics Division

FOR THE COMMANDER


LAWRENCE N. HJELM, Asst. Chief
Metals and Ceramics Division
Materials Laboratory

"If your address has changed, if you wish to be removed from our mailing list, or if the addressee is no longer employed by your organization please notify AFWAL/MLLN, W-PAFB, OH 45433 to help us maintain a current mailing list".

Copies of this report should not be returned unless return is required by security considerations, contractual obligations, or notice on a specific document.

Unclassified

SECURITY CLASSIFICATION OF THIS PAGE (When Data Entered)

REPORT DOCUMENTATION PAGE		READ INSTRUCTIONS BEFORE COMPLETING FORM
1. REPORT NUMBER AFWAL-TR-84-4031	2. GOVT ACCESSION NO. AD A142 273	3. RECIPIENT'S CATALOG NUMBER
4. TITLE (and Subtitle) A REVIEW OF CRACK CLOSURE		5. TYPE OF REPORT & PERIOD COVERED Interim Technical Report Aug. 1983 - Dec. 1983
		6. PERFORMING ORG. REPORT NUMBER
7. AUTHOR(s) Dr. S. Banerjee*		8. CONTRACT OR GRANT NUMBER(s) F33615-81-C-5015
9. PERFORMING ORGANIZATION NAME AND ADDRESS University of Dayton Research Institute 300 College Park Drive Dayton, Ohio 45469		10. PROGRAM ELEMENT, PROJECT, TASK AREA & WORK UNIT NUMBERS P.E. 61102F 2307P114
11. CONTROLLING OFFICE NAME AND ADDRESS Materials Laboratory (AFWAL/MLLN) Air Force Wright Aeronautical Laboratories, AFSC Wright-Patterson AFB, OH 45433		12. REPORT DATE April 1984
14. MONITORING AGENCY NAME & ADDRESS (if different from Controlling Office)		13. NUMBER OF PAGES 172
		15. SECURITY CLASS. (of this report) Unclassified
15a. DECLASSIFICATION/DOWNGRADING SCHEDULE		
16. DISTRIBUTION STATEMENT (of this Report) Approved for public release; distribution unlimited		
17. DISTRIBUTION STATEMENT (of the abstract entered in Block 20, if different from Report)		
18. SUPPLEMENTARY NOTES *Metallurgical Engineering Department Indian Institute of Technology-Powai Bombay 400076 INDIA		
19. KEY WORDS (Continue on reverse side if necessary and identify by block number) fatigue crack growth metals crack closure crack growth mechanisms fracture mechanics		
20. ABSTRACT (Continue on reverse side if necessary and identify by block number) A comprehensive review and critique of the literature on fatigue crack closure is presented. The elements of closure: its mechanisms, experimental procedures for its determination; the phenomenological study of its dependence on different variables, and methodologies for its prediction, are all discussed in detail. Suggestions for future work and interpretations of findings of other authors are presented.		

Unclassified

SECURITY CLASSIFICATION OF THIS PAGE (When Data Entered)

FOREWORD

This Technical Report was prepared by the Aerospace Mechanics Division of the University of Dayton Research Institute for the Metals and Ceramics Division, Materials Laboratory. Dr. Theodore Nicholas, AFWAL/MLLN is the project engineer.

The work was supported, in part, under Contracts F33615-81-C-5015 with the University of Dayton and Contract F33615-82-C-5001 with Universal Energy Systems. This review was completed during the period August 1983 through December 1983, when the author worked at the AFWAL Materials Laboratory as a Senior Visiting Scientist on leave from the Indian Institute of Technology, Bombay, India.

Some of the ideas contained in this report evolved out of the several sessions of discussion the author had with Dr. Theodore Nicholas of AFWAL Materials Laboratory and it is a pleasure to acknowledge his input, suggestions and interest in the preparation of this report. The author also acknowledges Dr. Noel Ashbaugh of the University of Dayton Research Institute for his suggestions and final editing of the manuscript.



Accession For	
NTIS	<input checked="" type="checkbox"/>
DTIC TAB	<input type="checkbox"/>
Unannounced	<input type="checkbox"/>
Justification	
Distribution/	
Availability Codes	
Dist	Avail and/or
A-1	Special

TABLE OF CONTENTS

<u>SECTION</u>		<u>PAGE</u>
1	INTRODUCTION	1
	<u>Closure and Its Origin</u>	1
	<u>Role of Closure in Crack Growth Rate Prediction</u>	7
	<u>Determination of Closure</u>	10
	<u>Closure in Plane Stress and Plane Strain Conditions</u>	12
2	MECHANISMS OF CLOSURE	14
2.1	PLASTICITY INDUCED CLOSURE	15
2.2	ASPERITY INDUCED CLOSURE	27
	2.2.1 <u>Single Asperity Model [8]</u>	30
	2.2.2 <u>Spring Clip Model [60]</u>	35
	2.2.3 <u>Fracture Surface Roughness Model [12]</u>	36
2.3	OXIDE INDUCED CLOSURE	41
2.4	COMMENTS ON THE MECHANISMS OF CLOSURE	47
3	EXPERIMENTAL DETERMINATION OF CLOSURE	53
3.1	THICKNESS AVERAGED BULK AND LOCAL CLOSURE BEHAVIOUR	58
	3.1.1 <u>CMOD Gage</u>	59
	3.1.2 <u>Strain Gage</u>	65
	3.1.3 <u>Ultrasonics</u>	68
	3.1.4 <u>Potential Difference</u>	70
	3.1.5 <u>Special Displacement Gages</u>	72
3.2	NEAR TIP SURFACE CLOSURE BEHAVIOUR	73
	3.2.1 <u>Interferometric Displacement Gage (IDG)</u>	74
	3.2.2 <u>Direct Observation Using SEM</u>	75
	3.2.3 <u>Optical Interferometry</u>	76
3.3	NEAR TIP INTERIOR CLOSURE BEHAVIOUR	77
	3.3.1 <u>Closure Measurement Before and After the Removal of Successive Surface Layers</u>	78
	3.3.2 <u>Push Rod Displacement Gage</u>	80
	3.3.3 <u>Vacuum Infiltration Technique</u>	80
	3.3.4 <u>Interferometric Technique in Transparent Specimen</u>	82
3.4	COMMENTS ON THE DETERMINATION OF CLOSURE	

TABLE OF CONTENTS (Concluded)

<u>SECTION</u>		<u>PAGE</u>
4	PHENOMENOLOGICAL STUDY OF CLOSURE	87
4.1	EFFECT OF K_{max} , K_{min} , and R UNDER CONSTANT AMPLITUDE LOADING	88
4.1.1	The Effect of R and K_{min}	92
4.1.2	The Effect of K_{max}	94
4.1.3	Normalization of da/dN Data Using K_{op}	101
4.2	OVERLOAD EFFECTS [27,32,36,55,65,80-94]	104
4.3	SHORT CRACK BEHAVIOUR	113
4.4	SURFACE CRACK BEHAVIOUR	116
4.5	EFFECT OF RESIDUAL STRESS	117
4.6	ENVIRONMENTAL FACTORS	122
4.7	MICROSTRUCTURAL AND FRACTOGRAPHIC FEATURES	125
4.8	MATERIAL PROPERTIES	129
4.9	EFFECT OF SIZE AND GEOMETRY	131
4.10	COMMENTS ON THE PHENOMENOLOGICAL STUDY OF CLOSURE	136
5	PREDICTION OF CLOSURE	139
5.1	ANALYTICAL PROCEDURES	140
5.2	FINITE ELEMENT BASED METHOD	143
5.3	COMMENTS ON PREDICTION OF CLOSURE	146
6	CONCLUDING REMARKS	148
	REFERENCES	152

LIST OF ILLUSTRATIONS

<u>FIGURE</u>		<u>PAGE</u>
1	Scheme of Fatigue Crack Closure. P is Load and K is Stress Intensity Factor.	3
2	Identification of K_{op} and K_{clo} From the Load Versus Displacement Plot (Figure 2a) and Load Versus Offset Displacement Plot (Figure 2b). P = Load, V = Displacement, and ΔV = Offset Displacement = V - C·P, Where C = Compliance = $\partial V / \partial P$.	4
3	Plastic Wake and Residual Compressive Stresses Developed on a Growing Fatigue Crack During a Constant Amplitude Cyclic Load Control Test.	16
4	Plastic Zone and Residual Compressive Stresses Developed on a Saw Cut Sharp Crack During a Constant Amplitude Cyclic Load Control Test.	18
5	Residual Stresses Developed in the Plane of Crack in CCP and CT Specimens Due to Plastic Wake Formed on Growing Fatigue Cracks, As Postulated in Plasticity Induced Closure.	20
6	Preferential Through-The-Thickness Yielding in the Surface Layers of a CT Specimen with a Straight Crack Front.	22
7	Residual Stress Developed Across the Thickness (See Section ZZ on Figure 6) Due to Preferential Yielding in the Surface Layers. The Effect of Residual Stress Reported in Figure 5 is not Taken into Account.	23
8	Preferential Through-The-Thickness Yielding in the Surface Layers of a CT Specimen With a Curved Crack Front (Compare with Figure 6).	25
9	Residual Stresses Developed in the Plane of Crack in CCP and CT Specimens Due to Asperity Induced Closure as Postulated. Compare with Figure 5.	29
10	Single Asperity Model [8].	31
11	Microroughness Induced Closure Model [12].	37
12	A Schematic Comparison of the Oxide Induced Closure Mechanism with the Other Mechanisms of Closure [12].	42

LIST OF ILLUSTRATIONS (Continued)

<u>FIGURE</u>		<u>PAGE</u>
13	Basis of Oxide Induced Closure - A Schematic Effect of Environment on ΔK_O and da/dN [22].	44
14	Basis of Oxide Induced Closure. Typical Variation of Excess Oxide Thickness, d , with Crack Length and Crack Propagation Rate [22].	45
15	Identification of Closure from Load Versus Displacement (P-V) and Load Versus Offset Displacement (P-AV) Plots. K_l Represents the Minimum Stress Intensity Factor at Which the Plots are Linear and P_{ct} is the Stress Intensity at Which the Two Tangents on the P-V Plot Intersect.	54
16	Schematic of the Typical P-AV Test Records. Friction and Misalignment may Change the Test Records from the Type Reported in Figure 16a to that in Figure 16b.	62
17	Preferred Locations of the Strain Gage in a CT Specimen for the Determination of Closure Using Strain-Gage Technique.	66
18	Determination of Closure Using Ultrasoncis Technique [41]. P_l and P_{ct} are Explained in Section 3.1.1.	69
19	Determination of Closure Using DC Potential Drop Technique. 1-1 and 2-2 - Potential Probe Position and 3-3 - Current Probe Position [3].	71
20	a - Variation of Closure Stress with Removal of Successive Surface Layers, b - The Effect of Specimen Thickness on Closure [2].	79
21	Push Rod Displacement Gage Technique for the Determination of Near Tip Interior Closure of an Elliptical Crack [65]. Note that the Technique can also be Used for a Through-The-Thickness Crack.	81
22	Effect of Load Ratio, R , on da/dN [2].	90
23	Variation of K_{Op}/K_{max} with a/W or K_{max} for (a) $R=0.5$ and (b) $R=0.1$ [32].	95
24	K_{Op} Has No Systematic Dependence on K_{max} . Each Data Point From Individual CT Specimens of $B = 4$ mm, $W = 50$ mm, and Varying a/W Values [31,34].	96

LIST OF ILLUSTRATIONS (Concluded)

<u>FIGURE</u>		<u>PAGE</u>
25	Decreasing K_{op}/K_{max} With Increasing K_{max} . The Unusual Behaviour of 2219 T87 is Attributed to Shear Lip Formation [18].	97
26	Plot of da/dN Versus ΔK_{eff} , Showing the Normalization of the Effect of R on da/dN as Reported in Figure 22 [2].	102
27	Variation of da/dN as a Result of Single Cycle Overload. The Crack Growth Rate at the Overload Cycle is not Represented in the Figure.	105
28	Experimental Crack Propagation Behaviour as Influenced by Overload Application - Comparison with Prediction by Various Models. The Inset Gives Details of Overload Application [84].	107
29	Crack Growth Rate Versus ΔK_{eff} Before and During Transient Effects After a Single Overload [32].	111
30	Comparison of Experimentally Observed da/dN Following Overload with the da/dN Inferred From Closure Measurement and Constant Amplitude da/dN Data for a Thumbnail-Shaped Crack with a =Crack Depth and c =Surface Crack Length [65].	112
31	Comparison of Experimental and Predicted Crack Growth Rates for Small Cracks Emanating From a Circular Hole in Steel Specimens [101].	115
32	Comparison of da/dN for Non-Stress Relieved and Stress Relieved Materials. The Agreement is Good when ΔK_{eff} is Used for Representing da/dN Data [110].	121
33	a - Effect of Environment on Crack Propagation in 7075-T651 Al Alloy, b - Normalization of the Data Reported in Figure 33a When da/dN is Plotted Against ΔK_{eff} [39].	124
34	Effect of σ_y on K_{op} in CT Specimens, $B=4$ mm, $W=50$ mm and Varying a/W . Scatter in K_{op} Values Reported is Attributed to Different Precracking History [31,34].	130
35	Fracture Surface Profile as Influenced by Specimen Size and Loading (a) Symmetric Profile, (b) Non-Symmetric Profile, and (c) Out of Plane Sliding in Thin Specimens with Non-Symmetric Profile Relaxes Compressive Force [89].	134
36	Displacement and Stress Along the Crack Line of a CCP Specimen at the Maximum and the Minimum Load.	135

1. INTRODUCTION

In a recent paper [1] titled 'Twenty Years of Reflections on Questions Concerning Fatigue Crack Growth; Historical Observations and Perspectives', Paris views 'crack closure as raising the most central question still to be resolved'. He further observes that 'crack closure is a key physical phenomenon in fatigue cracking process' particularly with reference to problem areas such as: variable amplitude load interaction effects, short cracks, threshold fatigue crack growth, and environmental effects. A review of crack closure in fatigue hardly needs a better justification.

The study of closure has been reviewed recently [2,3,4].; however, these reviews deal with only one or some of the aspects of closure.

The main purpose of this report is to review closure - its mechanisms, procedures for its determination, the phenomenological study of its dependence on the different variables, and the methodology of its prediction. As outlined below, the task is rather complex since it is difficult to provide answers to even the obvious questions concerning closure. What is attempted in this review is to define the positions and raise the critical questions concerning the above aspects of closure; hopefully, such an exercise would indicate meaningful direction of future work in closure studies.

Closure and Its Origin

The concept of crack closure was first proposed by Elber [5,6] in 1970. According to him, a fatigue crack in a body subjected to tension-tension

cyclic loading, is completely open only at high load levels; or in other words, at low load levels a part of the crack near the tip remains closed during the loading as well as the unloading phase of the cycle. The basic scheme of Elber's closure and the definition of the terms such as, K_{op} and K_{clo} are given in Figure 1.

The closure behaviour of a precracked body has three different aspects - K_{op} value, extent of closure, and residual strain due to closure. The three aspects are interrelated but they do not always change in an identical manner in response to a change in a given fatigue loading situation.

Among these three aspects, the K_{op} value is determined, studied, and calculated most often since it can be directly used for life prediction. K_{op} values can be identified from a simple plot of load versus crack mouth opening displacement (see Fig. 2a), provided the closure in the precracked body is extensive. The ratio of K_{op}/K_{max} can have a value anywhere between 0 and 1. A value of zero corresponds to no closure while a value of 1 indicates closure during entire fatigue cycle.

As regards the second aspect, closure is defined as extensive if a large fraction of the crack, $(\Delta a/a)$, remains closed at the start of loading, where a is the physical crack length and a_0 is the crack length measured from compliance at the start of loading and $\Delta a = a - a_0$. In a load versus displacement plot, the difference between the slope at the start of loading and the slope at a load higher than the closure load can be related to and, therefore, is obviously a measure of the extent of closure. The ratio of $\Delta a/a$ could have values between 0 and 1.

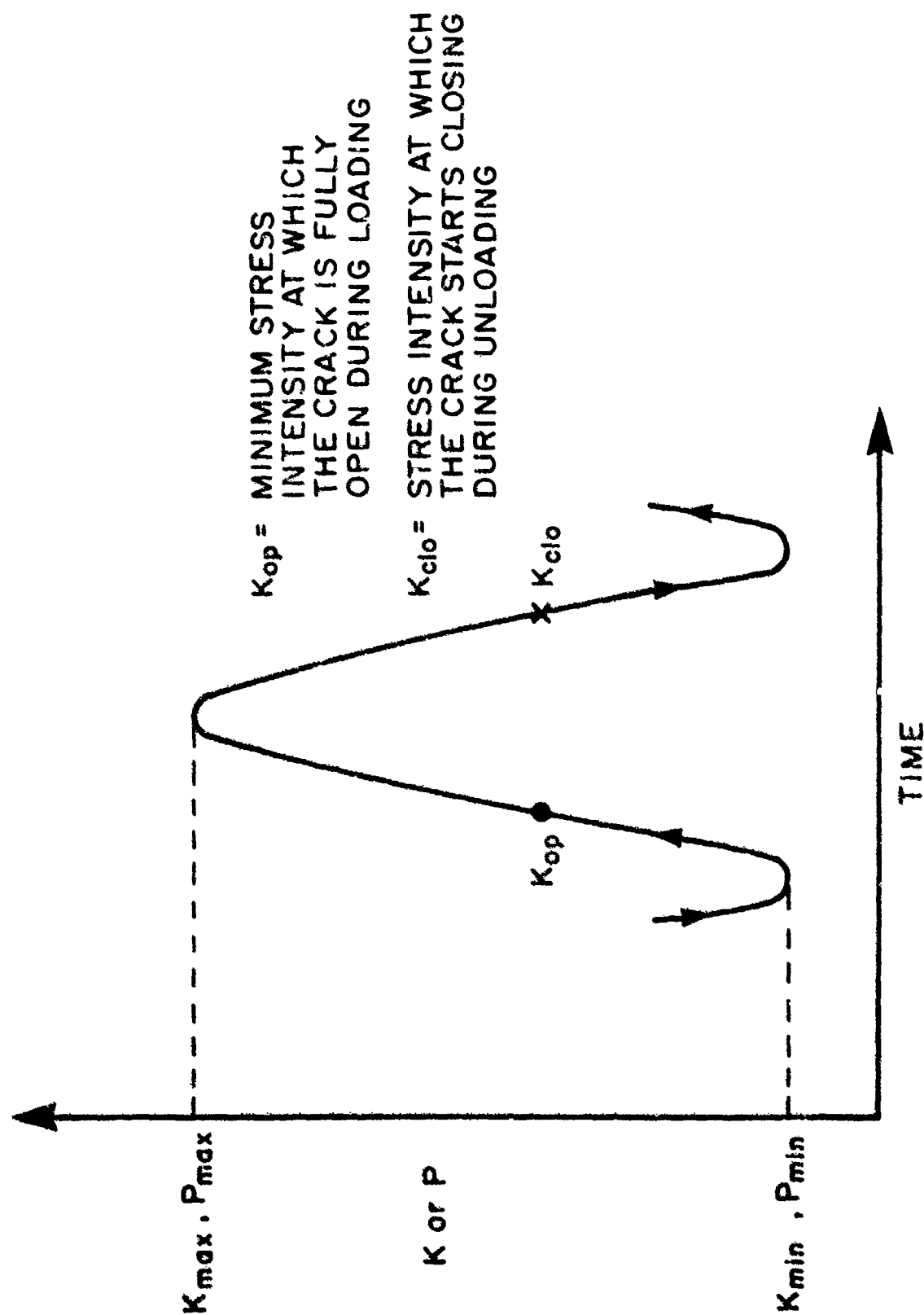


Figure 1. Scheme of Fatigue Crack Closure. P is Load and K is Stress Intensity Factor.

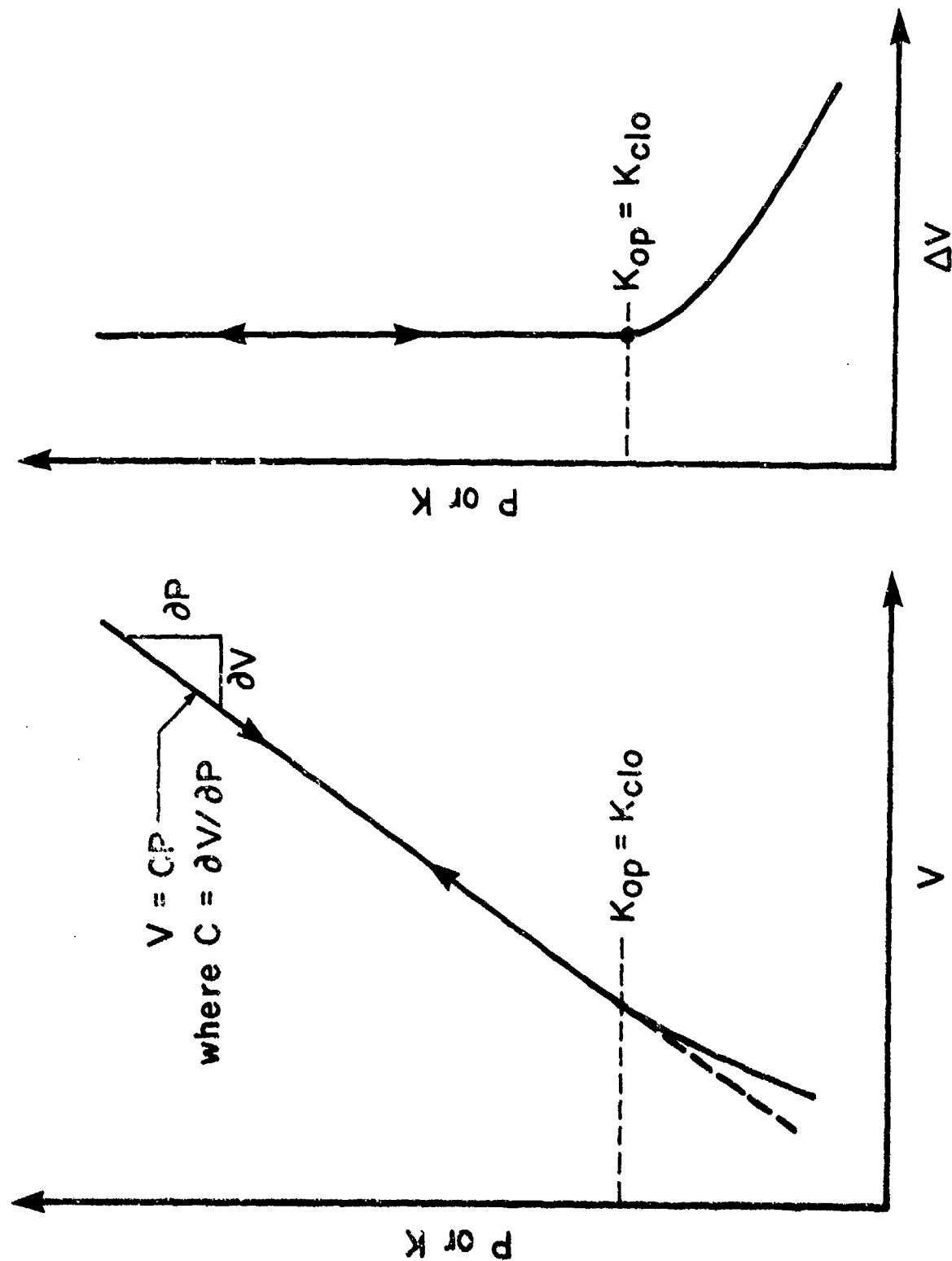


Figure 2. Identification of K_{op} and K_{clo} From the Load Versus Displacement Plot (Figure 2a) and Load Versus Offset Displacement Plot (Figure 2b). P = Load, V = Displacement, and ΔV = Offset

If the closure is not so extensive, that is $\Delta a/a$ has a small value, one can use a plot of load versus offset displacement to identify K_{op} as shown in Figure 2b; note that the plot in Figure 2b is derived from the data reported in Figure 2a. Alternatively, one can use a more sensitive instrumentation or data reduction technique to determine K_{op} .

The third aspect, that is the residual strain due to closure, is produced due to plastic flow at the crack tip during cyclic loading. This, in turn, leaves a strip of yielded material behind the crack tip, referred to as plastic wake. Elber proposed that the residual strain is produced by extension of the material within the plastic wake behind the crack tip. At zero load, the extended material in the plastic wake has to be accommodated by the rest of the precracked body which is elastic. As a result, residual compressive stresses are set up over the crack faces, and therefore, a part of the crack near its tip remains closed at low load levels. The usual argument is since there is no singularity at the tip of a closed crack, it cannot grow until it is fully open and this happens when $K > K_{op}$. However, the closure has some more basic consequences. The introduction of residual compressive stresses and also displacement in the wake of the crack alters the state of stress, strain, and displacement near the tip of the growing fatigue crack. This, in turn, will decrease the size of the monotonic, as well as the reverse plastic zones to values which are significantly less than conventionally assumed.

Elber's proposed concept is referred to as plasticity induced closure. Investigations of the closure behaviours such as, extent of closure and the residual strain due to closure are rather limited. But such investigations are essential for understanding the mechanism of closure and for the prediction of closure.

Elber [5] had originally proposed that K_{clo} should be greater than K_{op} . However, the difference between K_{clo} and K_{op} is less than the scatter observed in most experimental determinations of closure and for all practical purpose, one normally assumes $K_{clo} = K_{op}$ (see Figure 1). In all subsequent discussions, the symbol K_{op} would be used to represent the closure behaviour in general, unless a distinction between K_{clo} and K_{op} is warranted.

Elber had initially observed [5] that at very low load levels, the precracked body has a compliance which is identical to that of an uncracked body. On the other hand, this is not always true and many experimental compliance measurements show that a part of the crack can start opening as soon as the load is applied.

In addition to Elber's mechanism of plasticity induced closure, two other mechanisms of closure have recently been proposed: asperity induced closure [7-12] and oxide induced closure [13,14]. As discussed below, both of these mechanisms are based on a concept which can be more appropriately termed 'non-closure'. Furthermore, contrary to Elber's mechanism, K_{clo} should be less than K_{op} according to these mechanisms.

According to the asperity induced closure mechanism, the asperities on the two mating fracture surfaces interfere and keep the crack propped open even when the load is zero. On the other hand, according to the oxide induced closure mechanism, the formation of an oxide layer just behind the crack front wedges open the crack faces and keeps the crack open, even when the load is zero. It is obvious from these physical pictures that the concept of non-closure can produce only residual tensile stresses at the crack tip when the

external load is removed. It is interesting to note that even though the residual stress patterns near the crack tip, arising from closure and non-closure are opposite of each other, identical experimental techniques (see Figure 2) are used to identify the closure event, in both cases.

It is also rather surprising that even though the two different concepts postulate opposite patterns of crack tip residual stress at closure, the K_{op} derived from these two concepts is presumed to play an identical role in decreasing the fatigue crack growth rate. It shows how little we understand the manner in which closure decreases fatigue crack growth (FCGR) and the manner in which ΔK produces fatigue crack extension. The mechanisms of closure are discussed in greater detail in the next chapter.

Role of Closure in Crack Growth Rate Prediction

The concept of K_{clo} has been proposed mainly to achieve a more reliable fatigue crack growth rate (FCGR). In order to predict life of a component, several empirical laws have been proposed to characterize FCGR but all these are either derived from or are a variation of one form or another, of the law proposed first by Paris and Erdogan [16]. Paris-Erdogan law is represented by the equation

$$\frac{da}{dN} = A \Delta K^n \quad (1)$$

where A and n depend on the material and if these are known, one can separate variables and integrate to determine N , the component life. Since

the above relationship is independent of crack size and specimen geometry, the constants A and n when determined from a particular test specimen, can be used to calculate the fatigue life of any precracked body. Equation (1) applies only to constant amplitude loading. The equation fails to characterize fatigue crack growth rate if:

1. The ratio of minimum to the maximum load, R, in the test specimen and the component differs.
2. The crack length in the component is very short [15].
3. The loading amplitude varies and has hi-lo load sequence leading to load interaction and crack growth retardation or acceleration.

The concept of closure has been used to account for the effect of these factors on fatigue life. Accordingly, one defines an effective ΔK which is given by

$$\Delta K_{\text{eff}} = K_{\text{max}} - K_{\text{op}} \quad (2)$$

Elber proposed that crack growth rates are determined by ΔK_{eff} and, accordingly, Equation (1) should be appropriately modified by substituting ΔK_{eff} for ΔK . It could then be used for the calculation of life of a component.

In fact, Equation (1), when modified in a manner as described above, has been shown to account for the effect of the above three factors on the FCGR in some instances [1,2,5]. Furthermore, K_{op} as influenced by residual stresses, microstructure, and environment, has also been used to account for the effect of these variables on FCGR and life. Thus, a scatter band of 2, usually observed in a log-log representation of FCGR, could probably decrease if K_{op} is taken into account in representing FCGR.

Since closure depends on the formation of plastic zone and inelastic deformation in the vicinity of the crack tip, the closure could also be influenced by specimen size and geometry. As a result, the K_{op} observed in a test specimen could differ from that in another cracked body even though K , R , and the uniaxial yield strength, σ_y , are identical. Since reliable FCGR prediction of a component depends on K_{op} , the K_{op} in a precracked body must be known. Experimental determination of K_{op} for all cracked body geometries would require extensive testing which is not generally feasible. However, a systematic evaluation of the effect of size and geometry on closure would be invaluable in developing a procedure for calculation of K_{op} of any cracked body. Unfortunately, such evaluation has not yet been performed. In formulating such a procedure, it would also be essential to ascertain the mechanism of closure, the nature of residual stress distribution that a given mechanism produces at the crack tip and elsewhere in the specimen, and the manner in which such stress distribution decreases crack growth rate, da/dN . One could then propose and validate models of closure for the calculation of K_{op} in an arbitrary precracked body.

A phenomenological study of the different factors which influence both K_{op} and da/dN can provide the appropriate basis to ascertain the above. The several factors include K_{max} , K_{min} , R , short crack behaviour, step overload, surface crack behaviour, thickness, W , a/W , specimen geometry, microstructural and fractographic features, environment, residual stresses, elastic and flow properties of the material, and loading history. However, the reported results of phenomenological studies on the effect of even the more important ones amongst these variables, are quite confusing. For example, an examination of Elber's plasticity induced closure mechanism indicates that K_{op} should systematically depend on K_{max} if all other factors are identical. On the other hand, as would be discussed later (Section 4.1), some of the investigators report that experimental K_{op} increases with K_{max} , while others report that K_{op} is independent of K_{max} ; and yet still others report that K_{op} decreases with K_{max} ! One must interpret with caution the results of such phenomenological studies undertaken in the past, since K_{op} can depend very significantly on a host of different factors including the experimental technique used for its determination.

Determination of Closure

As discussed earlier, Figure 2a shows that the closure load can be determined experimentally from a load versus CMOD test record. For better resolution, one can identify closure from a plot of load versus offset displacement (see Figure 2b). The offset displacement can be obtained through the use of a simple operational amplifier circuit or by processing the load-CMOD test record numerically in a microprocessor. Besides the

CMOD-based approach, there are other experimental procedures for closure determination which are based on techniques using strain gage, ultrasonics, electrical potential, laser/optical interferometry, and optical methods including replication. The agreement amongst the different methods is not always good and the reason will be evident from the following discussion.

Closure can be identified from measurements made either near the crack tip or at points relatively far away from the crack tip. The measurements made either at points far away from the crack tip or those which involve the whole specimen cross section give a thickness-averaged global K_{op} of the precracked body. On the other hand, the K_{op} determined through the measurement of displacement near the crack tip are influenced significantly by the complex three-dimensional residual stress pattern localized near the crack front due to either preferential through-the-thickness yielding in the surface layers and/or due to crack tunneling. As a result, the K_{op} at the interior (say mid thickness) of a specimen near the crack tip can be quite different from the K_{op} observed at the near tip surface. In most instances, closure determined near the crack tip is based on surface measurement. Obviously, K_{op} values obtained from all three different measurements can be different.

Techniques such as CMOD gage, back face strain gage (BFS), electrical potential, and ultrasonics give a thickness-averaged global K_{op} value. The Elber gage and near tip strain gage in some instances, and the interferometric technique, and the optical and SEM technique including surface replication can give near tip K_{op} values at the specimen surface. Only a few investigators

(see Section 3.3) have determined near tip interior closure behaviour; techniques such as the optical interferometry in transparent specimens, the push-red clip gage technique, and the measurement of closure before and after the removal of surface layers have been used for this purpose.

Indeed, only a few investigators make a distinction between these different K_{op} values and the question as to which one of these closures should be used to arrive at ΔK_{eff} as per Equation (2), has not been properly addressed. The consequences of the lack of such distinctions are contradictory phenomenological observations and multiplicity of the proposed mechanisms of closure.

Closure in Plane Stress and Plane Strain Conditions

Plane stress and plane strain are convenient assumptions for analytical formulation of fracture problems. However, these terms have limited practical relevance in defining the state of stress in a precracked specimen which is loaded. The plane stress condition exists only at the surface of the specimen; the rest of the interior cross section is neither plane stress nor plane strain. The actual state of stress at the interior is intermediate or three-dimensional. This is especially true since a plastic zone forms at the crack tip and grows as K/σ_y increases. The growth of the plastic zone relaxes the stresses and therefore, the state of stress becomes closer to plane stress as K/σ_y increases. Besides this, the terms such as plane strain or plane stress are often used by investigators of closure phenomenon with the tacit assumption that increasing specimen thickness strongly decreases plastic zone sizes while the specimen width has only a

mild effect on plastic zone size. Both of these assumptions are incorrect [17]. Therefore, the interpretation, correlation, and comparison of results based on such assumptions are questionable. While examining the reported experimental results in this review, whenever possible, the use of concepts such as plane stress and plane strain will be avoided. Indeed, the different experimental closure situations can be better classified and compared in terms of extent of closure and extent of plasticity.

In the next section, the proposed mechanisms of closure are examined. In Section 3, the different approaches to closure determination are reviewed very briefly to better evaluate the significance of closure related phenomenological observations as discussed in Section 4. Section 5 briefly outlines the proposed methodology for the prediction of closure. To reiterate the important points, comments are made at the end of these respective sections. Also, the concluding remarks summarizes the major points made in the review.

2. MECHANISMS OF CLOSURE

Three mechanisms have been proposed for the closure of a fatigue crack: plasticity induced closure [5,6], asperity induced closure [7-12,60], and oxide induced closure [13,14,21]. The plasticity induced mechanism can be truly termed closure since according to such a mechanism, a fatigue crack near the tip remains closed even when the external load is tensile. The other two mechanisms can be more appropriately termed 'non-closure' since, according to the basic scheme of these mechanisms, a fatigue crack fails to close near the tip when the external load is zero, or even mildly compressive.

A study of the mechanism of closure is important due to two reasons: First, the prediction of closure in a cracked component of arbitrary size, geometry, and loading is based on a given closure model. The closure model, in its turn, is based on a proposed mechanism of closure. Thus, one must first know the mechanism in order to develop a procedure for the prediction of closure. Second, the study of closure mechanisms helps us to identify and explain the role closure plays in determining da/dN and thus helps us to develop materials with better fatigue resistance. It helps us to ascertain the validity of a given closure mechanism or a model. It also helps us to answer more basic questions. For example, it is presumed that fatigue crack cannot grow as long as it remains closed. However, could not the strain intensification ahead of a closed crack cyclically loaded to a K_{max} level which even if less than K_{op} , be enough to promote plastic flow at the crack tip and therefore cause growth?

A closure mechanism has to be validated through experimental observations. Any proposed mechanism of closure should be consistent with all the phenomenological observation concerning the effect of the different variables on closure. Such observations are presented and discussed later in Section 4. However, reference will be made in the present section to a few of these selected observations to comment on the validity of the different mechanisms.

Presented in this section is an examination of the different mechanisms of closure and their validity and limitations.

2.1 PLASTICITY INDUCED CLOSURE

Elber [6] proposed that during fatigue crack propagation, a zone of residual tensile deformation is left in the wake of a moving crack tip (see Figure 3). The residual tensile deformation is produced due to the envelope of plastic zone (see Figure 3) which is referred to as the 'plastic wake'. Note that the plastic wake increasingly spreads in the y direction as the crack grows since K_{\max} increases with crack growth for most test geometries under constant amplitude loading. At zero external load, the material within the plastic wake continues to remain extended and can no longer be accommodated within the surrounding elastic field without producing a corresponding strain mismatch. Thus, in the unloaded condition, this strain mismatch will produce residual compressive stresses over the plastic wake (see Figure 3) which, in turn, transmits the compressive stresses normal to the crack surface and thus keeping the two crack surfaces pressed and closed together.

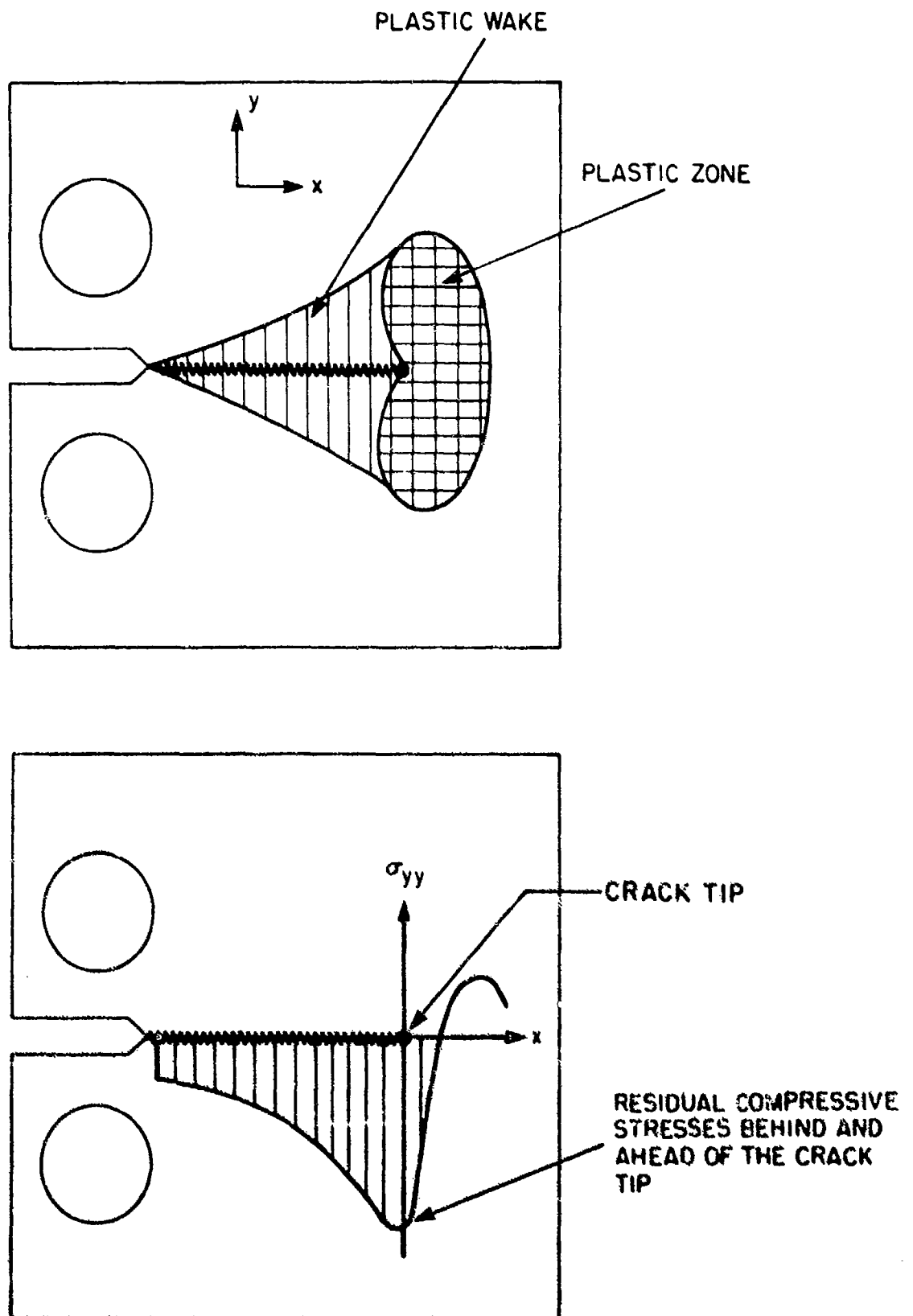


Figure 3. Plastic Wake and Residual Compressive Stresses Developed on a Growing Fatigue Crack During a Constant Amplitude Cyclic Load Control Test.

The plastic wake behind the crack front is produced due to the formation of the monotonic plastic zone ahead of the crack front during the tensile phase of the cyclic loading. This zone extends incrementally as the fatigue crack grows. However, on unloading, the monotonic plastic zone experiences compressive stresses for the reason mentioned above and this causes yielding in compression over a distance where the compressive stress exceeds the yield strength. This is referred to as reverse plasticity and the plastic zone formed as a result is referred to as cyclic or reverse plastic zone. The effects of plastic wake and the reverse plasticity can be distinguished by their respective residual compressive stress patterns in the two examples as discussed below.

When a sharp saw-cut crack (not grown by fatigue) is subjected to one cycle of loading, monotonic and cyclic plastic zones form and the residual compressive stress pattern produced is shown in Figure 4. Note that unlike in Figure 3, the residual compressive stresses behind the crack front is absent in Figure 4. As a result of Bauschinger effect, the stress increment to cause yielding during unloading or reversed plasticity, is twice the yield strength observed during monotonic loading. Since plastic zone size is inversely proportional to the square of yield strength, the reverse or cyclic plastic zone size is approximately one fourth the monotonic plastic zone. The presence of the reverse plastic zone modifies somewhat the pattern of residual compressive stress in the monotonic plastic zone.

On the other hand, in the case of a growing sharp fatigue crack, in addition to the monotonic and reverse plastic zone, a plastic wake (of the type shown in Figure 3) forms along the cracked part of the specimen. Therefore, the residual stresses in the plane of the crack in CCP and CT

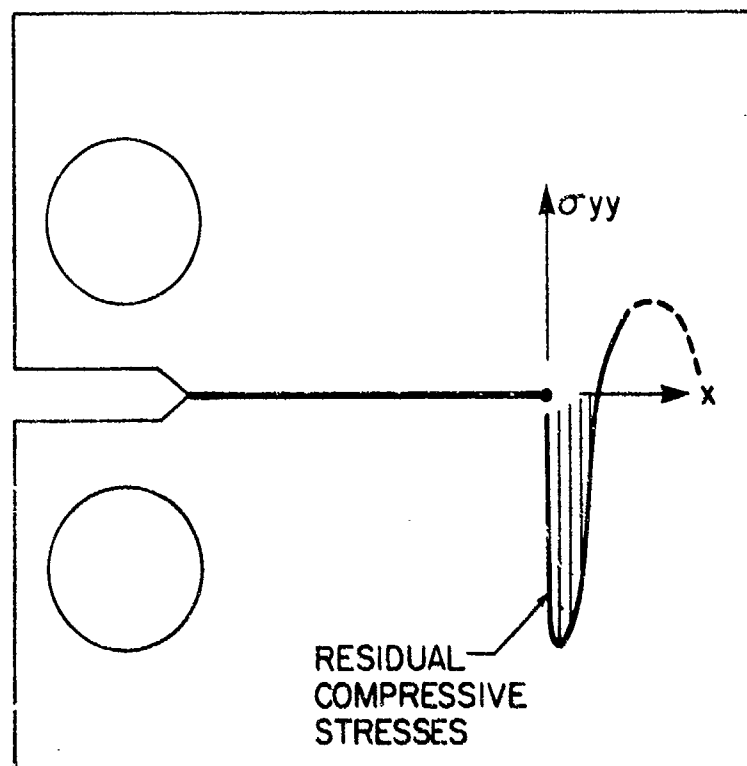
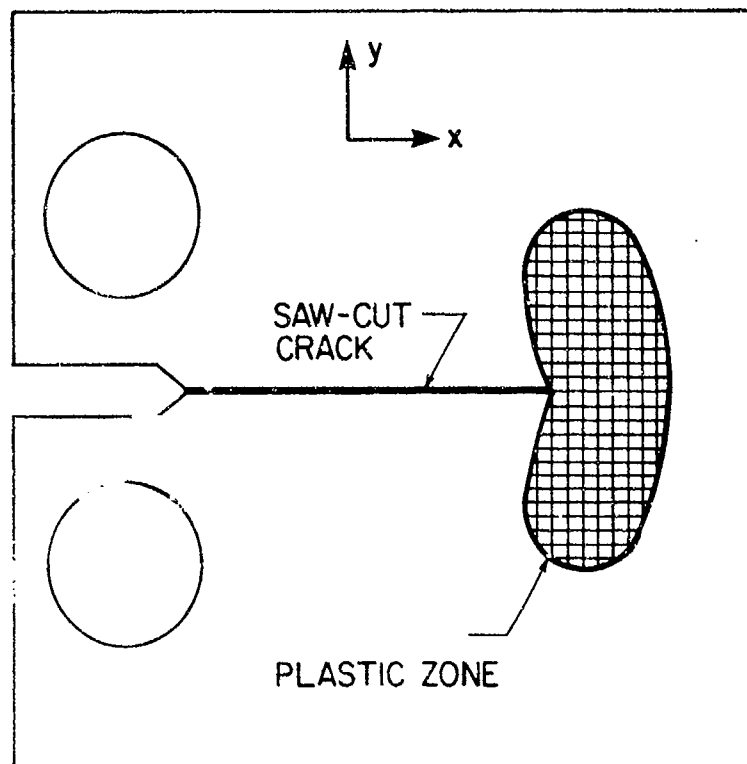


Figure 4. Plastic Zone and Residual Compressive Stresses Developed on a Saw Cut Sharp Crack During a Constant Amplitude Cyclic Load Control Test.

specimens are expected to exhibit patterns as shown in Figure 5. The plasticity induced residual stress pattern in the ligament of a compact tension specimen is not known and is expected to be rather complex. However, unlike in the case of a centre cracked panel, the residual stresses at the back face of a compact tension specimen should be compressive. This is discussed further in Section 4.5. One can surmise that the magnitude and distribution of residual compressive stress, depends on the distribution of ϵ_{yy} along the y direction at different points along the length of the wake and the distribution of displacement in the y direction at various points along the length of the crack. Obviously, if the closure were to be produced by the compressive stress over the whole length of the wake and the monotonic plastic zone, one should then take into account the residual stress distribution both ahead and behind the crack tip, as reported in Figure 5.

The two above sources of stress distribution can be examined separately. The residual compressive stress pattern produced by the plastic wake would probably influence the bulk closure behaviour and cause an extent of closure which is large and easily detectable. On the other hand, the effect of compressive residual stress within the plastic zone would be localized near the crack tip, cause an extent of closure which is small, and therefore can be detected only if the method of determination is highly sensitive. During constant amplitude loading, the residual stress distribution over the length of the wake as well as the plastic zone is expected to be smooth and continuous and, therefore, produce only one single closure load which represents the bulk as well as the local behaviour. However, one can speculate that a large single overload cycle may produce a

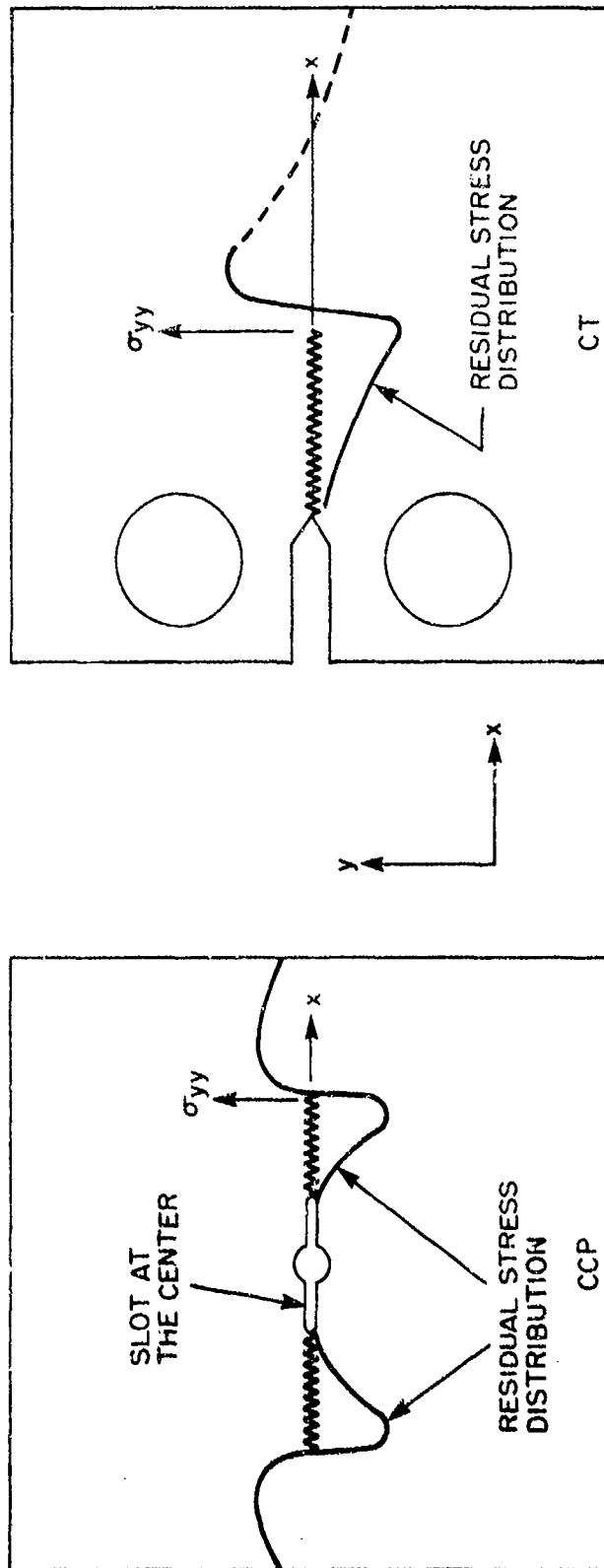


Figure 5. Residual Stresses Developed in the Plane of Crack in CCP and CT Specimens Due to Plastic Wake Formed on Growing Fatigue Cracks, As Postulated in Plasticity Induced Closure.

discontinuity in the residual stress pattern near the crack tip, and as a result, produce two closures - one representing the bulk and the other representing the local behaviour. This will be discussed in Section 4.2.

The residual stress pattern along the width direction as shown in Figure 5 is the primary factor which controls crack closure, and, therefore, plasticity induced crack closure models are based on such stress distribution. However, the residual stress distribution along the thickness direction can also influence closure.

The residual stress distribution along the thickness direction can be produced due to two factors: preferential yielding in the surface layers and presence of a curved crack front.

It is well known that in a relatively thick specimen, the yielding in the surface layers (see areas marked A in Figure 6) is more pronounced as compared to that at the interior. As a result, the dimension of the plastic wake in the y-direction in the surface layers is larger than that at the interior. If we assume that the residual stress pattern of the type given in Figure 5 were absent, one can then surmise that higher stretching of the yielded material along the y direction within the surface layer can introduce residual tensile stresses in the interior and correspondingly, reactive compressive stresses are introduced in the surface layer. The nature of such stress distribution is shown in Figure 7. In an actual specimen, the two stress patterns reported in Figures 5 and 7 are superimposed on each other. Thus, it is likely that the last fraction of opening during unloading or the

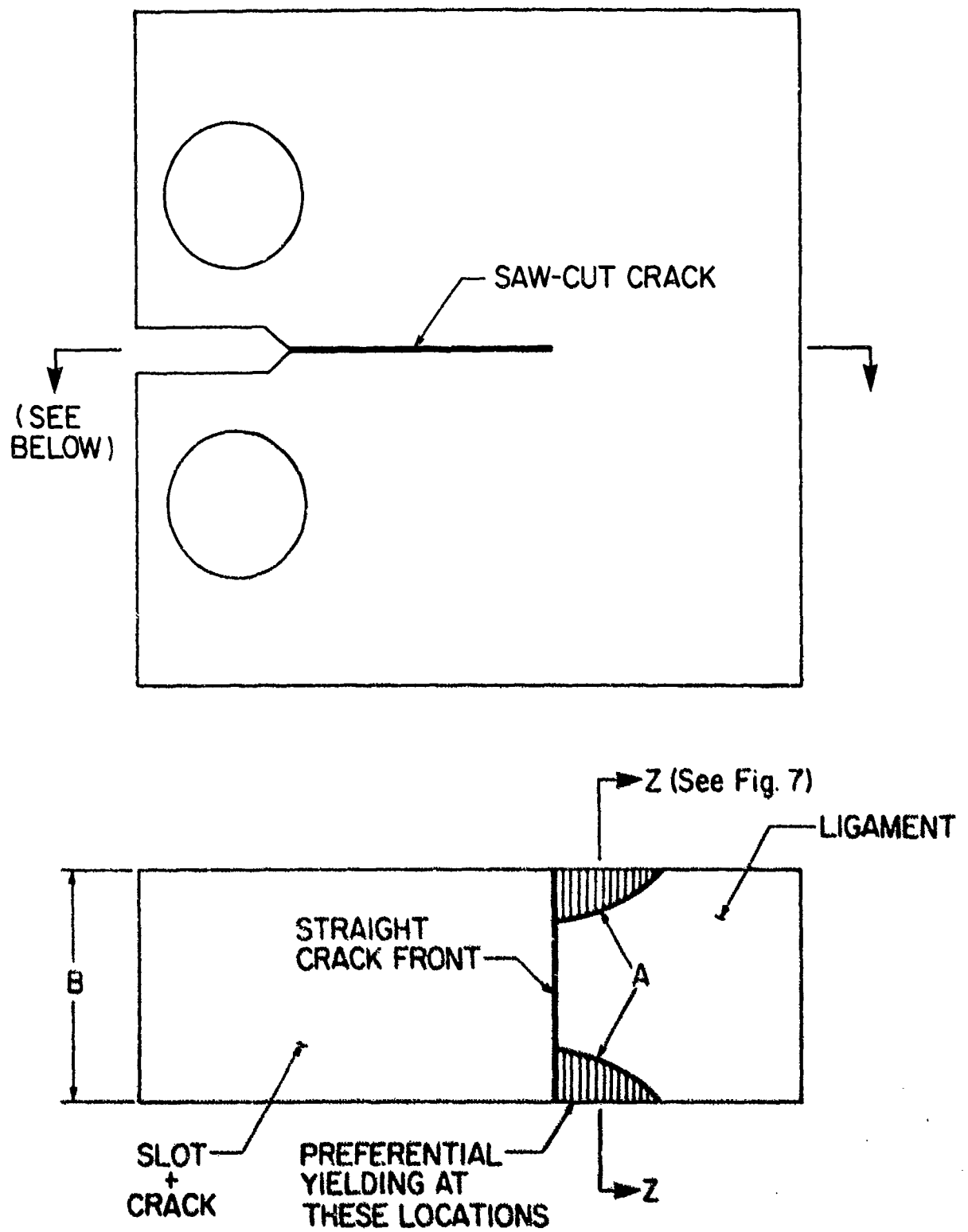


Figure 6. Preferential Through-The-Thickness Yielding in the Surface Layers of a CT Specimen with a Straight Crack Front.

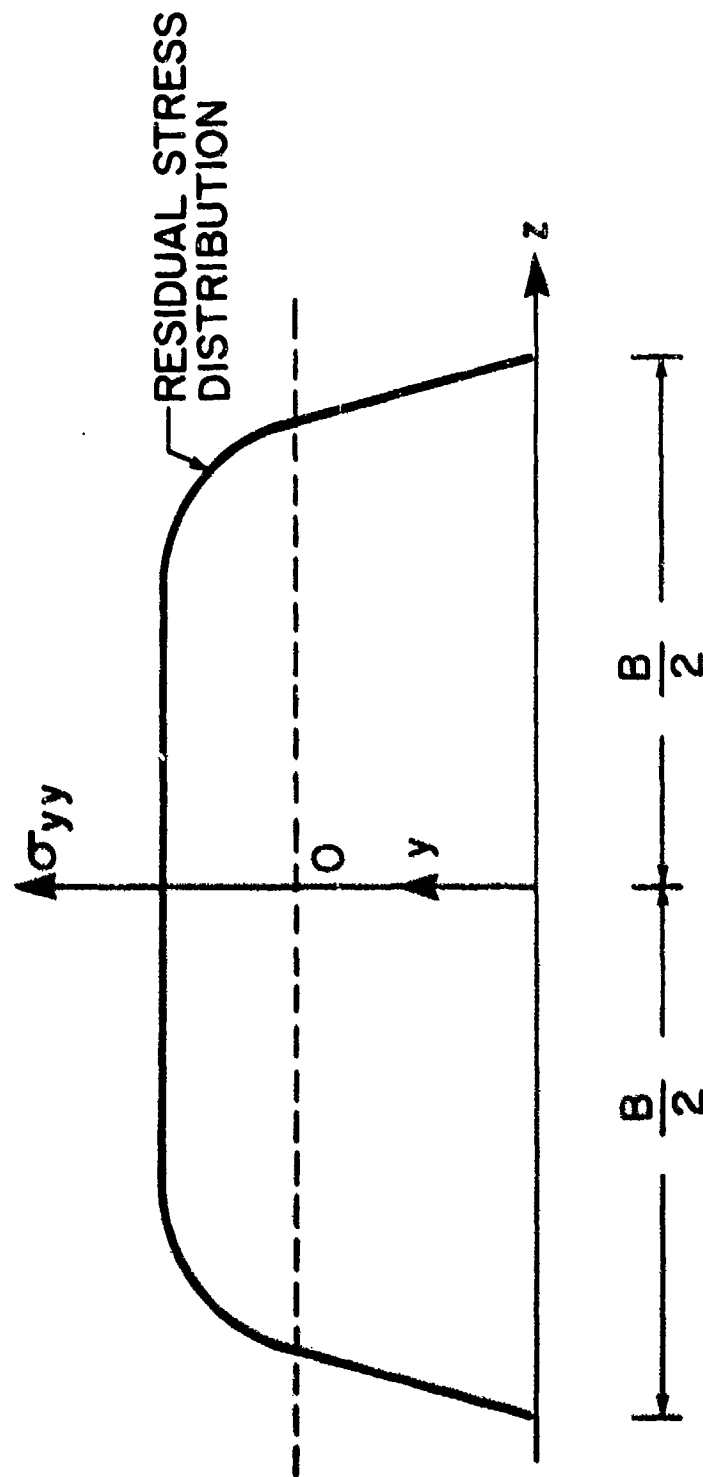


Figure 7. Residual Stress Developed Across the Thickness (See Section ZZ on Figure 6) Due to Preferential Yielding in the Surface Layers. The Effect of Residual Stress Reported in Figure 5 is not Taken into Account.

first fraction of closure during unloading could be influenced by the presence of the pattern of residual stress distribution along the thickness direction as reported in Figure 7. As a result, in the case of a thick specimen, the last fraction of opening in the surface layers would be difficult compared to that observed at the interior. In a relatively thinner specimen, the strains ϵ_{yy} and ϵ_{xx} are probably uniform across the thickness direction and the variation of residual stresses along the thickness direction may be negligible.

The presence of a curved crack front can cause preferential extension and plastic flow in the surface layers ahead of the crack front (see areas marked A in Figure 8). This may introduce a pattern of residual stress distribution along the thickness direction similar to that reported in Figure 7 and produce similar effects as discussed above. However, such an effect would be produced both in the thick and the thin specimen, as long as the depth of curved crack front is comparable to the thickness and is not negligible compared to the crack length. Obviously, a large crack length is preferable if the effect of curved crack front is to be ignored. The specimen then has to be correspondingly wide to accommodate a large crack length.

It is obvious from the above discussion that the analytical results obtained from closure models based on plasticity induced mechanism, are expected to agree with experimental closure data provided the specimen is thin and the depth of curved crack front is small. On the other hand, experimental results obtained from a thick specimen with a pronounced curved crack front, are not expected to agree with the analytical results based on

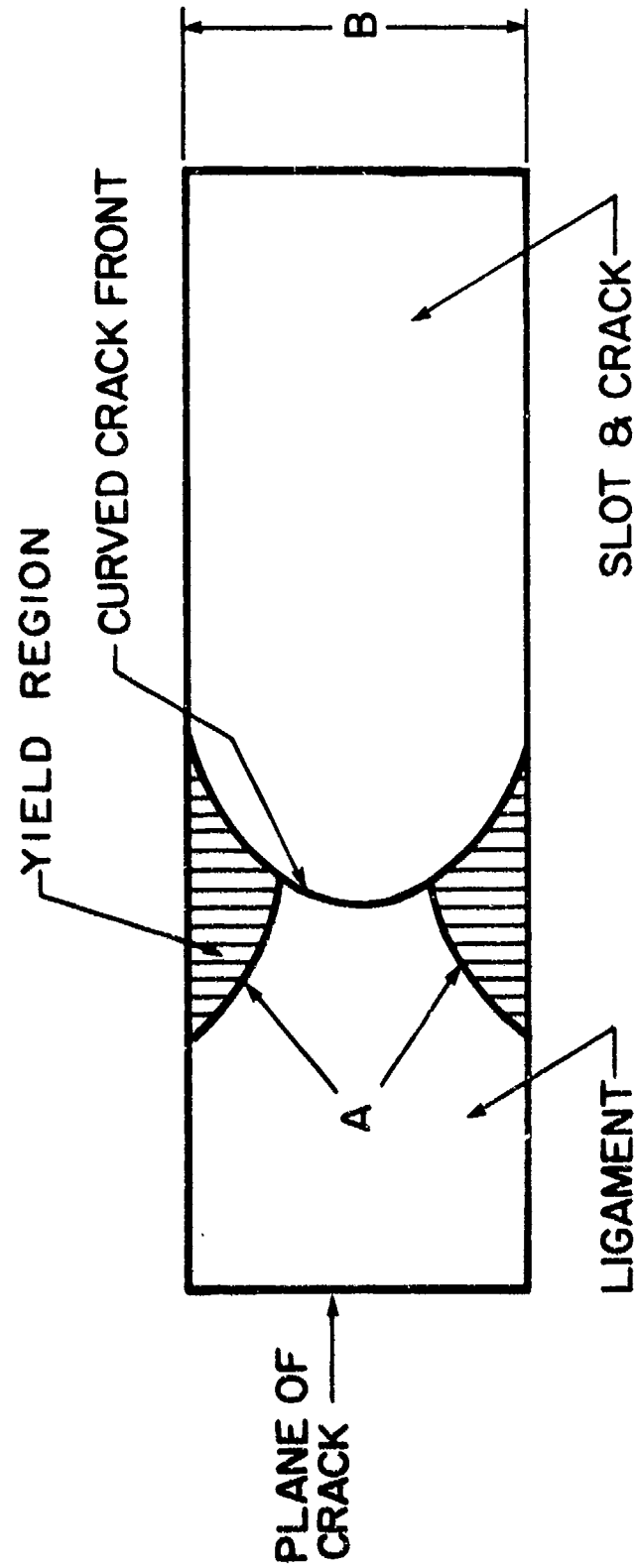


Figure 8. Preferential Through-The-Thickness Yielding in the Surface Layers of a CT Specimen With a Curved Crack Front (Compare with Figure 6).

plasticity induced closure. In fact, in the thick specimen with a curved crack front, the closure at the interior is expected to differ from that observed at the surface if plasticity induced mechanism were operative.

It is often stated [7-12] that Elber's plasticity induced closure mechanism is operative only in plane stress. A true state of plane stress does not exist anywhere in the specimen except at its surface. In that sense, the experimental condition at which the plasticity induced mechanism is applicable is not clearly defined. By plane stress, one implies that the K -value and the plastic zone sizes are large while the σ_Y and thickness of the specimen are low. On the other hand, it has been shown [17] that the state of stress in a thin specimen at low K/σ_Y value need not be plane stress. In fact, in a thin specimen, the state of stress can be quite close to plane strain if $K/\sigma_Y\sqrt{W}$ is small and the width is large [17]. In a thin specimen ($B \ll W$ or a), the whole thickness can be assumed to be approximately in the same state of stress. It has been suggested that probably ϵ_{yy} and ϵ_{xx} are the same across the thickness of a thin specimen [2]. Thus, the advantages of using a thin and wide specimen for closure studies is obvious.

It is often assumed without reliable experimental foundation, that K_{op} produced by the plasticity induced closure mechanism is independent of W , a/W , B (as long as the condition is the so called 'plane stress'), environment, microstructure, and geometry. In addition, such a mechanism would suggest that K_{op} should depend on K_{max} , K_{min} , R , σ_Y , presence of residual stresses, variable amplitude loading which produces load-interaction and retardation, and the short and surface crack behaviour.

Several investigators have reported experimental results which are broadly in agreement with the trends as indicated by the mechanism of plasticity induced closure. However, in view of the uncertainties in the determination of closure, one must carefully scrutinize any result on closure. There are anomalies and other contradictions which cannot be ignored. For instance, often, K_{op} is observed to be independent of K_{max} , K_{min} , and even R . The effect of W , a/W , geometry, and short crack behaviour have not been systematically investigated and the studies on the effect of B on K_{op} are very few. Interestingly enough, there are other investigators who report that K_{op} depends on environment and microstructure (see Sections 4.6 and 4.7). Such discrepancies are often explained in terms of plane stress and plane strain. However, the plane stress and plane strain conditions in terms of experimental situations, are not clearly defined or distinguished by these investigators. It is thus obvious that even though the mechanism of plasticity induced closure is conceptually logical, several anomalies and contradictions concerning the mechanism needs to be resolved.

2.2 ASPERITY INDUCED CLOSURE

The concept of asperity induced (or roughness-induced) closure was first reported by Walker and Beevers [7] and later by McEvily and Minakawa [10] and Ritchie and Suresh [11]. Subsequently, three models based on the asperity induced closure have been proposed by Suresh and Ritchie [12,19], Mays and Baker [60], and Beevers, Carlson, Bell, and Starke [8,9].

It is proposed by these workers that the asperity induced closure mechanism is encountered in situations where the maximum plastic zone size is less than the order of the grain size [9], the reverse plastic zone becomes of the order of dominant microstructural elements [11] or where the size scale of fracture surface roughness is comparable with crack tip opening displacement [10]. In such situations, crack extension occurs along a single slip system resulting in serrated or zig-zag fracture paths with out of plane crack trajectories [9-11]. Extension of the crack along such paths results in significant mode II displacement which plays a role in promoting such closure. Normally, this type of crack extension is observed near threshold ($da/dN < 10^{-6}$ mm per cycle) when the conditions are predominantly 'plane strain'.

The asperities on the mating fracture surfaces interfere and thus provide discrete contact points across the crack surfaces where load transfer occurs and thereby preventing the crack from completely closing. According to the asperity induced closure models, the wedging action of such interference or contact is small and is localized over very short distance behind the crack front. As a result, such wedging action is locally accommodated permitting the rest of the crack to close except a very short distance behind the crack front where the crack fails to close. Under such circumstances, the failure to close or 'non-closure' as one may term it, produces residual tensile stresses at the crack tip. In a centre crack tension panel, the residual stress pattern produced by this mechanism will be tensile throughout the ligament and in the case of a compact tension specimen, the residual stresses would be tensile near the crack tip and compressive at the back face as shown in Figure 9. Such residual stress distributions are obviously different from those reported in Figure 5.

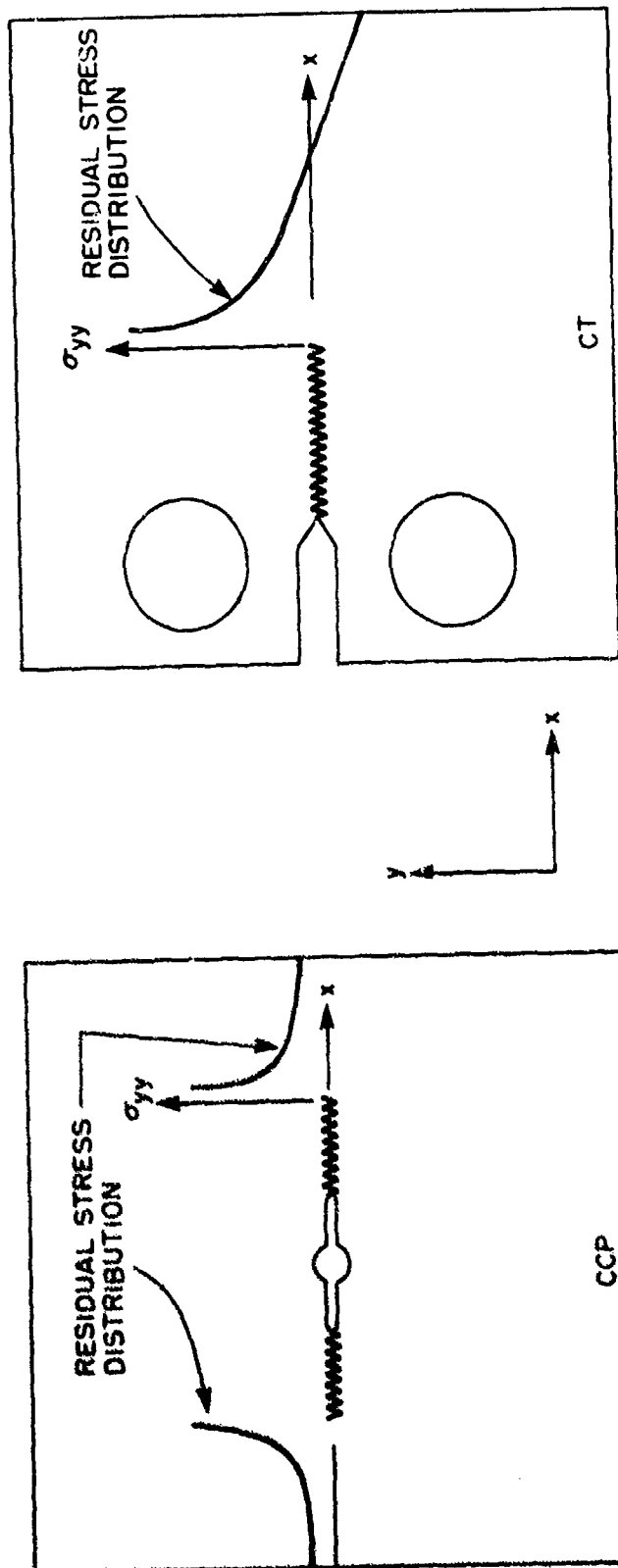


Figure 9. Residual Stresses Developed in the Plane of Crack in CCP and CT Specimens Due to Asperity Induced Closure as Postulated. Compare with Figure 5.

The three models [8,12,60] proposed for asperity induced closure are examined below.

2.2.1 Single Asperity Model [8]

Beever et al. [8] represents the asperities through-the-thickness by an effective precompressed spring which makes line contact across the thickness. This model is termed a single asperity model and is illustrated in Figure 10, wherein the crack faces are loaded with a force P at an asperity of height L , and width B , located at a distance c . The asperity undergoes a change in its height by ' e ' due to the force P . The local stress intensity factor due to force P is given by

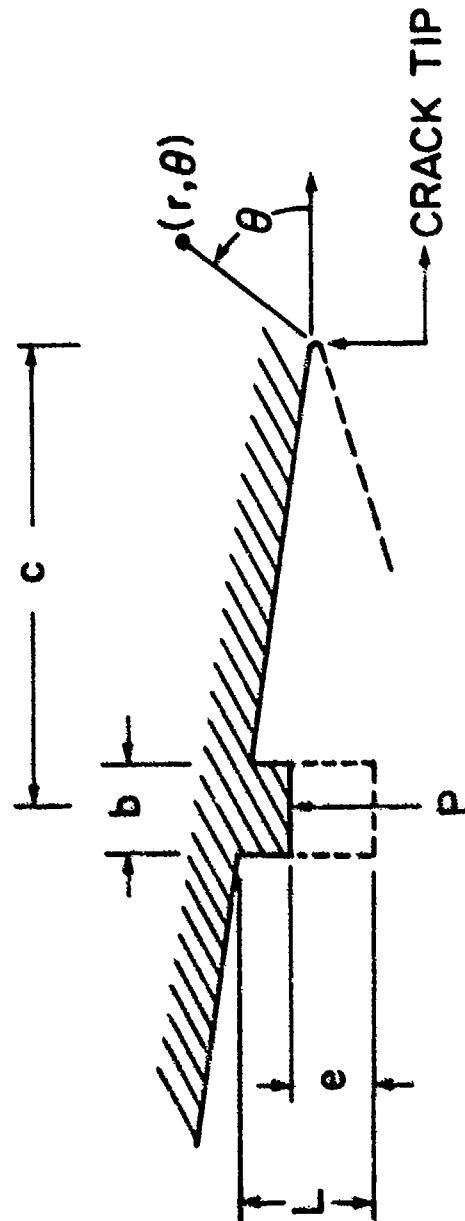
$$K_{\text{local}} = \left(\frac{2}{\pi c}\right)^{1/2} \frac{P}{B} \quad (3)$$

The corresponding displacement, V , at a point $r = c$ behind the crack tip at $\theta=180^\circ$ is obtained from the Westergaard solution

$$V = \frac{2(1-\nu)K_{\text{local}}}{G} \sqrt{\frac{c}{2\pi}} \quad (4)$$

Substitution of Equation (3) and (4) gives:

$$V = \frac{2P(1-\nu)}{\pi GB} \quad (5)$$



- L = Magnitude of Interference by the Asperity.
- P = Force Developed by an Asperity.
- c = Distance of the Asperity from the Crack Tip.
- b = Effective Width of the Asperity.
- e = Change in Asperity Height Due to the Compression by Force P.

Figure 10. Single Asperity Model [8].

Closure occurs when the crack surfaces make contact behind the asperities and at this point, the stress intensity factor due to externally applied load, K_{global} , is zero. At this point, $K_{\text{total}} = K_{\text{local}} = K_{\text{clo}}$ and $v = L - e$ where $e = PL/Eb.B$. Substitution of these and Equation (3) in Equation (5) and elimination of P gives

$$K_{\text{clo}} = \sqrt{\frac{2}{\pi c}} \left[\frac{1}{Eb} + \frac{2(1-\nu)}{\pi GL} \right]^{-1} \quad (6)$$

where E , G , ν are the usual elastic constants.

K_{op} can be obtained from similar equations and represents the situation when asperity load $P=0$ and the compression $e=0$. In such a case, $K_{\text{op}} = K_{\text{global}} = LG\sqrt{2\pi}/2(1-\nu)\sqrt{c}$. Obviously, according to this model, K_{op} should be higher than K_{clo} . The model envisages that the formation of plastic zone of effective length ' r_y ' increases the dimension of c to $c + r_y$ and one would then expect K_{clo} and K_{op} to decrease as σ_Y decreases.

The dimensions L , b , and c have been measured using replicating technique and these when substituted in Equation (6) give a K_{op} value which agrees with the experimentally determined K_{op} value in the near threshold regime for a wrought nickel alloy. The typical values are $c = 15$ to $30 \mu\text{m}$, $L = .1$ to $.125 \mu\text{m}$, and $b = 9-11 \mu\text{m}$.

The asperity induced closure models are important and interesting because they indicate a method for explaining and predicting the effect the dimensions of the microstructural features may have on closure. The idea

that K_{op} may be determined from the fractographic features is itself very attractive. However, one should not overlook the following points while applying such a model in practice:

1. The compressive stress, σ_c , in the asperity is given by

$$\sigma_c = \frac{Ee}{L} = \frac{P}{Bb} \quad (7)$$

Substitution of (3) in (7) gives

$$\sigma_c = \frac{K_I \sqrt{\pi c}}{\sqrt{2}b} \quad (8)$$

Substitution of the typical values $K_I = 4.5 \text{ MNm}^{-3/2}$, $c = 30 \text{ }\mu\text{m}$, and $b = 10 \text{ }\mu\text{m}$ in Equation (8) yields a value of $\sigma_c = 10,000 \text{ MPa}$. This is almost 30 times the yield strength of the nickel alloy investigated. Since the asperity is in compression, the amount of stress relaxation by plastic flow of the asperity is limited. The question then is would such an asperity survive the battering experienced during the fatigue loading? For example, the growth of the crack over the next $3 \text{ }\mu\text{m}$ (10% of c) would take about 100,000 cycles at $K_{\max} = 6 \text{ MNm}^{-3/2}$, but would alter the compressive stresses only by a small amount. Would the nickel alloy asperity survive the 100,000 cycles at a compressive stress of 10,000 MPa? This question is difficult to resolve since there appears to be little scope for the manipulation of the values of b and c so that one can obtain a more realistic value of σ_c from Equation (8) at which the asperity can survive 100,000 cycles.

2. According to the model, the closure behaviour is observed due to crack surface contact over dimensions of the order of 15 to 30 μm . This would correspond to an extent of closure, $\Delta a/a \sim .001$. It is difficult to detect K_{op} from the load-CMOD plot as done by the authors [9], if the extent of closure were as small as .001.

3. The model is supposed to apply to a plain-strain situation whereas all measurements of L , b , and c are made at the specimen surface. In addition, because of the characteristic variation of the fractographic features being what it is, it would be rather difficult to measure L , b , and c with confidence. This is particularly true for L which has a dimension of the order of 0.1 μm .

4. The model shows that K_{op} should increase as σ_Y increases. On the other hand, the trends of experimental results on the effect of σ_Y on K_{op} are just the opposite. To explain such trends, it appears that one has to use rather unrealistic values of L , b , and c .

5. The relationship for crack opening stretch width (COSW) is given by

$$CTOD \approx 2 \text{ COSW} \approx J/\sigma_Y = \frac{K^2(1-\nu)}{2E\sigma_Y} \quad (9)$$

Substitution of $K = 4.5 \text{ MNm}^{-3/2}$ and $\sigma_Y = 350 \text{ MPa}$ and $E = 200 \text{ GPa}$ gives $COD = .50 \mu\text{m}$. In fact, experimentally observed COD values are either in agreement or somewhat larger than those predicted by Equation (9). However,

it seems that the model does not take into account a crack opening of $0.5 \mu\text{m}$ and assumes that it plays little role in influencing the force P on the asperity whose height is as low as $0.1 \mu\text{m}$.

2.2.2 Spring Clip Model [60]

Mayes and Baker [60] have attempted to calculate closure induced by roughness by considering an infinite number of compression springs along the crack flank. The springs are in contact, and, therefore, transfer load only when the displacement is less than a minimum. Equating moment and force due to the springs, they obtain a relationship for load which is given by

$$P = \frac{m\epsilon}{c} - \frac{0.83 E B a l_o^2}{m^2 \epsilon^2}$$

where P is the applied load, ϵ is back face strain experimentally determined, B is thickness, E is Young's Modulus, a is crack length, C is compliance, m is a constant relating ϵ and load displacement, and l_o is the effective spring length.

The relationship exhibits a P versus ϵ relationship, similar to the one experimentally determined. Also, the residual strain, $\epsilon = \epsilon_r$, obtained by substituting $P=0$ in the above equation, obeys a relationship with crack length which is similar to the experimentally observed. These observations are the justification for the validity of the model. The model explains the observed effect of R and σ_y on ΔK -threshold.

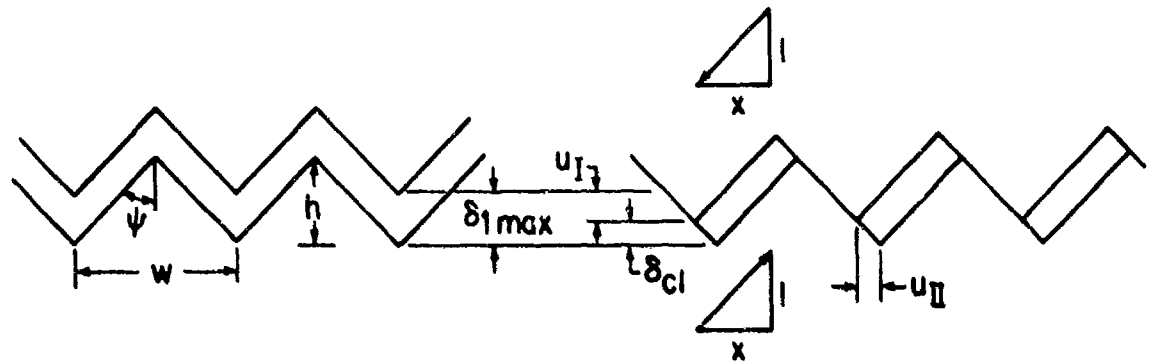
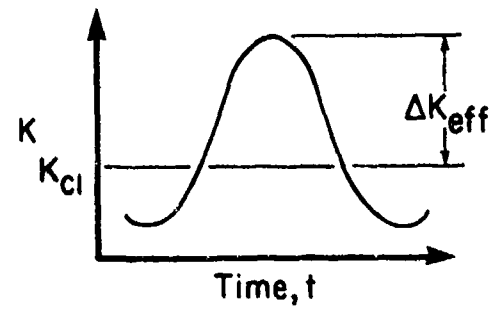
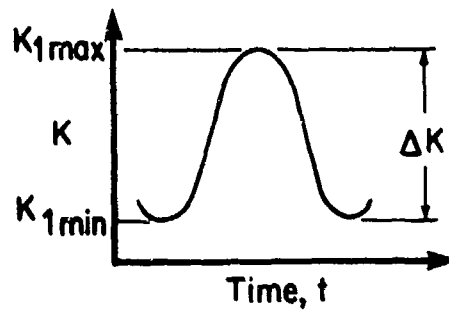
In the model, the effective spring length, l_0 , characterizes the surface roughness. Calculations show that l_0 changes with the material and its value ranges in the neighborhood of .01 to 0.1 μm . However, the roughness has not been measured and related to the equation as done by Beever and coworkers [8].

Spring clip and single asperity models are similar in most respects. Accordingly, some of the points made with regard to the single asperity model in Section 2.2.1 viz the items 3 and 5 are particularly relevant to the spring clip model.

2.2.3 Fracture Surface Roughness Model [12]

The concept of fatigue crack closure induced by fracture surface roughness was first outlined by Minakawa and McEvily [10,18]. Following similar scheme, Suresh and Ritchie [12,19] proposed a model which is reproduced in Figure 11. In this model, fracture surface roughness is idealized in terms of asperities assumed to be of triangular cross section of height, h , base, W , and all asperities are assumed to be equal in size. The failure to close produces a corresponding residual displacement. The final relationship is:

$$\frac{K_{clo}}{K_{max}} = \sqrt{\frac{2\gamma_x}{1+2\gamma_x}} \quad (10)$$



$$K = K_{1\max}$$

$$\delta_{cl} = \delta_{1\max} - u_I$$

$$x = u_{II} / u_I$$

$$\cot \psi = h / (w/2) = \delta_{cl} / u_{II}$$

$$\delta_{cl} = \frac{2hx\delta_{1\max}}{w + 2hx}$$

$$\frac{K_{cl}}{K_{1\max}} = \sqrt{\frac{\delta_{cl}}{\delta_{1\max}}} = \sqrt{\frac{2\gamma x}{1 + 2\gamma x}}$$

or in nondimensional form, with $\gamma = h/w$,

$$\left[\frac{K_{cl}}{K_{1\max}} \right]_{MR} = \sqrt{\frac{2\gamma x}{1 + 2\gamma x}}$$

$$[\Delta K_{eff}]_{MR} = K_{1\max} - K_{cl} = K_{1\max} \left[1 - \sqrt{\frac{2\gamma x}{1 + 2\gamma x}} \right]$$

Figure 11. Microroughness Induced Closure Model [12].

where γ is the roughness factor and x is the ratio of Mode I to Mode II displacements. The value of γ estimated from surface coating and profilometric studies when substituted into Equation (10) together with the experimentally determined K_{clo} and K_{max} values, give a value of x or mode II displacement, u_{II} , which is consistent with the experimental examination of crack tip motion using stereomaging procedure. This is how the model is validated.

It should be noted that roughness induced closure can occur only if $R < \sqrt{h/\delta_{max}}$ and this happens when the δ_{min} exceeds the scale of roughness, h . The symbols δ_{max} and δ_{min} refer to the crack tip displacement at the maximum and the minimum loads, respectively.

Such a concept of closure may be useful in explaining why ΔK_{th} is higher and da/dN just above the threshold regime is lower in coarser grained or lower strength material [11,12]. For such materials would give rougher surface and therefore higher γ . It can similarly explain why introduction of a soft phase in a duplex microstructure increases ΔK_{th} . The soft phase causes the crack path change direction frequently producing higher roughness induced closure. It may also explain the lower ΔK_{th} and higher da/dN in short crack (with crack length $<$ grain size) as compared to those observed in the case of long cracks. For a short crack, closure is expected to be much less [11,12] since the roughness is yet to develop.

The roughness and the single asperity models are derived from similar considerations. Some of the difficulties of the single and the spring clip models were pointed out earlier. In the case of the roughness model, more comprehensive and direct experimental measurements are required to clearly establish the validity of the model. But it seems that most of the points made earlier with regard to the single asperity model are also valid when one examines the roughness model. Some discussion would be appropriate as regards the first point made.

In the case of the roughness model, it is reasonable to assume that the mode II displacement, u_{II} , is microscopic and not global and therefore, it can be accommodated by regions local to the crack tip; for if the displacement is global, it would give very large and an absurd value of the extent of closure, such as $\Delta a/a \approx 1$. Thus, u_{II} may not be observable at distance much behind the crack tip. In that case, the distance behind the crack tip over which contact between asperities transfer compressive stresses due to the presence of Mode II displacement, becomes an important factor. Obviously, this distance must be long enough to distribute the compressive force generated by non-closure so that the stress level in the asperity are sufficiently low that they survive battering. On the other hand, this distance should be consistent with the extent of closure observed in an experiment. This is an important aspect and needs to be ascertained while verifying the proposed roughness model.

An examination of the fractured surface of a fatigue crack shows a battered appearance; the sharp edges one sees in the asperities of a monotonically loaded fracture surface are not usually observable in a fatigue fracture surface. On the other hand, one should note that large facets are present on the fracture surfaces obtained in the fatigue threshold regime. However, their presence neither guarantees that large mode II displacement have been experienced by the cracked body nor is it proof that the asperity induced mechanism of closure is operative. The mode II displacement and its distribution behind the crack length should be measured using suitable experimental technique to ascertain its role in asperity induced closure.

In a recent investigation [4], fatigue crack growth of Ti-Al alloys have been studied at room and elevated temperatures in air, vacuum, and argon in which crack closure was also determined. It was concluded that the crack closure mechanism is related to the macroscopic surface topography. The surface topographies of the different fractured specimens were examined and one can estimate that the asperity heights are in the range of hundreds of microns. Such asperity heights are three to four orders of magnitude higher than the roughness contemplated in the three asperity induced models outlined above.

Indeed, the roughness induced closure needs improved foundations of experimental and analytical work.

2.3 OXIDE INDUCED CLOSURE

Paris et al. [20] was the first to speculate that in a reactive environment, a freshly created fatigue fracture surface oxidizes and builds up corrosion product. According to them, this causes crack tip interference which effectively impedes crack growth in a manner similar to that described by Elber's crack closure mechanism. A similar argument was used by Stewart [21] to explain his experimental results on environmental effects. Following a similar approach, Ritchie, Suresh, and Moss [13] postulated the concept of oxide induced closure.

The oxide induced closure arises when the corrosion products having a thickness (typically several microns thick) comparable to the size of the crack tip opening displacement, build up near the crack tip and as a result, wedge-open the crack at $K_I > K_{min}$. Accordingly, during the closing portion of the cycle, contact between fracture surfaces will occur earlier, thereby raising closure loads and correspondingly reducing ΔK_{eff} [13,14]. Like asperity induced closure, oxide induced closure is observed at low growth rates ($da/dN < 10^{-6}$ mm/cycle) associated with near threshold condition at low load ratios under the so called plane strain condition [7-12]. Such a mechanism of closure [13,14,21] can explain some surprising observations relating to the effect of environment on da/dN and ΔK_{th} .

Figure 12 illustrates how the oxide deposits formed on freshly exposed surfaces at the crack tip in a moist environment can effectively wedge-close the crack at stress intensities above K_{min} and how such a

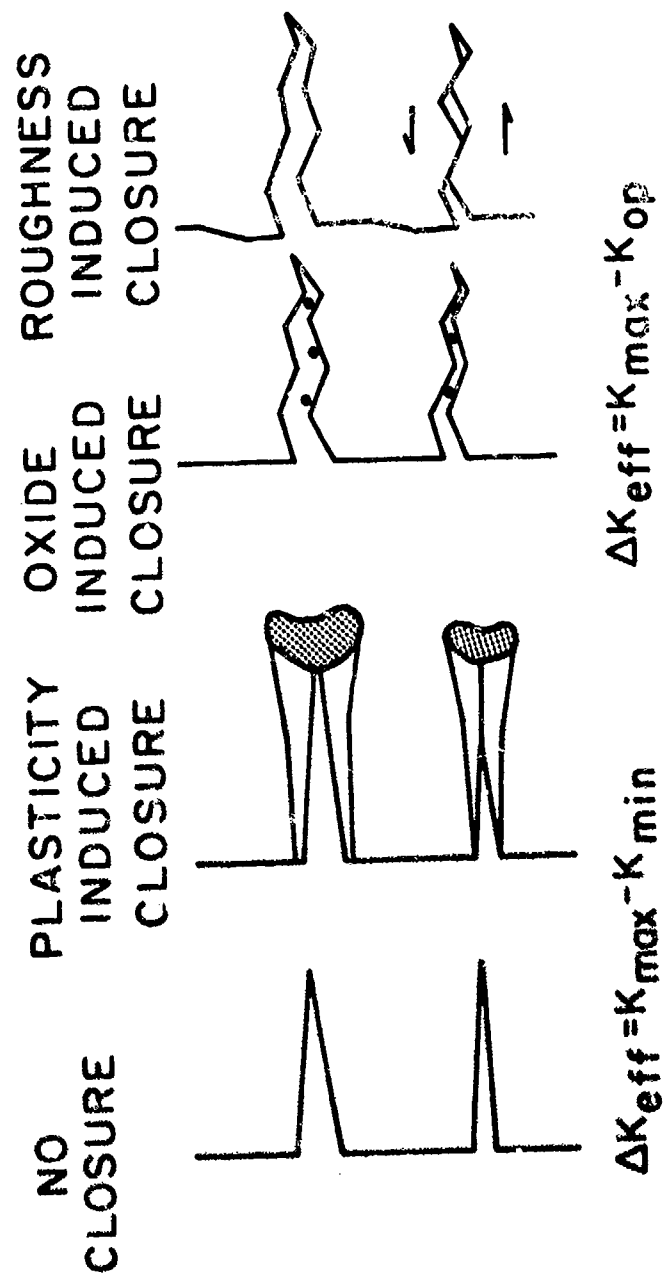


Figure 12. A Schematic Comparison of the Oxide Induced Closure Mechanism with the Other Mechanisms of Closure [12].

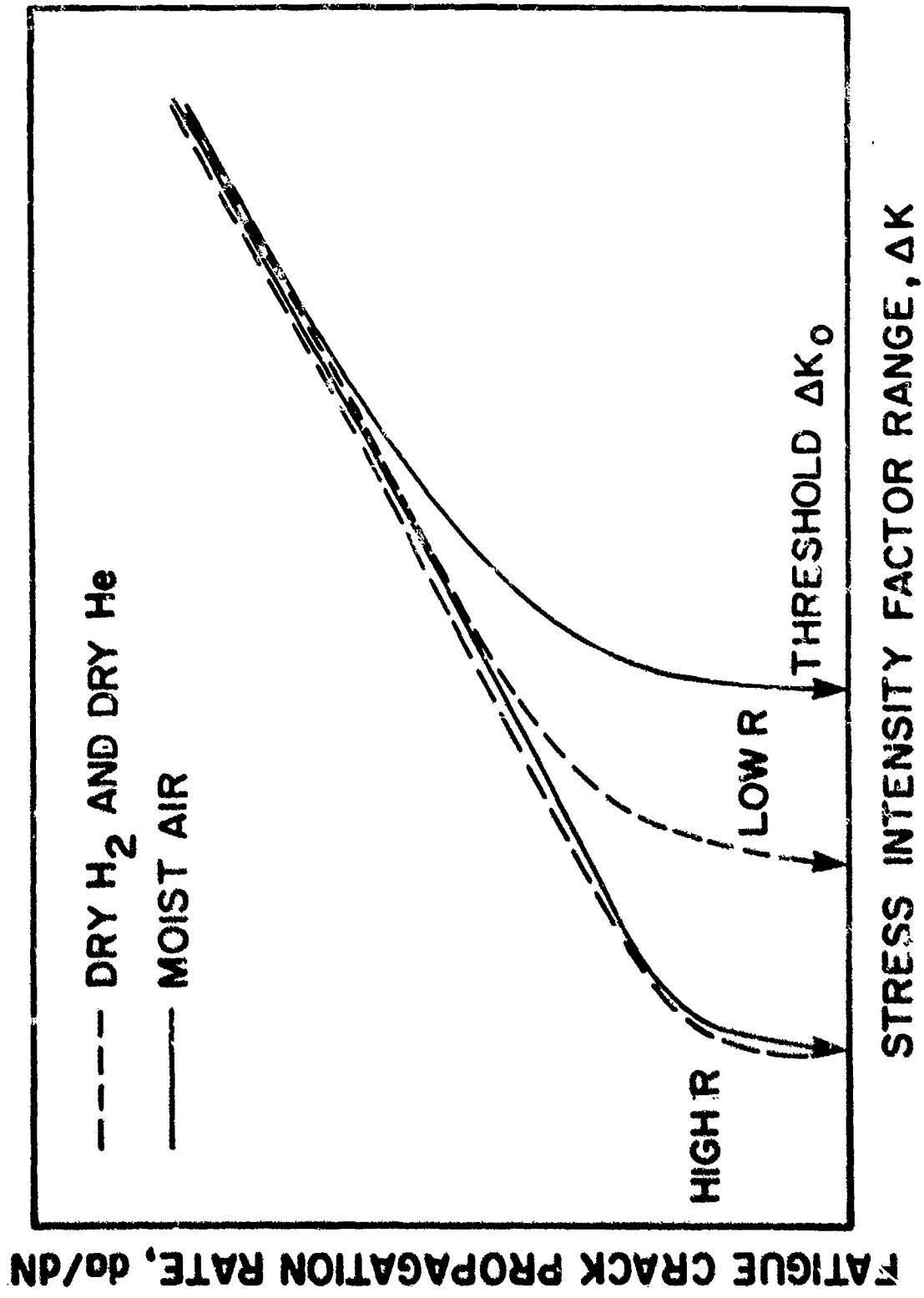


Figure 13. Basis of Oxide Induced Closure - A Schematic Effect of Environment on ΔK_0 and da/dN [22].

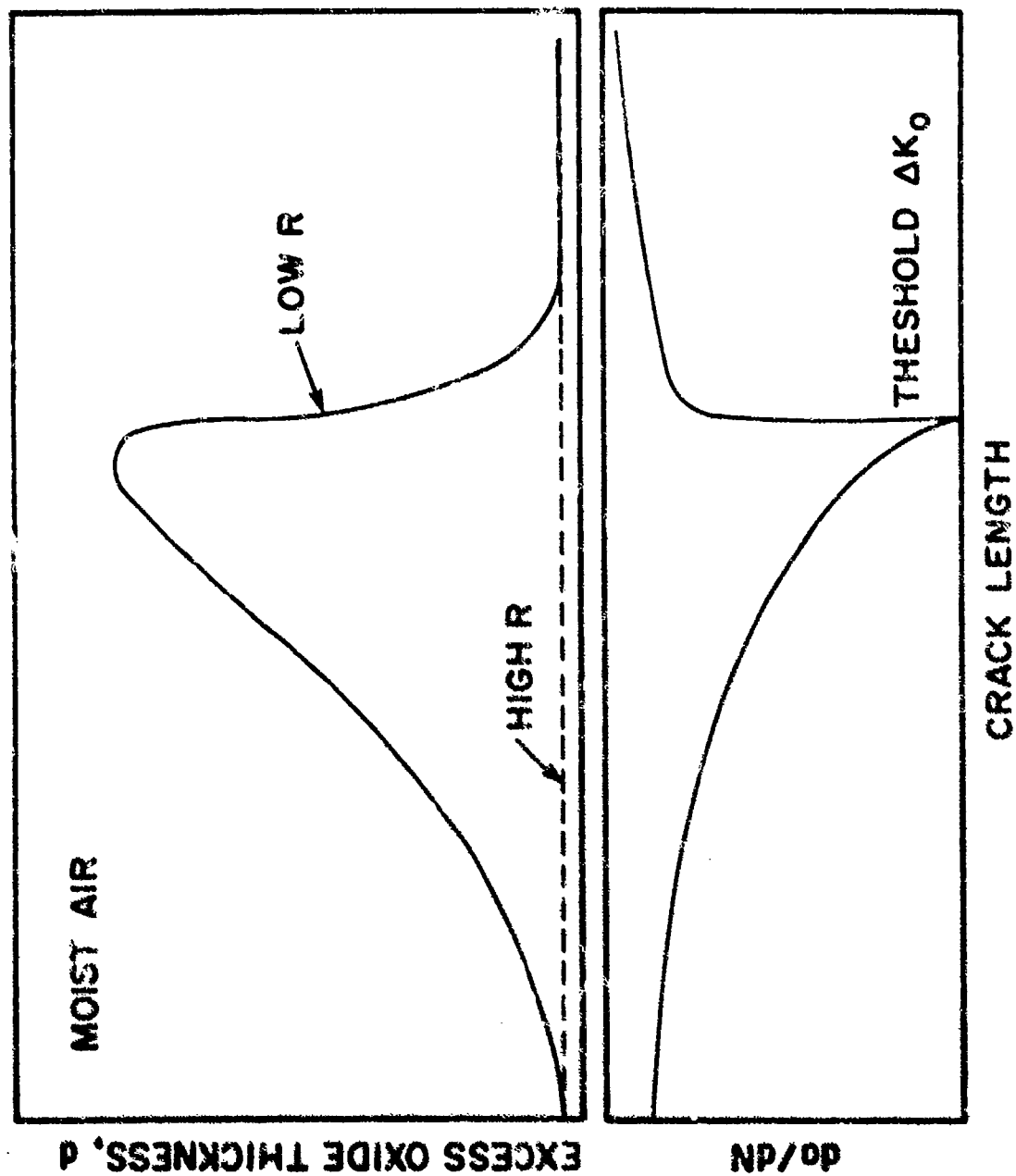


Figure 14. Basis of Oxide Induced Closure. Typical Variation of Excess Oxide Thickness, d , with Crack Length and Crack Propagation Rate [27].

One must note that oxide induced crack closure does not play a primary role in the near-threshold crack growth behaviour of 2021-T6 and 2024-T3 and peak-aged 7075-T6 aluminum alloys [22], where the thickness of oxide is small compared to the CTOD. This is also true for high strength steel [23] where it has been reported that the crack growth rates in regime just above the threshold are slower in hydrogen or argon as compared to in air. There are also instances such as in overaged 7075-T7 aluminum alloy where the oxide formation is significant and comparable to CTOD leading to crack arrest although ΔK_{th} is unexpectedly low. This has been attributed to the concurrent action of oxide induced closure and hydrogen embrittlement [22].

A few comments on the oxide induced closure mechanism are in order.

As is to be expected, oxide induced closure plays a major role only in specific combinations of material and environment. However, the same material when exposed to an environment which produces no oxide, does indeed exhibit finite K_{op} value. Also, it has been stated [14] that unless plasticity induced closure or mode II rubbing produces the fretting contact, no oxide formation or oxide induced closure can take place. Thus, whereas plasticity and asperity induced mechanisms can produce closure in all instances, the oxide induced mechanism produces additional closure only in specific instances.

The experimental observations [13,14,21,22] reported, qualitatively support the the main postulates of the oxide induced closure mechanism. However, no quantitative model interrelating K_{op} with oxide thickness and its properties has been proposed. One can conceive that such a model could be

along lines similar to the single asperity model. However, the difficulties in such a model as pointed out earlier, has to be kept in mind. Nonetheless, at present, the understanding of oxide induced closure is not adequate to predict or calculate the contribution of oxide formation to K_{op} .

One must also note that experimental verification of the extent of closure and the residual stress distribution which are characteristic of oxide induced closure have not been investigated and verified. For instance, oxide induced closure should exhibit a residual stress distribution similar to the one reported in Figure 9, although this has not been ascertained.

2.4 COMMENTS ON THE MECHANISMS OF CLOSURE

From the above discussion, the differences between plasticity induced closure on the one hand and the asperity and oxide induced closure on the other, are quite obvious. First, the nature of the residual stress distribution near the crack tip are expected to be quite different (see Figures 5 and 9). Second, the asperity and the oxide induced closure mechanisms apply to situations where plasticity, ΔK , K_{max} , da/dN , and the extent of closure that is $\Delta a/a$, are all very small. Presumably, plasticity induced closure applies to the opposite situation. However, it is interesting to recall a point made earlier: plastic zone formation is essential for the generation of closure by the oxide induced mechanism, even though the plasticity under such circumstances is extremely limited. The role of plasticity is considered to be secondary in asperity induced closure. However, a plastic wake forms even if the K_{max} value is low and the plastic wake will produce the

characteristic compressive residual stress pattern and the crack opening stretch at the crack tip. Neither the oxide nor the asperity induced closure mechanism takes into account the presence of such residual stresses.

One of the major discrepancies in plasticity induced closure is that K_{op} is observed to be practically independent of K_{max} even when the plasticity is not negligible. An increasing K_{max} should increase the size of the monotonic and reverse plastic zone. Therefore, it is not the reversed plasticity near the crack tip but the integrated effect of the residual displacement produced by the plastic zone and the wake, which plays the predominant role in determining closure. Similarly, contrary to expectations, K_{op} is observed to be independent of K_{max} even at K_I levels where asperity and oxide induced mechanism are assumed to be inapplicable. Thus, a mild dependence of K_{op} on K_{max} is not necessarily a characteristic of oxide or asperity induced closure. On the other hand, the observation that K_{op} decreases with increasing σ_y even at very low K_{max}/σ_y levels of loading indicates that asperity and oxide induced closure are either dependent of crack tip plasticity or, alternatively, the mechanisms play only a small role in producing crack closure.

In evaluating the effect of K_{op} on da/dN , it is assumed that a fatigue crack cannot grow as long as it remains closed. This, in turn, is based on the assumption that fatigue crack growth rate is generated by the strength of the singularity or rather the stresses and strain around the crack tip. Since the stresses and strains near the crack tip are comprehensively represented by K , K becomes the crack driving force for the growth of

a fatigue crack. In a cyclic loading situation, one would then expect alternating levels of K or ΔK to be the crack driving force and this then would control da/dN . Since there is no detailed micromechanism interrelating da/dN with ΔK level and material properties, the constants A and n in Equation (1), which represent material behaviour, are based on empiricism and have to be obtained from experimental measurement.

It is clear from the above discussion that the exact mechanism by which ΔK controls da/dN is not known. Therefore, the role of the different patterns of residual stress distribution obtained through the different mechanisms in influencing da/dN is hard to analyze and predict. However, one can speculate that a residual compressive stress distribution at the crack tip produced by plasticity induced closure, effectively decreases K_{max} and thus lowers ΔK . On the other hand, the residual tensile stresses at the crack tip produced by the asperity or oxide induced closure increases K_{min} . In either case, ΔK_{eff} would be decreased even though alternative schemes of closure produce opposite patterns of residual stress distribution. Such an explanation can provide the rationale for decreased da/dN due to K_{op} corresponding to two opposite patterns of residual stress distribution.

The above rationalization appears too simplistic since it is well known that fatigue crack growth rate is a more sensitive function of K_{max} than K_{min} . In fact, this is evident from a close examination of the usual data showing increasing da/dN with increasing R for a given value of ΔK . Thus, a decrease in K_{max} value due to residual compressive stress (produced by plasticity induced closure) cannot produce da/dN which is the same as that

obtained by an increase in K_{min} due to residual tensile stress (produced by asperity or oxide induced closure). Thus, the above rationalization is not consistent with the observed dependence of experimentally determined da/dN on K_{max} , R , and K_{min} .

There is another point with regard to the asperity and the oxide induced mechanisms which needs careful examination. If K_{op} decreases da/dN by increasing K_{min} as implied by these mechanisms, one would then expect da/dN to be independent of varying K_{min} in an experimental situation where $K_{op} > K_{min}$ and K_{max} is held constant. This is not observed to be true [67]. Thus, the manner in which the two opposite patterns of residual stresses as well as the two different schemes of closure decrease da/dN is rather confusing.

Notwithstanding the discussion above, one can formulate roughness and oxide induced closure models, wherein the additional residual displacement and the wedging action produced by roughness or oxidation, is not localized just behind the crack front but is spread evenly over the whole length of the fractured surface. Such a distribution of displacement will produce a residual compressive stress pattern over the crack faces and ahead of the crack which is identical to that produced in the case of plasticity induced mechanism and accordingly, plasticity, asperity, and oxide induced mechanisms will then produce identical effects on da/dN , thus resolving the discrepancy discussed above. Based on such a formulation of asperity and oxide induced closure, K_{op} can be calculated by using methodologies normally adopted for plasticity induced closure mechanism discussed later in Section 5, wherein the microstructural roughness parameters and the volume generated by oxidation could be the additional inputs.

One can possibly use back face strain gage together with the CMOD technique to determine the residual stress pattern corresponding to a given mechanism of closure. The measurement of residual strain at the front and back of the centre crack panel specimen at zero load would indicate the nature of residual stress distribution which is characteristic of a given mechanism of closure. In the case of CT specimen, one has to measure the strain also at the intermediate points in the ligament to ascertain the pattern of residual stress distribution.

In the case of plasticity induced closure, it may be necessary to distinguish between the role and the effect of plastic wake and the monotonic plastic zone in producing closure. The former probably produces bulk closure behaviour, generates a large extent of closure and residual displacement, and is easily detectable. On the other hand, the latter probably produces local closure, generates a small extent of closure and residual displacement, and requires sensitive technique for its detection. In a constant amplitude test, the role and the effect of these two closures may not be distinguishable but in a situation where an overload is applied, the distinction between the role and effect of these two closures would be quite obvious.

Finally, one must note that asperity and oxide induced closures operate only in the near threshold regime. There are no models for oxide induced closure and the models proposed for asperity induced closure are in their preliminary stage and require validation through systematic experimental measurement. Thus, these closure models cannot be used for calculation of closure in a component even though roughness and oxide induced closures are

feasible. On the other hand, the closure observed at higher K levels can be calculated only on the basis of plasticity induced closure. The approaches used for such calculation to predict closure in a precracked body are examined in Section 5.

3. EXPERIMENTAL DETERMINATION OF CLOSURE

The determination of closure is based on the measurement of one or more of the parameters such as: displacement, electrical potential, strain gage output or transmitted ultrasonic intensity from the specimen, as the load increases or decreases. The point of transition in the plot of one of these parameters against load is identified as closure. It is not easy to identify the transition point in such plots with certainty. Often the last fraction of opening during the loading phase of the cycle can be rather difficult because closure produces compressive forces which are larger near the crack tip (see Figure 5).

Some investigators consider the transition point as the minimum stress intensity factor above which the crack is fully open and therefore identify it as the lowest point at which the plot becomes linear (marked K_{ℓ} in Figure 15). Others draw two tangents on the plot - one corresponding to the minimum load and the other corresponding to the fully open crack. As shown in Figure 15, the point of intersection of the two tangents, that is K_{ct} , gives the load at closure. The advantage of the tangency method is that it gives consistency between the closure values obtained by two different techniques when simultaneously used in a specimen.

The transition point determined during load and unloading usually occurs at the same load but some investigators prefer to determine the transition point from the plot obtained during the unloading phase. It was pointed out in the introduction that the transition point can be identified with less difficulty if one generates a load-offset displacement plot instead of the usual load-displacement plot.

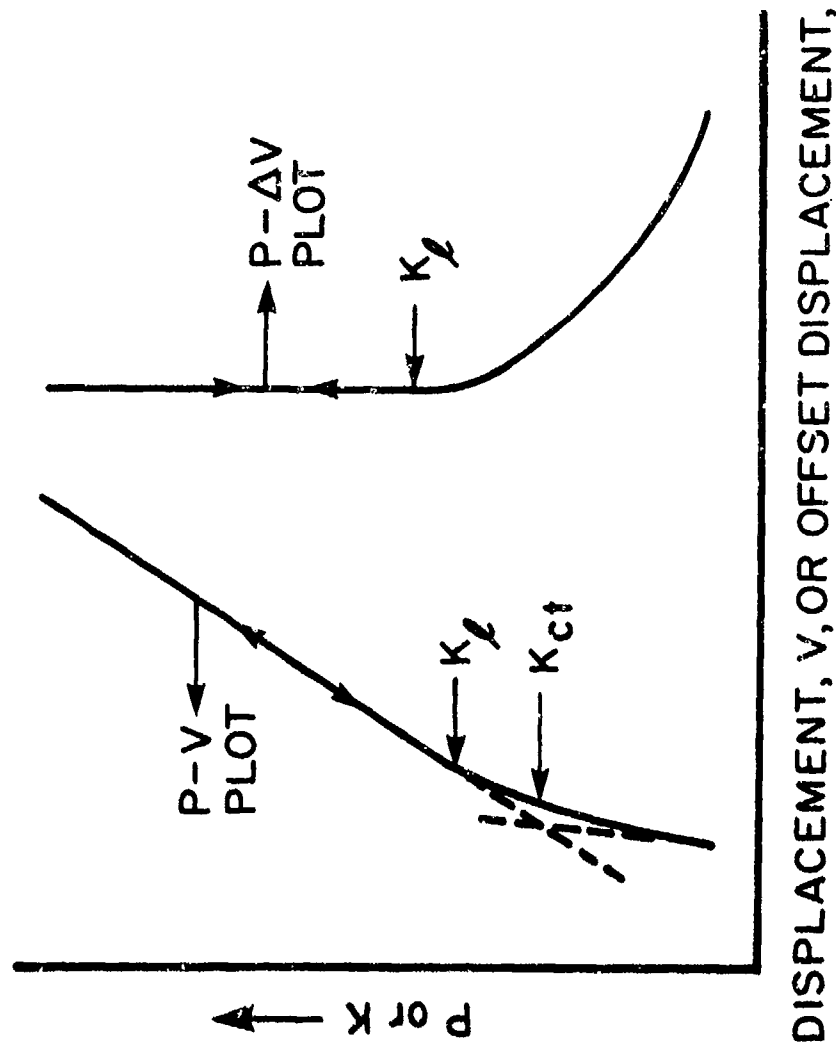


Figure 15. Identification of Closure from Load Versus Displacement (P-V) and Load Versus Offset Displacement (P- ΔV) Plots. K_ℓ Represents the Minimum Stress Intensity Factor at Which the Plots are Linear and P_{ct} is the Stress Intensity at Which the Two Tangents on the P-V Plot Intersect.

The other way to conveniently identify the closure load is to use a more sensitive instrumentation technique. It is argued that since the near tip region of the crack is last to open during loading, the displacement measured at points close to the crack tip would have a larger contribution from closure and therefore, such a measurement is expected to reveal the transition point more clearly. This has indeed been the rationale for the use of Elber type gages as well as the strain gages near and across the crack; for all these measurements can be made at points close to the crack tip.

The thickness averaged global closure behaviour has been determined by techniques such as CMOD, back face strain gage, electrical potential, and ultrasonics. But even the techniques such as the Elber gage or strain gages bonded across the crack or near the crack tip as referred to above, could give thickness averaged global closure behaviour if the distance between the location at which the displacement is measured and the crack tip is large compared to the depth of the curved crack front, the plastic zone size, and the specimen ligament.

As pointed out earlier in the introduction, the closure behaviour determined from the displacement measured at points very close to the crack tip would exhibit a trend which is quite different from the thickness averaged global closure behaviour. It was also pointed out in Section 2.1 that the residual stress may vary across the thickness near the crack tip and exhibit a complex pattern due to preferential plastic flow in the surface layers of the specimen and due to the presence of a curved crack front at the interior of a specimen. Accordingly, the closure behaviour based on the measurement at the surface and those at the interior of the specimen near the crack tip are expected to be different from each other.

The more successful techniques for the determination of closure based on the near tip surface measurements are the methods based on optical interferometry. These can measure displacements localized over small areas (say gage lengths less than 0.5 mm) with a precision better than 0.5 μ m. In addition, one can use the technique of surface replication followed by SEM observation to determine near tip surface closure behaviour. If the depth of crack tunneling, the plastic zone size, and the ligament length are large, the difference between the interior and surface closure behaviours is easily detectable. In such cases, techniques such as small strain gages glued either across the crack or near the crack tip or Elber gages mounted very near the crack tip can also give closure behaviour which has a significant contribution from the near tip surface displacement. For this, the gage length of the strain gage or the clip gage should be small compared to the dimension of the plastic wake in the y-direction. The K_{op} values determined on the basis of near tip surface measurements are usually greater than thickness averaged global K_{op} values.

At present, experimental observations are too meager to define the dimension over which the near tip closure effects would be observed. Obviously, such dimension would depend on the depth of curved crack front, plastic zone size at the specimen surface, and the depth of penetration of plastic zone across the thickness and the ligament of the specimen.

As discussed earlier in Section 2.1, the residual stress in the interior near the crack tip is tensile and therefore, the closure would be observed at a lower load level in the interior as compared to at the surface. Only a few investigations have been carried out to determine the closure

at the interior and the following techniques have been used for the purpose: optical interferometry in transparent specimen, the measurement of closure before and after the removal of a surface layer, and the push rod gage technique.

The thickness averaged bulk closure behaviour would be primarily influenced by the residual stress pattern across the width of the precracked body. But this closure behaviour could also be influenced to some extent by the pattern of residual stress across the thickness near the crack tip. In fact, one can visualize that the closure of the last part of the crack could be influenced by the residual compressive stresses in the surface layers, particularly when the crack front is significantly curved. It has been observed that the closure effects determined on the basis of near tip surface measurements are higher than thickness averaged global closure. Similarly, it has also been shown that K_{op} at the surface is higher than that observed at the interior. However, whether the near tip interior K_{op} corresponds to the thickness averaged global closure is not conclusively established.

The above discussion concerns constant amplitude loading where the bulk and local closure behaviour could be identical as pointed out in Section 2.4. It was proposed that application of a single cycle overload could produce two closures - representing the global and the 'local' behaviours, respectively. The term 'local' refers to the average near tip closure behaviour and probably corresponds to the upper closure point reported by some investigators [32]. One can speculate that in a specimen of intermediate thickness, one would observe some difference between the 'local',

the near tip interior, and the near tip surface closure behaviours. Possibly, the offset displacement procedure technique could be developed and standardized to determine local closure behaviour. This prospect will also be examined in this section.

In this section, the different procedures for closure determination will be discussed under three sub-headings.

1. Thickness Averaged Bulk and Local Closure Behaviour
2. Near Tip Surface Closure Behaviour
3. Near Tip Interior Closure Behaviour

3.1 THICKNESS AVERAGED BULK AND LOCAL CLOSURE BEHAVIOUR

The following techniques are used for the determination of the thickness averaged bulk closure behaviour.

1. CMOD Gage [3,24-32]
2. Strain Gage [3,27,28,33-37]
3. Ultrasonics [12,38-41,52]
4. Potential Difference [3,4,28,30,42-46,60,65]

5. Special Displacement Gage [2,3,6,28].

While using the special displacement gages such as Elber and Nowack gage or strain gages bonded across or near the crack tip to determine thickness averaged bulk closure behaviour, one must remember that the location of such gages has to be far behind the crack tip so that the gage outputs are not influenced by the presence of curved crack front or through-the-thickness yielding at the surface layers or surface strains near the crack tip.

The thickness averaged local closure behaviour could be determined from CMOD gage output using offset displacement technique.

3.1.1 CMOD Gage

The displacement is measured from a clip gage mounted across the notch mouth and located either at the load-line or at the cracked edge (in case of single edge-cracked specimen). A plot of the type shown in Figure 15 is obtained from which the transition point can be identified. The standard CMOD gage, the fixtures used for locating the gage into the specimen, and other details of the related instrumentation are described in the standards (ASTM E399 or E647). As pointed out earlier, the transition point can be more clearly identified from a load versus differential displacement plot (see Figure 2b). Such a technique has been used by several investigators [3,31,32,68]. The basic idea of the measurement of the offset displacement is discussed below.

When the specimen is fully open, the displacement, V , is related to load, P , linearly through

$$V = CP \quad (11)$$

where C is the compliance of the specimen. However, the P - V plots have nonlinearity which can be represented by the offset displacement as given by

$$\Delta V = g (V - CP) \quad (12)$$

where ' g ' is the gain of the amplification and ΔV gives the nonlinear part of the displacement or the offset displacement. Thus, at loads higher than the closure load, $\Delta V = 0$ and a plot of P - ΔV is a vertical line (see Figure 2b). At loads less than the closure load, the P - ΔV plot is nonlinear. The point of transition from linear to nonlinear gives the closure load. Accordingly, the closure load can be identified with a higher sensitivity and less subjective error from such a plot. Offset displacement can be obtained using analog circuitry or digital data in a microprocessor.

It cannot be overemphasized that the accuracy of the P - ΔV plot depends primarily on the accuracy of the measurement of the load and the displacement. Accordingly, the errors in displacement measurement due to the misalignment and friction in the loading fixture or clevis and the clip gage support has to be minimized. One can use clevis with ball bearings [32,141] and special support point for the clip gage [3] to achieve this.

In addition, one must note that the identification of the closure load has some inherent uncertainty. The minimum stress intensity factor at which the P-V plot is linear if identified as the closure point (marked K_{ℓ} in Figure 15) would be somewhat higher than the closure point identified by the tangency technique (marked K_{ct} in Figure 15). One can use a regression analysis to determine K_{ℓ} from the P-V plot. But a small amount of inherent nonlinearity in the upper part will introduce uncertainty in determination of the true K_{op} from P-V test record. Because of higher sensitivity of P- ΔV test records, K_{ℓ} determined from such a record could be higher than that obtained from the P-V test record (see Figure 15).

If one uses P- ΔV plot, the identification of closure is easier, but even this procedure is not free from some degree of uncertainty. Figure 15 gives an idealized representation of the P- ΔV plot. The actual P- ΔV test records tend to develop a loop area since the signal ΔV is amplified in such records. To generate P- ΔV plots, one normally uses a value of C in Equation (12) corresponding to that experimentally observed at loads which are higher than P_{op} but which are somewhat less than P_{max} . As a result, the P- ΔV plots are curved as illustrated in Figure 16. The identification of K_{op} from such test records would be unambiguous, only if the upper part of the P- ΔV record is a straight line. But the upper part of the P- ΔV test record always tends to curve. The origin and interpretation of this curvature are discussed next.

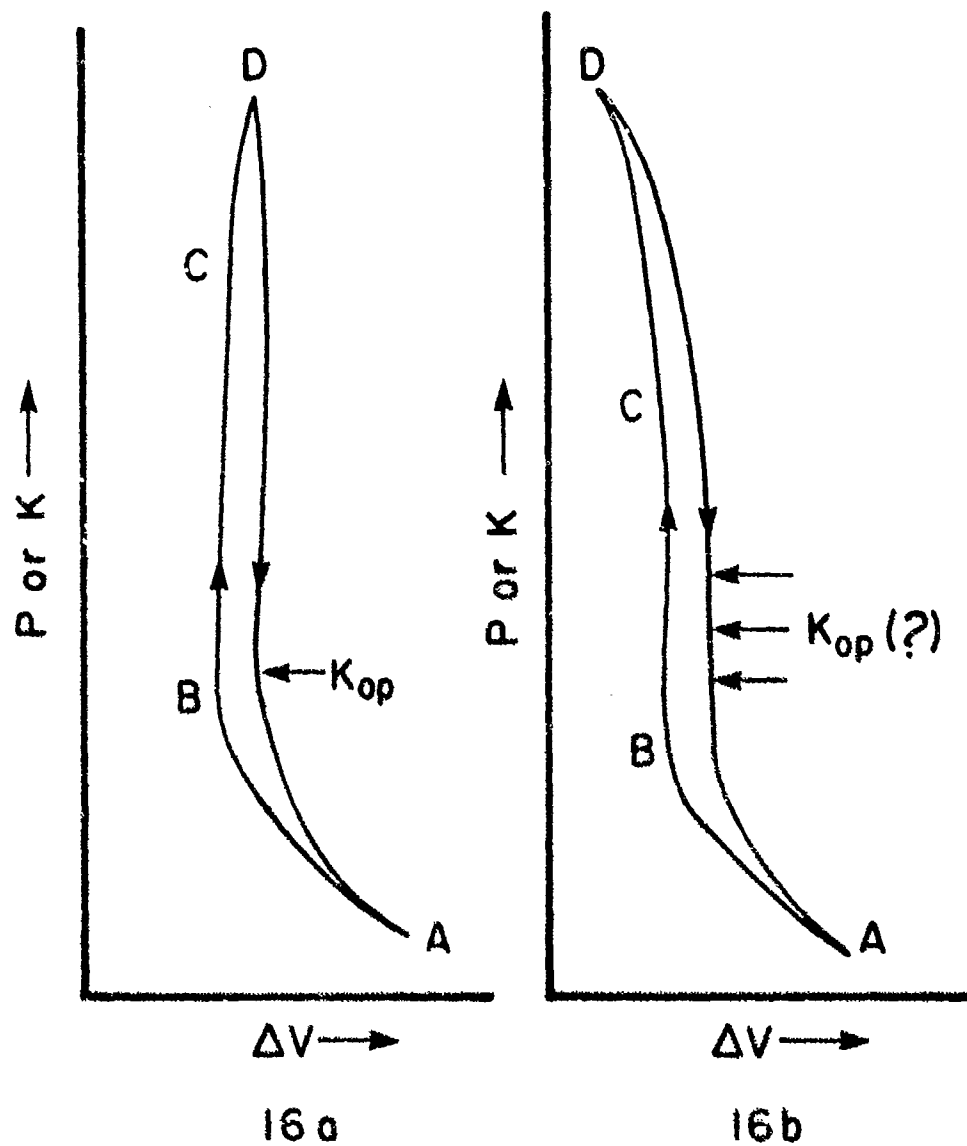


Figure 16. Schematic of the Typical P- ΔV Test Records. Friction and Misalignment may Change the Test Records from the Type Reported in Figure 16a to that in Figure 16b.

It is obvious from Figure 16 that at low load levels, that is between the points marked A and B, the bulk of the crack opens up as the load increases and the curve bends clockwise. At intermediate load levels, that is between B and C, the curve is nearly vertical and this facilitates identification of K_{op} as shown in Figure 16a. However, uncertainties in the identification of K_{op} from the plots of the type reported in Figure 16a can arise if the amplification is high or if the plasticity is large for they tend to decrease the interval between B and C and increase loop area. As the load increases further, the P- ΔV test record again bends clockwise between C and D due to one or more of the following reasons.

1. Incremental growth of plastic zone
2. Crack extension
3. 'Local' opening of the crack near the tip
4. Misalignment and out of plane bending

If crack extension is absent and incremental growth of plastic zone is negligible, as happens after a single cycle overload, and the misalignment and out of plane bending effects are negligible, the clockwise bend in the P- ΔV test record in the region C to D would indicate a local opening of the crack. Thus, an identification of the local or an upper [32] closure behaviour from the P- ΔV test record is possible. However, in the case of constant amplitude loading, such identification would be erroneous.

On the other hand, a P- ΔV test record of the type shown in Figure 16b shows that the curve in the region between C to D bends counterclockwise. Such a test record is encountered quite often, both in constant and variable amplitude loadings. The counterclockwise bend indicates that the crack is closing as load increases. Since a crack cannot close with increasing load, a counterclockwise bend in the upper part of the P- ΔV test record (that is between B and D in Figure 16b) occurs due to friction and misalignment as stated earlier.

Even if one eliminates misalignment and friction, the vertical part of P- ΔV test plot tends to bend in a clockwise manner due to the growth of plastic zone at large $K/\sigma_Y\sqrt{W}$ values or due to further opening of the crack at the 'local' opening point. The determination of K_{op} is difficult if the curve bends either in a clockwise or a counterclockwise manner. Finally, at higher amplification or higher $K/\sigma_Y\sqrt{W}$ value, the loop areas are excessive and this tends to further complicate the identification of K_{op} . Thus, some amount of arbitrariness is unavoidable if one uses P-V or even the P- ΔV plots, for the identification of closure.

K_{op} , as identified from the P- ΔV test record, need not correspond to K_ℓ or K_{ct} obtained from the P-V plots. And, the question as to which of these - that is K_ℓ and K_{ct} - more appropriately represents closure is, therefore, not significant. If the specimen has a curved crack front, then the crack tip at the interior may be open at a stress intensity factor less than K_{op} . On the other hand, there is every likelihood that at $K = K_{ct}$, the last fraction of the crack might not have opened up, even in a constant amplitude loading situation. In a hi-lo load sequence, in addition, one has to also consider the possibility of a local closure.

CMOD gage is an attractive, convenient, and popular technique for the determination of thickness averaged K_{op} since most often one has to determine compliance of the specimen during fatigue crack growth studies. Even though using such a technique together with the offset displacement procedure enables one to achieve a highly sensitive detection of the last fraction of crack opening, the techniques need further improvement and standardization with regard to specimen alignment and minimization of friction at the clevis pins and at the clip gage support. In addition, further investigation is required to properly interpret the various features of a load versus offset displacement plot so that the occurrence and the identification of an upper closure point [32] can be properly ascertained.

3.1.2 Strain Gage

In order to measure thickness averaged bulk closure behaviour, strain gages can be bonded to the specimen at various locations, A, B, C, and D in Figure 17. A commonly used location is on the back face of a specimen, marked A in Figure 17. The strain gage at D straddles the crack and only the ends of the gage length of the strain gage are bonded onto the lower and upper part of the specimen across the crack. The middle part of this strain gage is unbonded. In all cases, the signal from the strain gage is recorded against load. One can then use either the criterion of deviation from linearity or the intersection of tangents to determine the closure load.

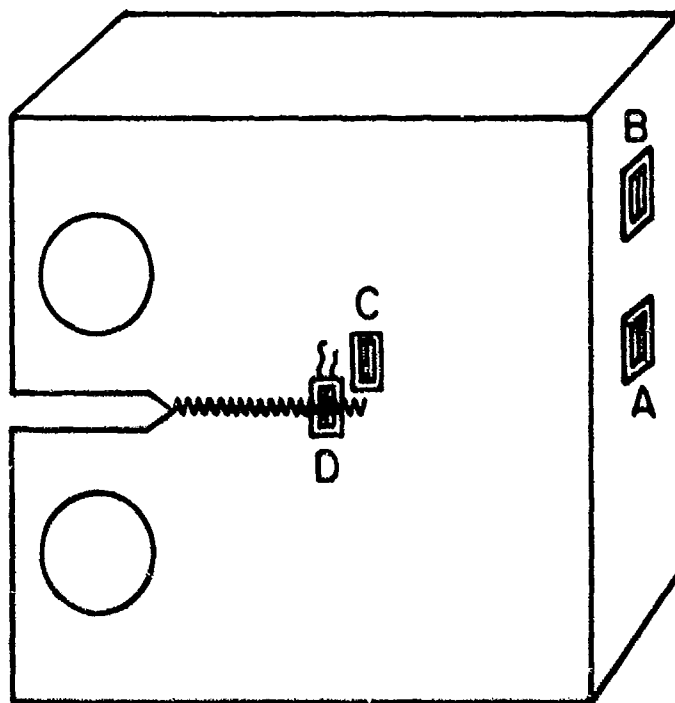


Figure 17. Preferred Locations of the Strain Gage in a CT Specimen for the Determination of Closure Using Strain Gage Technique.

The back face strain gage technique usually gives results which agree well with those obtained from CMOD gage unless the crack length is very short. Besides, the back face strain gage shows less hysteresis. Therefore, back face strain gage technique is widely used for the determination of closure.

The strain gage mounted at location B, C, or D (see Figure 17) can also give thickness averaged bulk K_{op} if the strain gage is large and is not located very close to the crack tip. In fact, K_{op} results obtained from such measurements are also in excellent agreement with those obtained from CMOD.

There are stress-free regions in a precracked specimen, particularly at points which are behind the crack tip but just above and below the crack. Thus, a strain gage located at such points may not experience any strain, therefore, it gives either no erroneous closure [3,34]. It was observed that strain gage of 1x2 mm located with its centre at $a/W = 0.5$ in a $B = 4$ mm and $W = 50$ mm CT specimen at a point 3 mm above the crack faces can sense the closure over the whole range of $0.4 < a/W < 0.65$ [34]. There could be other locations also in the plane of the specimen.

The strain gage, particularly at the back face, has advantages over the CMOD clip gage for the determination of closure. If proper strain gage procedure is followed, one can dispense with the problems of friction at the clip gage support. Besides, at high frequencies and high temperatures, strain gage technique has some obvious advantages in determining closure.

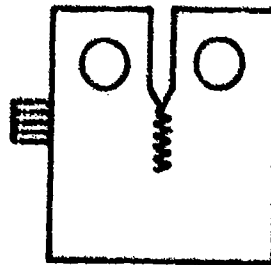
3.1.3 Ultrasonics

As the crack closes, the acoustic resistance of a specimen changes and, therefore, the intensity of the ultrasonic signal reflected from or transmitted through a fatigue crack changes as closure takes place. The basic scheme of the technique is illustrated in Figure 18a. A schematic plot of the load versus transmitted ultrasonic intensity is shown in Figure 18b. In this figure, P_{op} based on deviation from linearity and P_{ct} based on tangency method, give two different closure loads.

However, ultrasonic methods do not always give closure loads which agree with those obtained from CMOD or strain gage techniques. It is reasoned that the asperities on mating crack surfaces slide past one another and the contact between the asperities keeps the crack surfaces acoustically closed even though it is mechanically open [28,46]. The sliding is introduced due to the presence of mode II which, in turn, is produced either due to specimen misalignment or crack branching. However, ultrasonic techniques, unlike the electrical potential technique, can be used even if the specimen surfaces are oxidized [12].

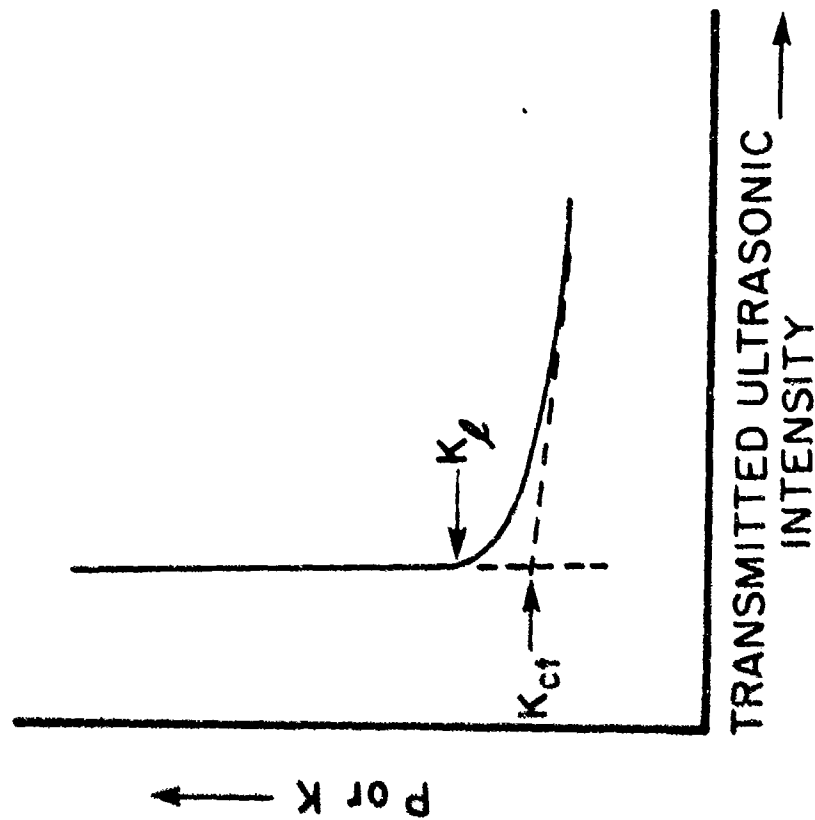
The ultrasonic technique has been successfully and consistently used by one group of workers [38-41]. However, the experience of some others with regard to this technique is not so satisfactory [52].

ULTRASONIC
TRANSMITTER



ULTRASONIC
RECEIVER

18a



18b

Figure 18. Determination of Closure Using Ultrasonics Technique [41]. P_l and P_{ct} are Explained in

3.1.4 Potential Difference

The electrical resistance of a specimen changes as the crack closes. This principle as applied in the potential difference technique is illustrated in Figure 19. A constant current source supply or a constant voltage source together with a resistor in series with the specimen, can be used to feed the current probe. The resultant signal across the potential probe is amplified and recorded. One can use the offset procedure to obtain offset output and examine the load-offset output plot for a more precise identification of closure [3].

Since the output signal from the specimen is small, necessary precaution against thermal drift is essential. Also, it is reported [3] that potential could be measured across the potential probe position 1 or 2 (see Figure 19). The tangential technique could be used to identify closure point.

However, one must note that potential difference technique gives results which do not agree with those obtained from CMOD or back face-strain gage, not only for titanium alloys [28,65], but also for steel [3,60]. This discrepancy could arise due to different reasons [28].

First, a tenacious and insulating oxide layer forms when the specimen is cyclically loaded in air and this prevents electrical contact and closure detection even when there is mechanical contact and the load is transferred across the crack surfaces. Second, but an opposite reason, is that when a specimen is cyclically loaded in vacuum, the asperities on the

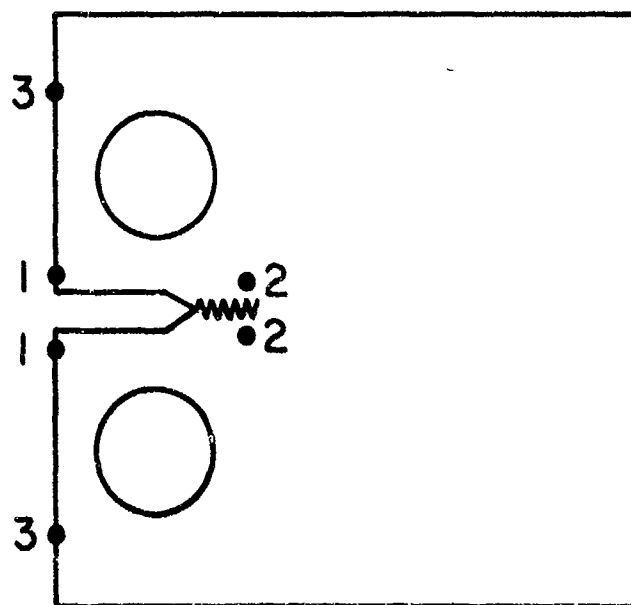


Figure 19. Determination of Closure Using DC Potential Drop Technique.
1-1 and 2-2 - Potential Probe Position and 3-3 - Current
Probe Position [3].

mating fracture surfaces may slide and make electrical contact without effectively transferring load across the crack surfaces. Finally, plasticity at the crack tip and varying contact resistance at the specimen/pin contact can contribute to the potential drop measured. In fact, it has been stated that the results of potential drop technique have to be interpreted with extreme caution [2].

3.1.5 Special Displacement Gages

Special displacement gages such as single cantilever Elber gage [6], Nowack gage reported in Reference [28], and twin cantilever gages [3] have been developed for the measurement of displacement over small gage lengths across the crack on the specimen surface and at points very close to the crack tip. These gages have high sensitivity, exhibit low hysteresis, and give P-V plots with higher slope change at the transition point for the identification of closure. Thus, in the initial stages of closure studies, they were widely used for the determination of closure. One can also use load-offset displacement procedure [3] for a more precise identification of the closure point from the outputs of these gages.

As pointed out earlier, such displacement gages can be used for the determination of bulk closure. But in situations where the depth of crack front, plastic zone size, thickness, and width of the specimen are relatively large, such displacement gages can be used for the determination of near tip surface closure.

In case of ordinary clip gages located near the crack mouth, the displacement signals are large and therefore, closure which changes the compliance of the specimen contributes only a small fraction of it. However, if the displacements were measured over small gage lengths close to the crack tip, the total displacement would be small and closure would make a large contribution to the total displacement measured. As a result, the transition point can be identified more easily [2,3].

It has been pointed out [62] that surface strains behind the crack tip may influence the displacement values measured by special displacement gages of small gage length and located very close to the crack tip and this can affect the closure value somewhat. Thus, such special displacement gages should be used with caution. On the other hand, it has also been reported [3] that special displacement gages located near the crack tip give closure values which are identical to those obtained by CMOD or back face strain gage technique.

3.2 NEAR TIP SURFACE CLOSURE BEHAVIOUR

It has been pointed out earlier that the special displacement gages or strain gages located very close to the crack tip can measure near tip surface closure behaviour in certain circumstances. However, the more reliable method for the measurement of near tip surface closure behaviour are the following:

1. Interferometric displacement gage [49-54]

2. Direct observation using SEM [3,7,8,9,47,55,56,62]
3. Optical interferometry [52,53,63,89].

3.2.1 Interferometric Displacement Gage (IDG)

IDG is a laser based technique which measures the relative displacement between two shallow reflecting indentations located .05 to 1 mm apart across the crack. The indentations are produced by microhardness indenter. The two interference fringe patterns form due to overlapping diffracted laser beams. The motion of the fringe pattern is a measure of the displacement. The resolution of the technique is $0.25\text{ }\mu\text{m}$ for a range of $400\text{ }\mu\text{m}$; the corresponding error band is 1 percent. Since the gage length of IDG could be as small as $50\text{ }\mu\text{m}$, it can measure displacement within a very small region around the crack tip. Such measurements are bound to be influenced by preferential yielding through the thickness in the surface layer and the presence of curved crack front and shear lips. This can indeed produce a much stronger closure effect than exhibited by the typical bulk measurements such as CNOD or back face strain gage techniques. Indeed, closure measured [52,53] using IDG technique show the above trend. However, IDG measurements can also be influenced by surface strains near the crack tip [62].

IDG technique is powerful since it is a non-contact method so it has all the advantages of avoiding friction, high temperature, or environment. One can numerically process the fringe data and obtain real time measurement. Its use at a location far behind the crack tip can give reliable through-the-thickness bulk closure behaviour.

3.2.2 Direct Observation Using SEM

One of the convincing techniques for determining near tip surface closure is direct observation of a two stage replica taken of the crack tip region of the specimen. The two stage replication consists of acetate tape, evaporation of gold on it, and the final support of the replica using electrodeposited copper [8,9]. Almost a similar procedure but different somewhat in the details, was used by another investigator [3]. Since the acetate has a resolution of $.01 \mu\text{m}$, displacements as small as $.01 \mu\text{m}$ can be measured.

Replicas have to be taken at fixed loads; thus, several replicas are required to determine the closure load. However, the use of replicas is a direct method of closure observation and if properly carried out, is free from ambiguity of closure determination when other techniques are used.

A variation of this method consists of producing a fine scratch mark running along the specimen surface at an angle to the crack [36]. As the crack opens, the scratch mark splits at the crack line and therefore, shifts a certain distance along the x direction. This shift can be related to the crack opening. One can probably further modify this method to determine the near tip mode II displacement produced by the K_{II} component, if the scratches are marked at fixed intervals of say $50 \mu\text{m}$ or so. It must be noted that at a higher magnification, the crack changes path frequently and appears to branch. Such change of path of crack propagation has been observed even when ΔK was significantly higher than threshold [3]. In fact, at higher ΔK ,

the branches could be longer. It is doubtful if such extensive branching occurs at the interior during constant amplitude loading. What, however, is interesting is that a direct observation using SEM gives closure values which agree very well with the CMOD or back face strain gage [3,62] which measure bulk K_{op} values. On the other hand, one [3] of these two investigators observed that direct observation gives closure values which agree very well with the closure value obtained from special displacement gage located very near the crack tip whereas the other [62] reported just the opposite.

3.2.3 Optical Interferometry

The optical interferometry technique can be used to measure the transverse displacement at points close to the crack tip. A collimated beam of monochromatic light is directed through an optically flat quartz plate positioned directly on the polished specimen surface. With load, the specimen surface separates from the quartz plate and produces an optical interference pattern. Knowing the fringe order, the transverse displacement can be measured with a resolution of $0.25 \mu\text{m}$ at a given point at various times during loading. A combination of the load-time and transverse displacement time data gives load versus transverse displacement record from which one can determine closure.

The optical interferometry gives results which agree very well with those obtained by IDG technique. This is indeed interesting for optical interferometry measurements can yield a displacement ahead of the crack whereas IDG measures a displacement behind the crack tip. This supports the viewpoint that there is probably a fair degree of continuity in the

distribution of residual displacement and compressive stresses across the crack front. On the other hand, these K_{op} measurements do not agree with K_{op} obtained from CMOD gages. This is to be expected. However, what appears confusing is that the replication of crack tip followed by direct observation under SEM give K_{op} which agree well with CMOD gage [3].

The use of optical interferometry for the determination of closure is limited but could be useful if one were to investigate the transverse displacement together with closure.

3.3 NEAR TIP INTERIOR CLOSURE BEHAVIOUR

The investigation of near tip interior closure behaviour is very limited. The following four techniques have been used:

1. Closure measurement before and after the removal of successive surface layers [2]
2. Push rod displacement gage technique [65]
3. Vacuum infiltration technique [64]
4. Interferometric technique in transparent specimen [58].

3.3.1 Closure Measurement Before and After the Removal of Successive Surface Layers

The closure was determined in a 10 mm thick 2024-T3 Al-alloy specimen ($W = 100$ mm, $a = 12.7$ mm) after successive removal of 1 mm surface layers from each side [2]. As can be seen from Figure 20a, K_{op} decreased drastically when the first layer was removed. The lowering was much less during subsequent removal but the lowering of K_{op} continued even to a reduced thickness level of 4 mm when it reached 50% of its original value. On the other hand, it can be noted from Figure 20b that closure measured on specimens of different thicknesses prepared from the same material show that increasing thickness decreases K_{op} [2]. Thus, the major part of the closure probably originates from the preferential through-the-thickness deformation in the surface layer. The presence of a curved crack front and the formation of large shear lips could also contribute to such a marked thickness dependence. Even though it is an interesting and straightforward technique, no similar investigations have been reported.

Since electrical potential technique had been used to detect closure in the investigation and the electrical potential technique is not entirely satisfactory in determining closure, one can suspect the results reported in Figure 20. But these results tend to agree with the result obtained from interferometric technique in a transparent specimen (see Section 3.3.4) and also by others on metallic materials [59].

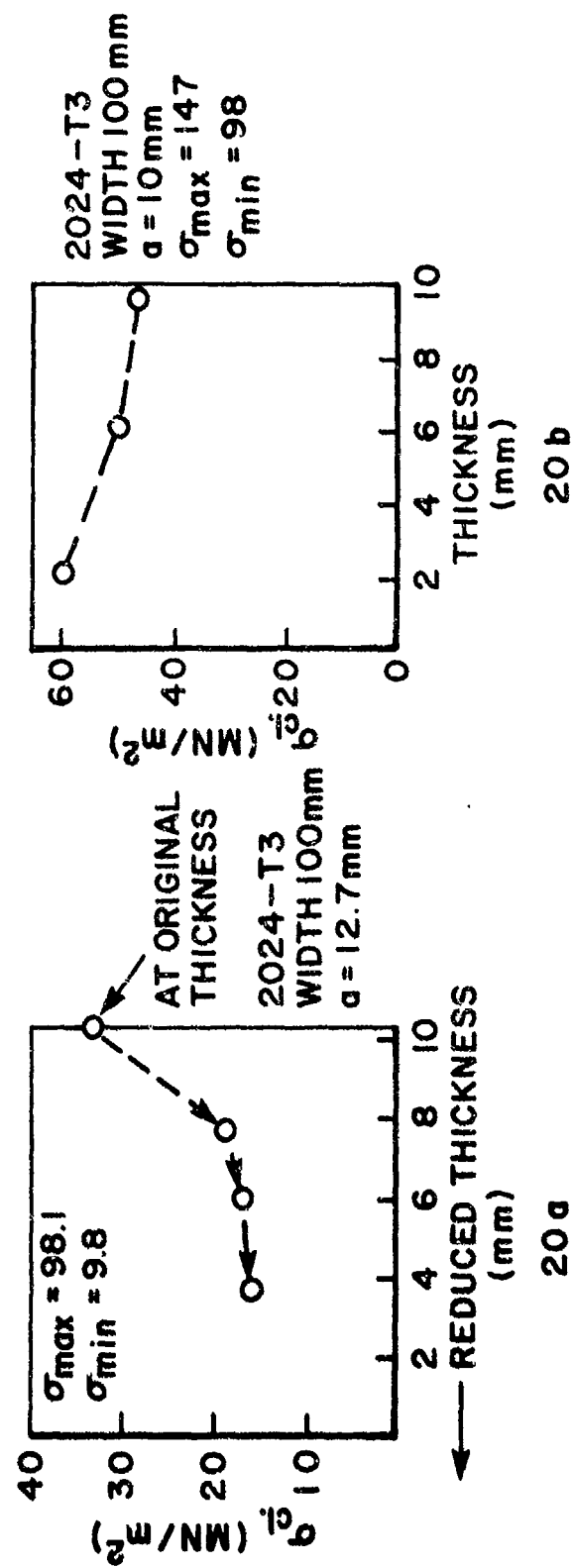


Figure 20. a - Variation of Closure Stress with Removal of Successive Surface Layers
b - The Effect of Specimen Thickness on Closure [2].

3.3.2 Push Rod Displacement Gage

This technique has been developed and used to determine closure at the interior of a thick specimen as well as at the interior of the part through elliptical crack [43,65] in a plate. Figure 21 illustrates the push rod displacement gage technique. The technique shows that closure at the interior is less than that measured at the surface using a near tip strain gage. These are interesting and important measurements and need careful reconfirmation by other techniques such as removal of the surface layer followed by a recheck of the closure behaviour at the first and subsequent cycles of loading.

3.3.3 Vacuum Infiltration Technique

The use of vacuum infiltration technique [64] in a 2024-T3 Aluminum alloys has shown that the primary closure contact points are in the center and within 1 mm of the crack tip, even though substantial shear lips are present.

Based on the observed sharpness of fractographic features in the shear lip and flat fraction region, it has been contended that closure does not take place at the interior at all and is confined only at the shear lips [62] of a very high strength steel ($\sigma_Y = 1677$ MPa). These observations contradict the results of vacuum infiltration technique. Probably, the difference is related to the yield strength of the materials investigated.

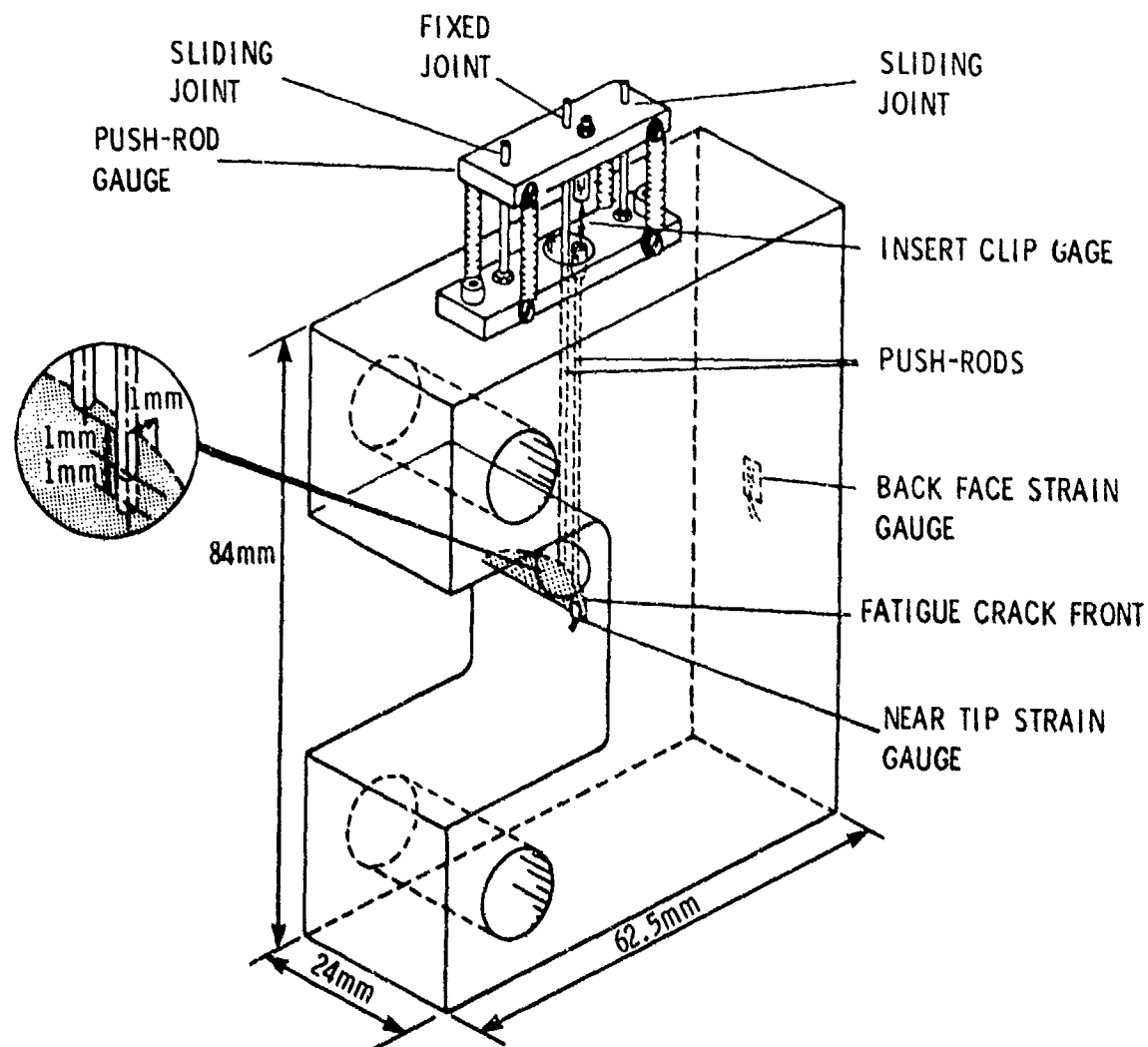


Figure 21. Push Rod Displacement Gage Technique for the Determination of Near Tip Interior Closure of an Elliptical Crack [65]. Note that the Technique can also be Used for a Through-The-Thickness Crack.

3.3.4 Interferometric Technique in Transparent Specimen

Monochromatic light interference fringe patterns produced at the fatigue crack during the loading of a transparent polymethylmethacrylate CT specimen were examined [58] to provide three-dimensional measurement of crack surface displacement with a resolution of 0.25 μm . In the unloaded condition, the crack is closed at the surface of the specimen and also along the curved front within the surface layers. But the crack is open at the interior. The results suggest that the closure effect or K_{op} observed on the specimen surface would be higher than those observed in the interior of the specimen.

Whereas the results support the expected trend that K_{op} observed near the crack tip at the surface would be higher than those observed at the interior of a specimen with a curved crack front, it must be noted that a material such as polymethylmethacrylate undergoes viscous flow. Thus, one may question the applicability of these results to an elastic-plastic material such as a metal. Unfortunately, only one such investigation could be located and such investigation cannot be carried out with metal.

3.4 COMMENTS ON THE DETERMINATION OF CLOSURE

Apart from the techniques discussed above, some other techniques -- such as photoelasticity [75], enlargement of photographs of the crack tip [74], direct observation of the crack tip under optical microscope [36] and SEM [55], fatigue crack growth rate at different R-values [48,76], and electron fractography [94] -- have also been used to determine closure.

The more mature and established methods for the determination of bulk closure appear to be based on the CMOD, back face strain gage, and the use of a special displacement gage such as Elber gage. The value of K_{op} determined by CMOD and back face strain gage technique tend to agree with each other in most instances. However, with uncertainties and contradictions in K_{op} determination being what it is, it is preferable to determine bulk K_{op} , using simultaneously two different techniques. In fact, important aspects of closure behaviour should be confirmed by simultaneously using two different techniques.

The offset procedure can be used to identify K_{op} from the signals obtained from these three techniques. The offset displacement technique is very sensitive and therefore, it can detect the last fraction of closure. However, the determination of a thickness averaged 'local' closure behaviour from the offset technique needs refinements of procedure. Even if such refinements are accomplished, it is not clear if the local K_{op} determined from the offset technique would differ from the near tip interior and surface K_{op} values.

In the case of plasticity induced closure, the difference in the roles of the plastic wake and the crack tip plastic zone in producing closure should be characterized. The offset displacement procedure can be improved and developed to identify the distinction between the closures produced by these two factors. The plastic wake probably produces bulk closure - whereas crack tip plastic zone and reverse plasticity could have a predominant influence on the local closure. The effect of reverse plasticity is important

and should be visible in experiments where a high-low load sequence leads to crack growth retardation; on the other hand, the effect of plastic wake is probably relevant in the case of constant amplitude loading where the effect on R on the da/dN has to be taken into account. In order to distinguish between the two closures, one could machine the material in the plastic wake by EDM and study the effect of its removal on closure detected by the offset procedure on da/dN . This could also help ascertain the origin of the upper and the lower closure points [32] wherein the former has been used to explain overload retardation effects.

The offset displacement procedure using either a differential amplifier or a microprocessor is sensitive and can easily identify the transition point. However, some workers [3] tend to identify the closure load at some point higher than the transition point. No definite procedure is reported to identify such closure points and it appears arbitrary. The offset procedure needs refinement and standardization to minimize the effect of friction, misalignment, and out-of-plane bending. Besides, the characterization of the load versus offset displacement plots and loops needs to be standardized. In the absence of these, even a sensitive technique such as offset procedure is not free from uncertainties.

The more attractive and reliable methods for near tip surface closure measurements appear to be the techniques such as interferometric displacement gage and replication followed by SEM measurements. Surface closure is expected to be higher than the closure at the interior and this has been confirmed by different investigators. However, to clearly

distinguish between the two, the more reliable technique is the progressive removal of surface layers from the specimen and the study of its effect on closure. Such a method, even though laborious and slow, is quite worthwhile in view of the contradictions in the closure behaviours reported by the different investigators.

The push rod gage technique [43,65] appears to be an interesting method of determining near tip interior closure behaviour, however, one has to shift gage location as the crack grows and drill more holes in the specimen. As pointed out above, the most certain method of determining the role of surface versus near tip interior bulk closure is to machine surface layers and measure closure by the offset procedure. Such an experiment can be used to distinguish between the bulk, the local, the near tip interior, and the near tip surface closure behaviours. In order to isolate the effects of a curved crack front and that of the thickness, one could produce specimens with a straight crack front using special notches [17].

Most of the closure determination studies report K_{op} . Yet, to understand, characterize, and predict closure, it is essential to measure the extent of closure and the residual displacement due to closure. Only a few studies report the extent of closure and residual displacement due to closure.

The use of terms such as plane stress or plane strain is confusing. In relation to closure studies, the experimental situations which correspond to two distinct groups of behaviour need to be clearly ascertained. Thus,

the effects of geometry, thickness, width and crack length on K_{op} , extent of closure, and residual strain (or displacement) require a careful investigation. During these investigations, the effect of machining of surface layers as well as the material from the wake in a few selected instances would ascertain and distinguish the closure at the surface and at the interior.

4. PHENOMENOLOGICAL STUDY OF CLOSURE

In this section, some observations concerning the effect of different variables on closure will be presented and discussed. Most of these facts are experimentally determined and only a few are numerically obtained. Most investigations report the effect of the different variables on K_{op} . Since the effect of the variables on the two aspects of closure, that is, the extent of closure and residual displacement produced by closure are rarely reported, the effects of these variables on K_{op} alone will be discussed. The effects of some of these variables are extensively studied, yet some of them are hardly investigated. The effect of the following variables on K_{op} are examined in this section:

1. K_{max} , K_{min} , and R Under Constant Amplitude Loading
2. Overload
3. Short Crack Behaviour
4. Surface Crack Behaviour
5. Residual Stresses
6. Environmental Factors
7. Microstructural and Fractographic Features

8. Material Properties

9. Size and Geometry

Elber [6] proposed that crack growth rates are determined by ΔK_{eff} rather than by ΔK . Accordingly, various investigators have shown that the effects of the stress ratio, hi-lo load sequence, the short crack, the residual stresses, and environment on fatigue crack growth rate can be suitably accounted for by substituting ΔK_{eff} for ΔK in the Paris-Erdogan law - see Equations (1) and (2). The applicability of these equations and their ability to account for the effects of these variables will also be briefly examined at the end of the respective sections.

4.1 EFFECT OF K_{max} , K_{min} , AND R UNDER CONSTANT AMPLITUDE LOADING

In any fatigue loading situation, the three variables, K_{max} , K_{min} , and R are interrelated through $R = K_{min}/K_{max}$. However, contrary to expectation, even in a relatively simple loading situation such as constant amplitude loading, the three variables exert independent influences on da/dN . This shows the inherent complexity of fatigue. A careful examination of fatigue crack growth rate data shows that amongst these three variables, K_{max} has a very strong and positive influence on da/dN in all types of constant amplitude tests. On the other hand, the influence of K_{min} on da/dN ranges between zero to positive and that of R between zero to negative, depending on the type of constant amplitude test. It is likely then that these three variables should also influence K_{op} independently; but the influence of an individual variable on K_{op} need not be identical to that on da/dN .

The effect of R on da/dN obtained under constant amplitude loading is shown in Figure 22. For a given ΔK , as R increases, da/dN increases. Life prediction would be obviously simple if all the da/dN data for different R values as reported in Figure 22 were to collapse to a single line. Accordingly, several approaches have been used to achieve this. The important ones amongst these are the empirical equations (13) and (14) given below.

Forman Equation [78]

$$\frac{da}{dN} = \frac{C \Delta K^n}{(1-R)K_c - \Delta K} \quad (13)$$

Walker Equation [2,79]

$$\frac{da}{dN} = f \left[\frac{\Delta K^m}{(1-R)^m} \right] \quad (14)$$

These equations have been used with some degree of success. However, in recent times, the closure based concept is increasingly being used to achieve the desired collapse of data. The closure based concept is more popular since the concept has a physical basis and can account for the effect of many other variables on da/dN.

Since the three variables are interrelated, the determination of K_{op} could be undertaken in three different types of constant amplitude test situations, as given below:

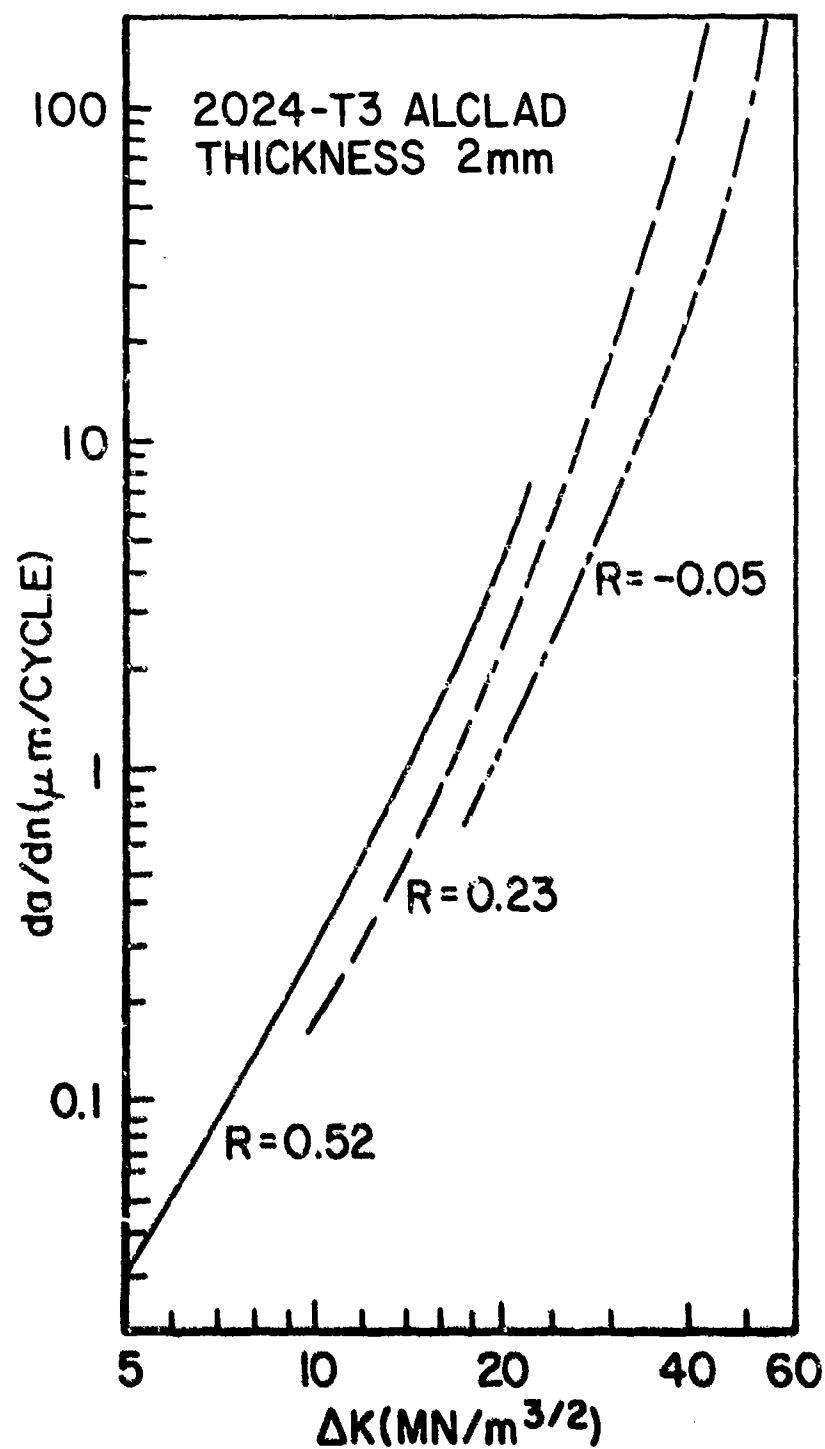


Figure 22. Effect of Load Ratio, R , on da/dN [2].

1. R is constant, K_{\max} and K_{\min} vary
2. K_{\max} is constant, K_{\min} and R vary
3. K_{\min} is constant, K_{\max} and R vary

Most of the investigations belong to the first type; only a few investigations which belong to the second or the third type have been undertaken so far. In fact, it appears that a comprehensive investigation of the effect of all these three different types of tests on K_{op} has not been carried out.

One must also note that most of the closure studies are carried out under load control test conditions. In a load control test, P_{\max} and P_{\min} are held constant and, therefore, K_{\max} and K_{\min} increase as the crack length increases. The K_{op} values obtained from such tests are usually plotted against K_{\max} presuming that a/W has no effect on K_{op} at constant P . In order to ascertain that crack length has no effect on K_{op} , it is necessary to perform K control tests. This will be discussed later.

In the subsequent paragraphs, the effect of R , K_{\min} , and K_{\max} on experimentally observed K_{op} during the three different test situations, are discussed successively.

4.1.1 The Effect of R and K_{min}

The effect of R on K_{op} has been studied by several investigators [6,24,32,44,66,67,68,70] first amongst these being Elber [6] who proposed the relationship

$$U = \frac{K_{max} - K_{op}}{K_{max} - K_{min}} = 0.5 + 0.4 R \quad (15)$$

Substitution of $\Delta K_{eff} = U \cdot \Delta K$ and the Equation (15) in Equation (1) enables us to evaluate the effect of R on da/dN . Based on their respective experimental results, Equation (15) has been modified by other investigators to forms such as $U = .68 + .91 R$ [67] and $U = .707 + .408 R$ [70]. Also, it has been reported that the value of U ranges from as low as 0.4, to as high as 0.85 for plane strain and 0.75 for plane stress [66,67]. Values of U as high as 2 have been reported [70,73] in the literature. However, it has been pointed out [125] that U values greater than 1 represent a contact free crack surface and, therefore, have no physical significance in fatigue crack growth.

Experimental data shows [63,69,70] above, that at a certain value of $R > R_c$, further increase in R has no effect on da/dN . It is also observed that at $R > R_c$, $K_{op} < K_{min}$. To represent fatigue crack growth rate using Equations (1), (2), and (15) at $R > R_c$, K_{op} is assumed to be equal to K_{min} and, therefore, $U = 1$, and accordingly, Equations (1), (2), and (15) give a da/dN which is independent of R as observed experimentally. However,

it has also be argued [73] that by assuming $U = 1$ in situations where $K_{op} < K_{min}$, one uses the same da/dN versus ΔK_{eff} relationship even though the crack tip opening ranges are quite different. And it has also been reported [36] that at $R > R_c$, da/dN increases with increasing R . Thus, the effect of R on U and on da/dN is unclear.

Substitution of $K_{min} = R \cdot K_{max}$ in Equation (15) gives

$$\frac{K_{op}}{K_{max}} = 0.5 + 0.1 R + 0.4 R^2 \quad (16)$$

Equation (16) should be independent of K_{max} or K_{min} ; or, in other words, Equation (16) should hold true for all the three different types of tests. However, as will be discussed in Section 4.1.2, K_{op}/K_{max} is observed to depend on K_{max} and a plot of K_{op}/K_{max} versus K_{max} (or a/W) shows a transition [29,32].

According to Equation (16), at constant K_{max} and positive R values, K_{op} should increase with R and the minimum value of K_{op}/K_{max} should be 0.5. On the other hand, K_{op}/K_{max} has been reported [24,31,32,43,52,65-68] to be ranging in values from 0.15 to almost 1, even at positive R ratios. Yet contrary to all these, in a recent investigation, it has been suggested that K_{op}/K_{max} is independent of R [32].

Elbers original tests were performed with CCP specimens prepared from aluminum alloys. It is hard to infer from these results to what extent specimen size, material, the type of test and test control parameters, and the method of K_{op} determination have influenced the trends of K_{op} results reported above. Indeed, such discrepancies in the experimental observations on K_{op} discredit a plasticity induced closure mechanism. However, as will be discussed shortly, the discrepancies could have alternative explanations.

In a recent investigation [67] where the tests were of the second type, the effect of varying R and K_{min} on K_{op} has been investigated at $K_{max} = \text{constant}$. An examination of the data shows that a sevenfold increase in K_{min} and R , raises K_{op} only by 40%.

4.1.2 The Effect of K_{max}

As regards the effect of K_{max} on K_{op} , the bulk of the investigations [3,6,29-34,44,48,66-68,70,71,73] have been carried out using type 1 test, where R is constant and both K_{max} and K_{min} vary. This is achieved by a load control test where K_{max} and K_{min} increase as the crack length increases. Such test results, discussed later, show apparently three different patterns: (a) K_{op}/K_{max} is almost independent of K_{max} [3,6,32,70] as shown in Figure 23a, (b) K_{op} is independent of K_{max} at constant R , even when K_{max} is in the Paris regime as reported in Figure 24 [4,31,34,48], and (c) K_{op}/K_{max} decreases systematically as K_{max} increases as shown in Figure 25. Such results have been obtained by several investigators [10,18,30,47,66,71,72], particularly when K_{max} values are in the threshold region.

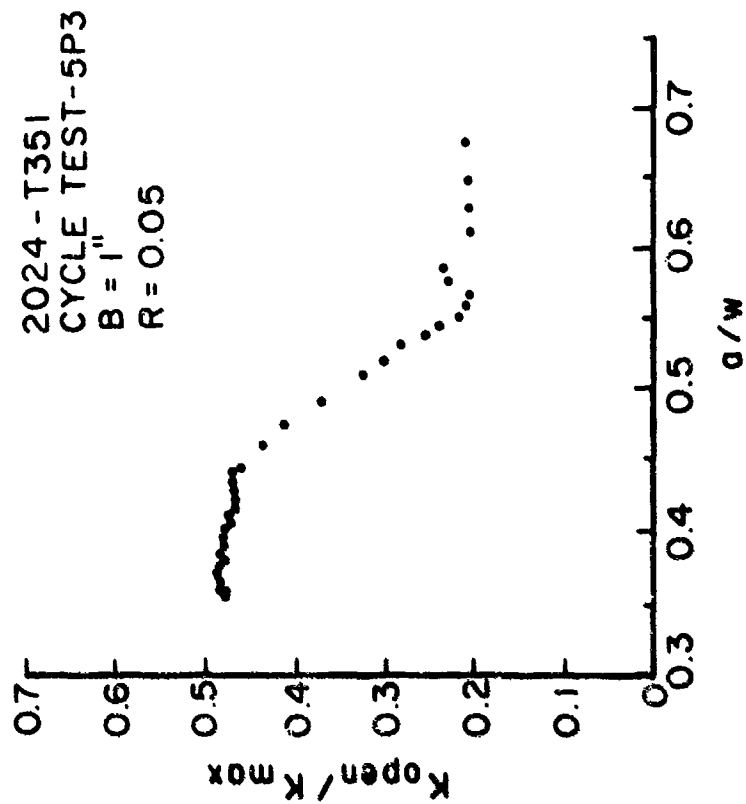
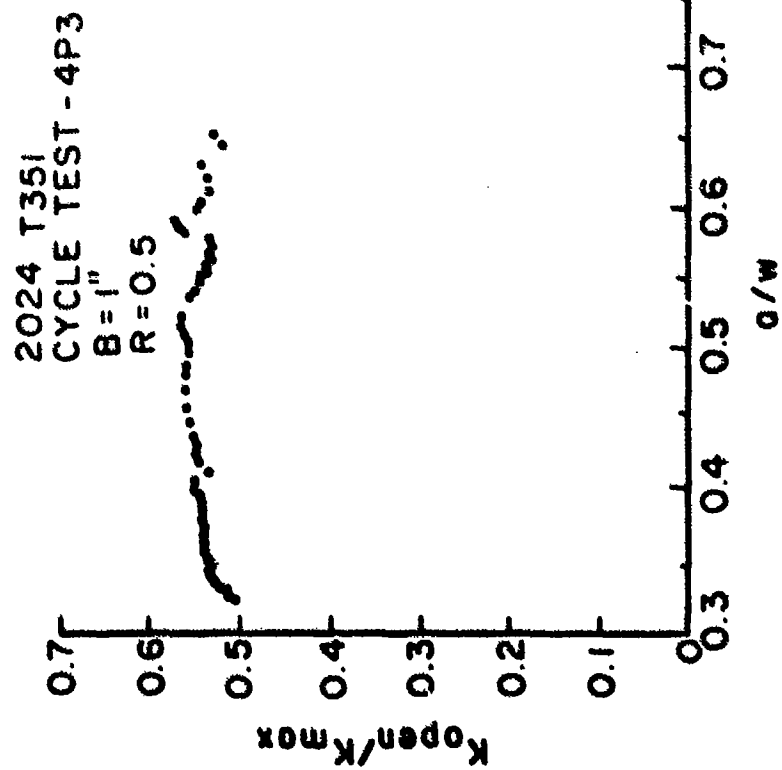


Figure 23. Variation of K_{op}/K_{max} with a/w or K_{max} for (a) $R=0.5$ and (b) $R=0.1$ [32].

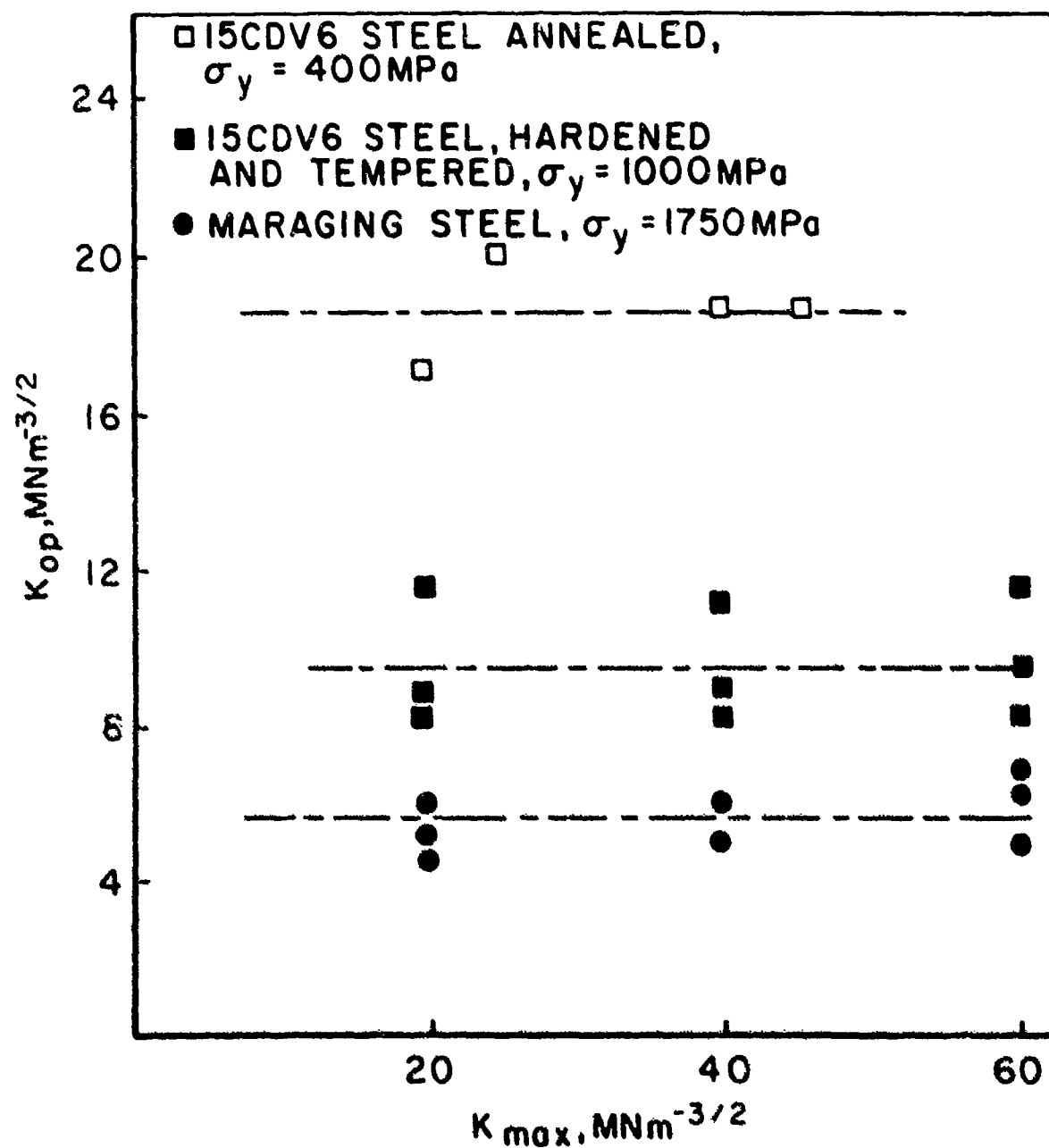
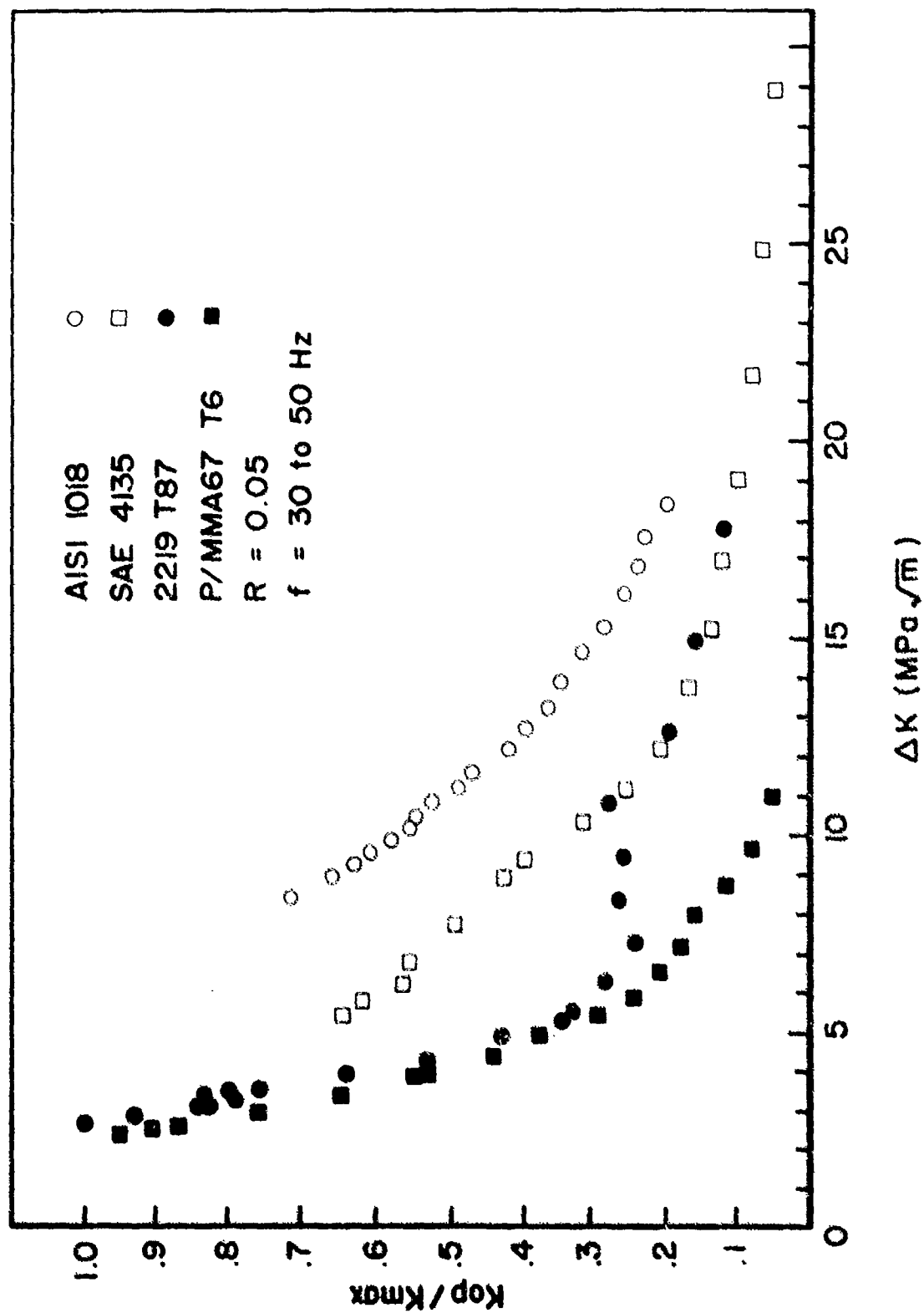


Figure 24. K_{op} Has No Systematic Dependence on K_{max} . Each Data Point From Individual CT Specimens of $B = 4 \text{ mm}$, $W = 50 \text{ mm}$, and Varying a/W Values [31,34].



The observation that K_{op}/K_{max} is independent of K_{max} at constant R and high K_{max} values (see Figure 23a) implies that K_{op} increases with K_{max} . Such an observation is consistent with the mechanism of plasticity induced closure irrespective of whether K_{op} originates from the plastic wake or the plastic zone ahead of the crack tip. However, as reported above, the bulk K_{op} has also been observed to be independent of K_{max} at constant R and high K_{max} values [4,31], particularly in a situation where the K_{max} is changed after the crack has grown with a certain history of loading. At low R values, sometimes it undergoes transition [32] to a lower K_{op}/K_{max} value as shown in Figure 23b. Such a transition is also reported by others [29,32,66]. Usually, such results are obtained in a load control test when K_{max} is in the Paris regime.

The history of loading probably has a strong influence on K_{op} but this has not been systematically investigated. If the prior history of loading were to exert a major influence on the bulk K_{op} value, it is more likely that the main contribution to bulk K_{op} originates from the plastic wake rather than the plastic zone ahead of the crack.

It was pointed out while discussing the first pattern of results that in the Paris regime tests, K_{op}/K_{max} undergoes a transition at higher a/W values (see Figure 23b). Such results are obtained under load control and at higher K_{max} values with $R = \text{constant}$. If the plastic wake is important in producing closure, then obviously, the crack length vis-a-vis the length of the wake in relation to the spread of the wake in the y direction should play a significant role in governing the K_{op} value. The effect of even a fairly wide plastic wake could decrease if the wake is

located at a far off point from the load line of the specimen. The observed transition in the K_{op}/K_{max} value is, therefore, not inconsistent with plasticity induced closure. In view of the above, it is necessary to isolate the effects of K_{max} and a/W in producing closure. Such isolation is possible if closure is determined at different a/W values, in a test where K_{max} and R are held constant. Such an investigation can also help to evaluate the effect of the plastic wake on K_{op} , a point which is particularly important in view of the observed dependence of plastic zone on a/W , recently reported by several investigators [11,121-124].

On the other hand, a systematic decrease in K_{op}/K_{max} with increasing K_{max} (see Figure 25) is considered inconsistent with Equation (16). In fact, this unusual pattern of closure behaviour is cited as important evidence that asperity or oxide induced closure is operative instead of plasticity induced closure at low ΔK regions close to the threshold value. While this logic appears reasonable, one should not overlook the following three points.

First, a close examination of the pattern of decreasing K_{op}/K_{max} with increasing K_{max} of the type shown in Figure 25 would indicate that K_{op} is either independent or is only mildly dependent on K_{max} . In fact, this trend agrees with the recent observation that K_{op} is practically independent of K_{max} . In one of these studies [31,34], K_{max} or ΔK was increased by 100 to 200% and the crack was grown for considerable length. Even then the change in bulk K_{op} was insignificant (see Figure 24). The results reported in other studies [4,48] confirm the above. Obviously, a change in

K_{\max} or ΔK changes the plasticity only at the crack tip; apparently, this change has only a minor influence on K_{op} . Even though plasticity induced mechanism is discounted [4] since K_{op} is observed to be independent of K_{\max} (see Figure 24), one should not ignore the possibility that bulk K_{op} probably originates from the plastic wake, and the wake previously developed is loading history dependent and such history effect on bulk K_{op} can override the effect produced by a change in a local crack tip plasticity during constant amplitude loading for some duration of crack extension.

The second point concerns the very high K_{op}/K_{\max} values observed in the threshold regime. The K_{op}/K_{\max} value is nearly equal to 1. To determine threshold, one normally precracks at a higher load and once the crack has grown outside the notch field, the load-shedding is started in order to determine ΔK_{th} . Thus, the threshold test as usually run, produces a characteristic plastic wake. The plastic wake established during precracking loading history could continue to determine K_{op} over a significant length of subsequent crack extension during a threshold test. Under such circumstances, if K_{op} remains constant, K_{op}/K_{\max} could be nearly equal to 1 as K_{\max} decreases during load shedding. If K_{op} is as significantly history dependent as speculated here, could there be a minimum K_{op} corresponding to the K_{th} , as postulated? Carefully conducted experiments may answer such a question.

The third point concerns the explanation of the observed pattern that K_{op}/K_{\max} decreases with K_{\max} . As discussed above, most threshold tests are conducted following a systematic load-shedding pattern as crack length increases. After the threshold is determined, if load is

kept constant, the K_{\max} value increases; but the initial plastic wake produced at low K_{\max} value during threshold tests, may continue to determine K_{op} value for quite some distance, thus producing a low K_{op}/K_{\max} at higher K_{\max} .

Since the relative roles of plastic wake and monotonic plastic zone in producing the closure at different a/W values is not known, all the above discussion is speculative. But the main point is that one should not ignore the effect of loading history, that is, the change in ΔK or K_{\max} with increasing crack length to suitably explain the observed facts through plasticity induced closure phenomenon.

The reported differences in the effects of K_{\max} , K_{\min} , and R on K_{op} by the various investigators exhibit no systematic pattern. A comprehensive experimental programme can sort out the contradictions and anomalies which partly originate from the method of determination, partly from the type of tests, and partly from the material, specimen size, and geometry.

4.1.3 Normalization of da/dN Data Using K_{op}

Several investigators [2,6,66,68,70] have reported that the effect of R on da/dN can be normalized if da/dN is plotted against $\Delta K_{\text{eff}} = K_{\max} - K_{\text{op}}$ instead of ΔK . One such result is reported in Figure 26. Yet there are some others [36,44] who report that crack closure cannot fully account for the effect of R on da/dN .

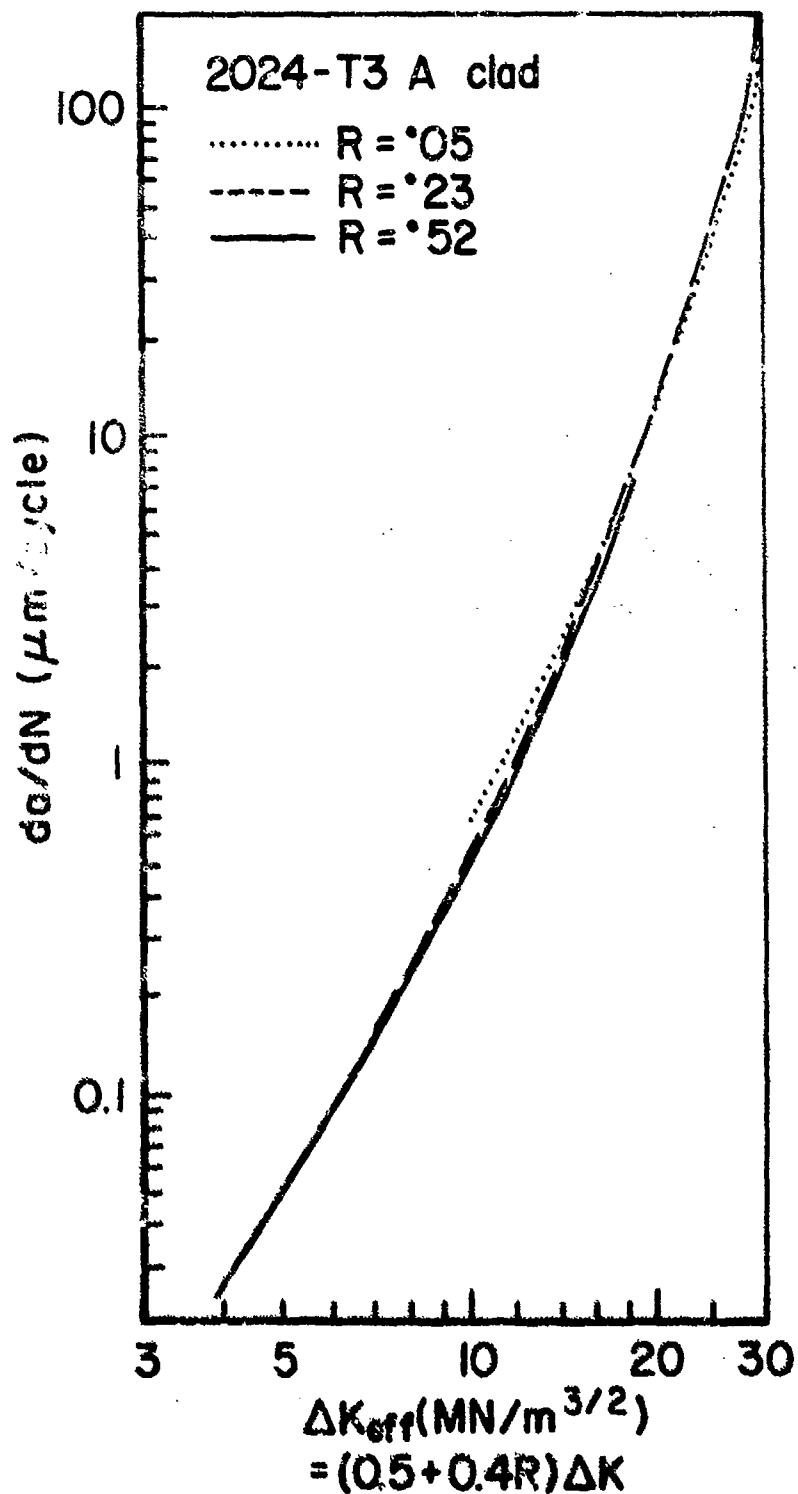


Figure 26. Plot of da/dN Versus ΔK_{eff} , Showing the Normalization of the Effect of R on da/dN as Reported in Figure 22 [2].

Indeed, it is intriguing that so many investigators find such good correlation between da/dN and ΔK_{eff} . When one considers the wide divergence in the observed effects of K_{max} , R , and K_{min} on K_{op} , the inherent uncertainties in the determination of K_{op} , our ignorance as to which K_{op} (bulk, local, interior, or surface) really controls da/dN , and the contradictions as to the precise mechanism by which closure decreases da/dN , ΔK_{eff} appears to be a rather powerful parameter. But to what extent a log-log plot with a permissible scatterband of 2 conceals any discrepancies that would have been otherwise observed, is hard to say. On the other hand, it is clear that the values of the constant A and m should change significantly if one were to change the basis and approach to closure determination. Under these circumstances, A and m can have hardly any physical significance even though considerable research is done to relate them to the basic material behaviour.

Instead of the anticipated straightline, a plot of da/dN versus ΔK is sometimes reported to be curved - sometimes concave [2,66] and sometimes convex with sharp bends [69]. Thus, in such cases, obviously Equations (1) and (2) fail to represent the da/dN data. The question is, do these effects manifest because closure is ignored in the representation of such data. On the other hand, the opposite question is equally valid. If for a given set of data, a plot of da/dN versus ΔK yields a straightline, would a plot of da/dN versus ΔK_{eff} also produce a straightline?

4.2 OVERLOAD EFFECTS [27,32,36,55,65,80-94]

The constant amplitude loading fatigue crack growth studies discussed in Section 4.1 are useful in understanding and characterizing fatigue crack growth. However, what is encountered in service is variable amplitude loading often with an ordered sequence such as a hi-lo sequence producing the so called load-interaction. This is referred to as an overload effect and it causes significant crack growth retardation. As a result of such effects, life prediction based on the crack growth data obtained through constant amplitude loading can be overly conservative. Thus, even though the characterization of overload effects are most important for a precise life prediction, it is a complex phenomenon and is not well-characterized. For the sake of simplicity, in this section, the discussion will primarily concern the overload effects produced by a single cycle step-load even though other loading patterns such as block overloads, compressive loads in compression-tension load cycle, or compressive loads in tension-compressive load also produce significant load-interaction effects.

The overload interaction effect is experimentally observed when a load excursion in the form of a single overload is applied during constant amplitude fatigue crack growth at a baseline ΔK level. The effect of the single cycle overload on 'a' versus N and da/dN versus 'a' at constant ΔK and R is shown in Figure 27. Before the overload, the da/dN has a constant value at region A. The overload has the following effects on da/dN : (1) accelerated da/dN due to overload from the baseline level as in A (this acceleration of da/dN is not shown in Figure 27, since da/dN for a single

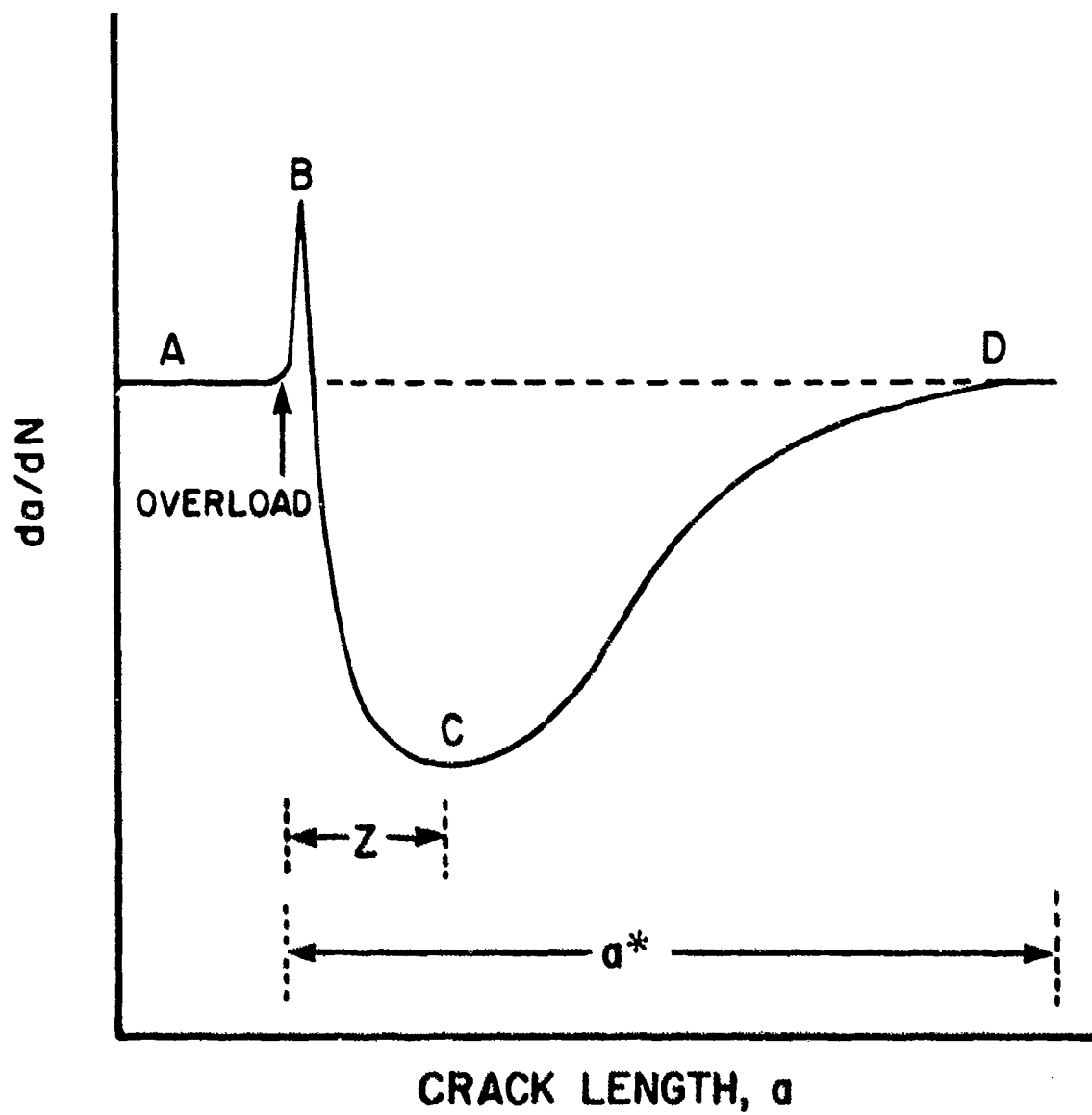


Figure 27. Variation of da/dN as a Result of Single Cycle Overload. The Crack Growth Rate at the Overload Cycle is not Represented in the Figure.

cycle is difficult to determine), (2) a short lived initial acceleration of da/dN at the baseline ΔK immediately after the overload, as in B, (3) a decrease in da/dN to a minimum as in C which is followed by an increase in da/dN to the baseline ΔK level as in C through D, and (4) continued growth with a da/dN value identical to that before the overload, as in D. Also indicated in Figure 27 is Z, the delayed retarded zone and a^* , the overload retardation zone. Whereas several investigators [80,83,85,94] show that a^* is nearly equal to the overload plastic zone size, sometimes in plane strain and sometimes in plane stress, many report [65,90] that a^* is four to five times larger than even the plane stress plastic zone size.

Several empirical models [95-98] have been proposed to explain the overload effect. A comparison of the experimental data and the results of calculations based on the models proposed by the various investigators are shown in Figure 28. The agreement between the models and experiments is not good. Part of this originates from the scatter in da/dN data. But basically, the factors which cause the observed decrease in da/dN are not properly understood.

Attempts have been made to explain the observed effects of the overload using the following concepts: (1) crack tip strain hardening [99,100], (2) crack branching or deflection [19,88], (3) fracture surface microroughness [19], (4) residual compressive stresses introduced due to overload ahead of the crack tip [6,96], and (5) crack closure [2,27,32,65,85,92,94].

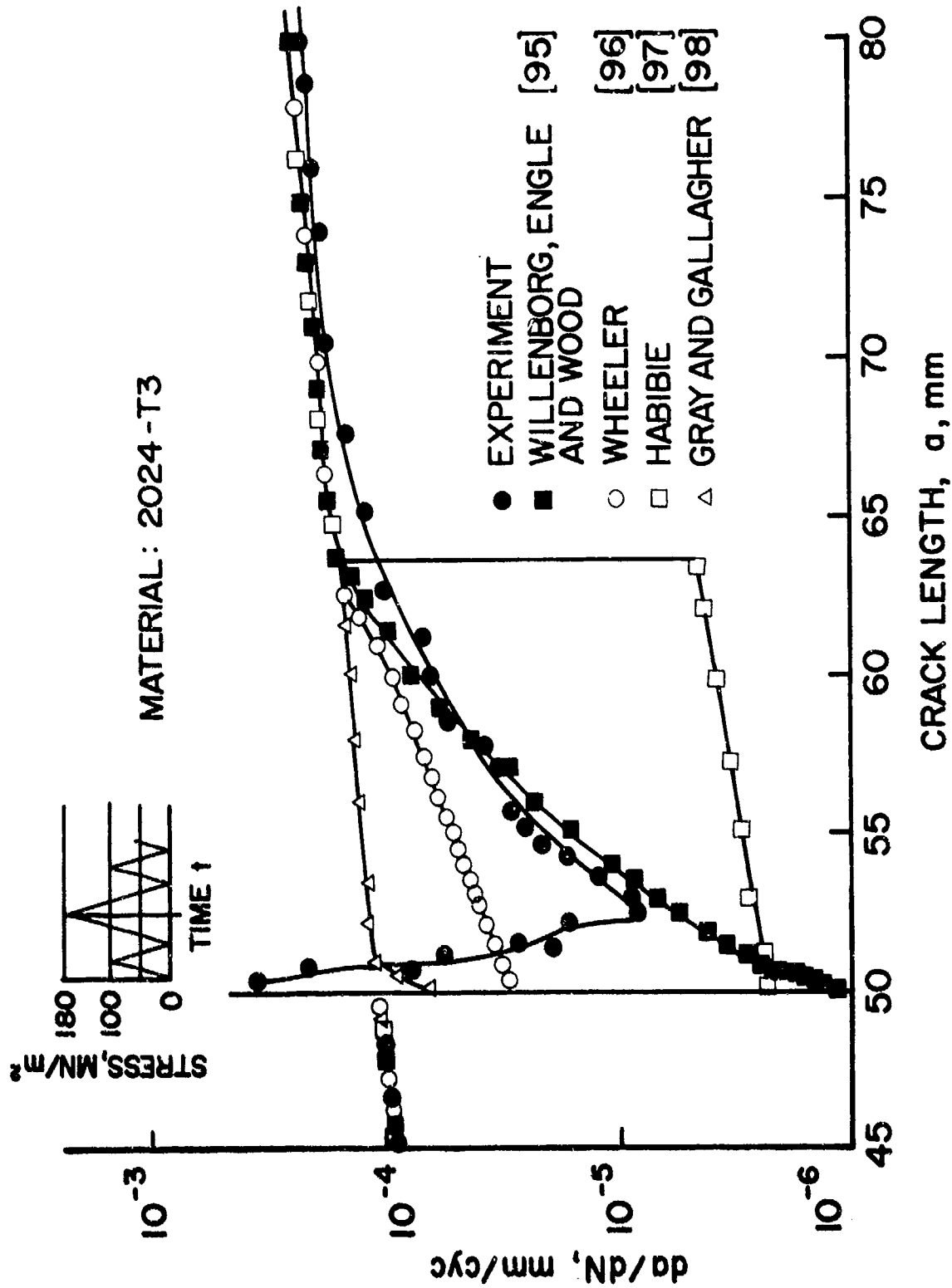


Figure 28. Experimental Crack Propagation Behaviour as Influenced by Overload Application - Comparison with Prediction by Various Models. The Inset Gives Details of Overload Application [84].

Even though crack tip strain hardening can explain some of the observed overload effects, it has also been shown [80] that the phenomenology of retardation behaviour is independent of whether the material is strain hardening or softening during cyclic loading. Recently, crack branching has been proposed to explain part of the observed retardation [19,88]. But the extent of such retardation could depend significantly on the geometry of loading, such as the presence of a bending moment. The role of fracture surface microroughness in producing closure and decreasing da/dN had been examined earlier in Section 2.2. While microroughness can be expected to play some role in producing closure at low ΔK values near the threshold region, the specific combination of K_{max} , σ_Y , size, and geometry at which the role of plasticity becomes negligible and the roughness plays a predominant role in producing closure and retarding da/dN is not clear. Besides this, the position is somewhat confusing. Because, whereas one group of investigators [84] show that a rougher fracture surface produced by intergranular fracture would decrease K_{op} and accelerate da/dN following overload, others [7-12] contend that roughness could produce more closure and decrease da/dN .

Residual compressive stresses ahead of the crack tip due to overload plastic zone and behind the crack front due to the plastic wake are produced by a mechanism discussed in Section 2.1. It is necessary to distinguish between them conceptually, such as considered earlier in Sections 2.1 and 3.4 in terms of 'bulk' and 'local' closure. Experimentally also, one can possibly distinguish between the two. The 'local' closure could be produced mainly by the residual compressive stresses ahead of the crack and therefore, this may play a predominant role in explaining overload retardation effects. On

the other hand, under constant amplitude loading, the distinction between the bulk and local K_{op} may disappear and the bulk K_{op} produced by the residual compressive stresses in the plastic wake behind the crack front is as good in explaining the observed effect of R , K_{max} , and K_{min} on da/dN .

An examination of Figure 27 would obviously show that in order to explain the observed pattern of the change of da/dN following the application of overload, ΔK_{eff} should increase at first, and K_{op} should decrease to account for the short-lived initial acceleration of da/dN . The short-lived initial acceleration marked B in Figure 27, is not observed sometimes. However, what always follows is a drop in da/dN to a minimum (see C in Figure 27) followed by a continuous increase in da/dN till it reaches its original value. These changes in da/dN should correspond to an increase in K_{op} to a maximum followed by a gradual decrease to the original K_{op} prior to overload. Since plastic wake does not change with overload, it is difficult to conceive that closure produced by the plastic wake can give rise to such initial sharp decrease and then a sharp increase in K_{op} followed by its steady decrease. In fact, the bulk K_{op} is not observed to change when K_{max} is changed during overload [31], implying that bulk K_{op} probably originates from the plastic wake. One, therefore, has to take into account the role of overload plastic zone formed ahead of the crack in modifying the residual stresses and displacement. The overload plastic zone can generate residual compressive stresses which have no correspondence with the compressive stresses in the plastic wake. It can, therefore, give rise to compressive stress humps at the peak load spot as postulated [125,126,138] and directly supported by the experimental measurements of near tip displacements [84] and indirectly supported by the identification of an upper closure point [32].

Even though overload retardation has been extensively investigated, only a few investigators [80-94] have used the closure concept to explain the observed effects. Only a few [27,32,65] have measured the K_{op} values before and after overload and correlated the resultant ΔK_{eff} with da/dN . Figure 29 reports one such result where the agreement is good. More impressive are the predicted versus observed da/dN preceeding and following an overload for a thumbnail shaped part through crack on the surface of a specimen which, as discussed later, has a pair of closure and da/dN values, one corresponding to the surface and the other corresponding to the maximum depth point in the interior. This is reported in Figure 30. Notwithstanding the above, some have reported that K_{op} cannot account for the observed overload effects [44, 43,144].

There is an even more important contradiction. Some investigators [85,94] have produced good correlation between ΔK_{eff} obtained from Equation (15), and da/dN during overload retardation. As discussed in Section 4.1, Equation (15) has doubtful validity. The others have used bulk measurements such as ultrasonics [27] and obtained excellent correlation between ΔK_{eff} and da/dN . On the other hand, recent K_{op} measurements which correlated ΔK_{eff} with da/dN very nicely [32,65] are all based on near tip or local closure behaviour of the crack tip measured using highly sensitive instrumentation. It was discussed in Section 3 that local and bulk behaviour in most test situations would give different K_{op} values. Yet a plot of ΔK_{eff} versus da/dN , even in the situation where the estimation or determination of K_{op} has doubtful basis, yield excellent correlation! It seems a log-log plot with the permissible scatterband of 2 can accommodate all such differences. If gross measurements and estimation can as well yield the normalized da/dN data as desired, what is the need for precision measurements?

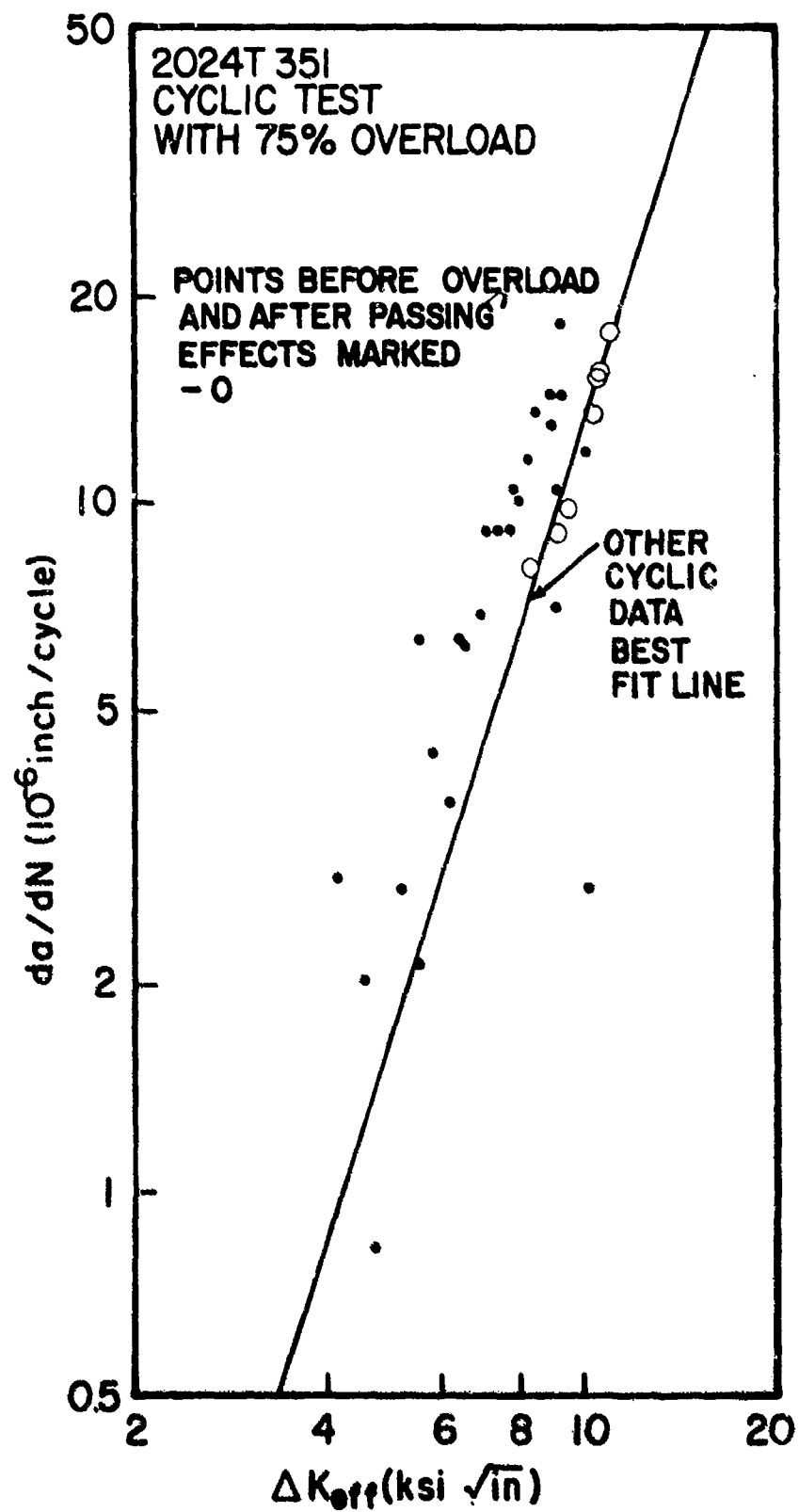
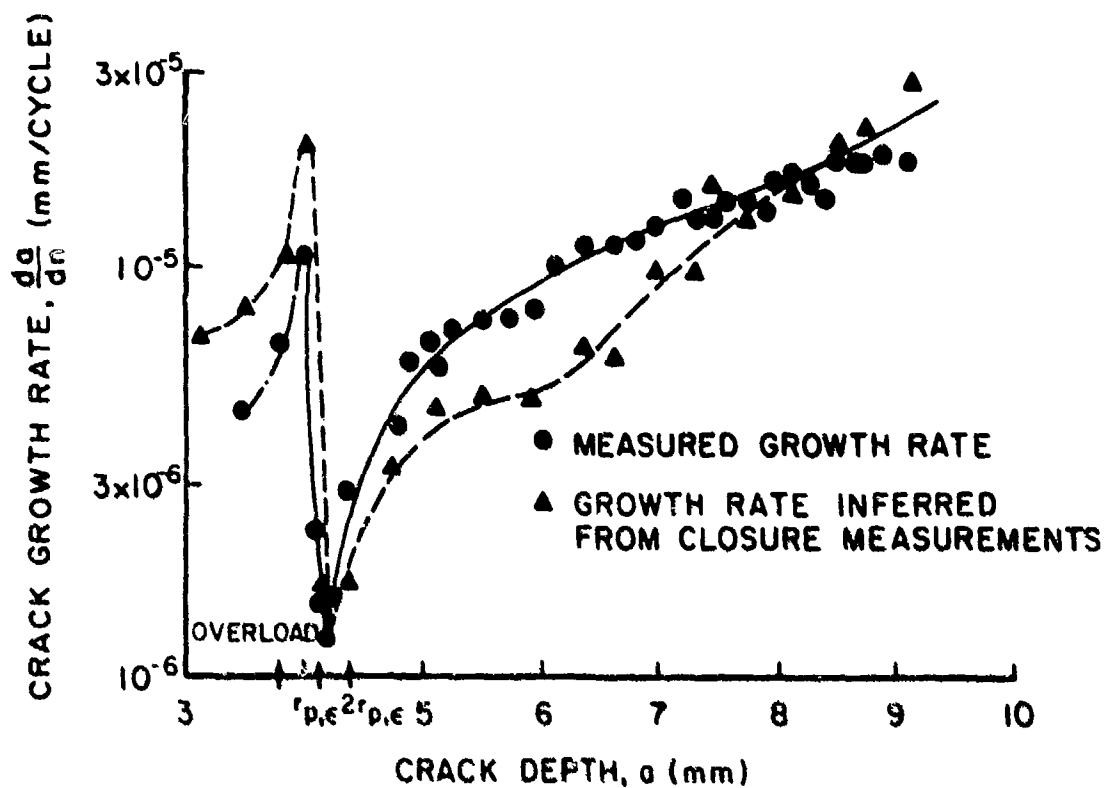
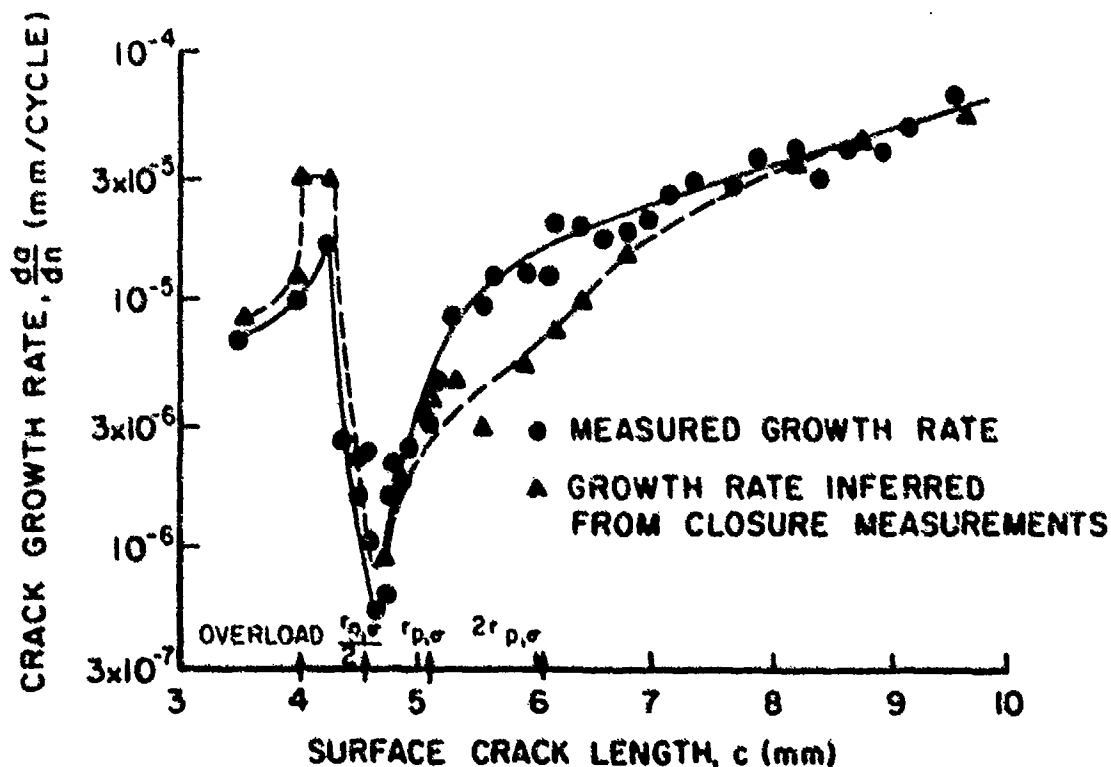


Figure 29. Crack Growth Rate Versus ΔK_{eff} Before and During Transient Effects After a Single Overload [32].



30a



30b

Figure 30. Comparison of Experimentally Observed da/dN Following Overload with the da/dN Inferred From Closure Measurement and Constant Amplitude da/dN Data for a Thumbnail-Shaped Crack with a =Crack Depth and c =Surface Crack Length [65].

If the K_{op} originating from the overload plastic zone were to be responsible for the observed overload effects, the determination of K_{op} produced by such small effects at regions close to the crack tip require precision measurements. As discussed in Section 3, such measurements as well as the interpretation of test records, require standardization.

4.3 SHORT CRACK BEHAVIOUR

A component spends a major part of its life when the crack present in it, is short. It is well established that a short crack grows at a rate much faster than that of a long crack [11]. Life prediction could be significantly non-conservative if this is ignored. Therefore, reliable life prediction requires that short crack behaviour be properly understood and characterized.

The fast growth of short cracks is attributed to several factors: first, continuum requirements are no longer satisfied, second, K or LEFM is no longer applicable and finally, closure is much less, in the case of a short as against a long crack [11]. A short crack is hard to define for its length depends on the material and K level at which the crack is grown. However, most experiments report short crack behaviour in the range of 25 μm to 2 mm [11].

In order to understand and characterize the fast growth of short crack in terms of closure, some numerical and experimental investigations have been carried out. Newman [101,102] has used Dugdale's strip yield plasticity

analysis to devise a 'ligament model' which permits the calculation of closure in CCT specimen geometry using a finite element technique. The closure has been calculated for a short crack emerging out of a hole in a plate specimen and also a CCT specimen without a hole [101]. Newman did not measure closure but compared the experimental crack growth rate with the crack growth rate predicted for a short crack, taking into account the closure effect as obtained from the finite element calculations. Such comparison for the cases both with and without the hole shows a reasonable agreement [101] as reported in Figure 31. The implication is that the crack closure effect in a short crack is less than that of a long crack.

On the other hand, the experimental determination of K_{op} shows a different trend. The experimental investigations of closure in short cracks are few [56,104]. One of the investigators [56] reports results which indicate that the closure behaviour of a short crack is not radically different from that of a long crack; for example, for a .36 mm crack, at $R = 0$, $K_{op}/K_{max} \sim 0.6$. In fact, if K_{op} is as high as reported, the closure effect in short cracks cannot explain the high crack growth rates exhibited by a short crack. Accordingly, the applicability of K-based representation of fatigue crack growth rate is questionable.

It is difficult to characterize closure for a short crack via the plasticity induced mechanism unless the respective roles of plastic wake and plastic zone as dependent on crack length are properly established. Ritchie has proposed [11,12] that a short crack grows fast since the roughness does not develop in a short crack and consequently, closure is less

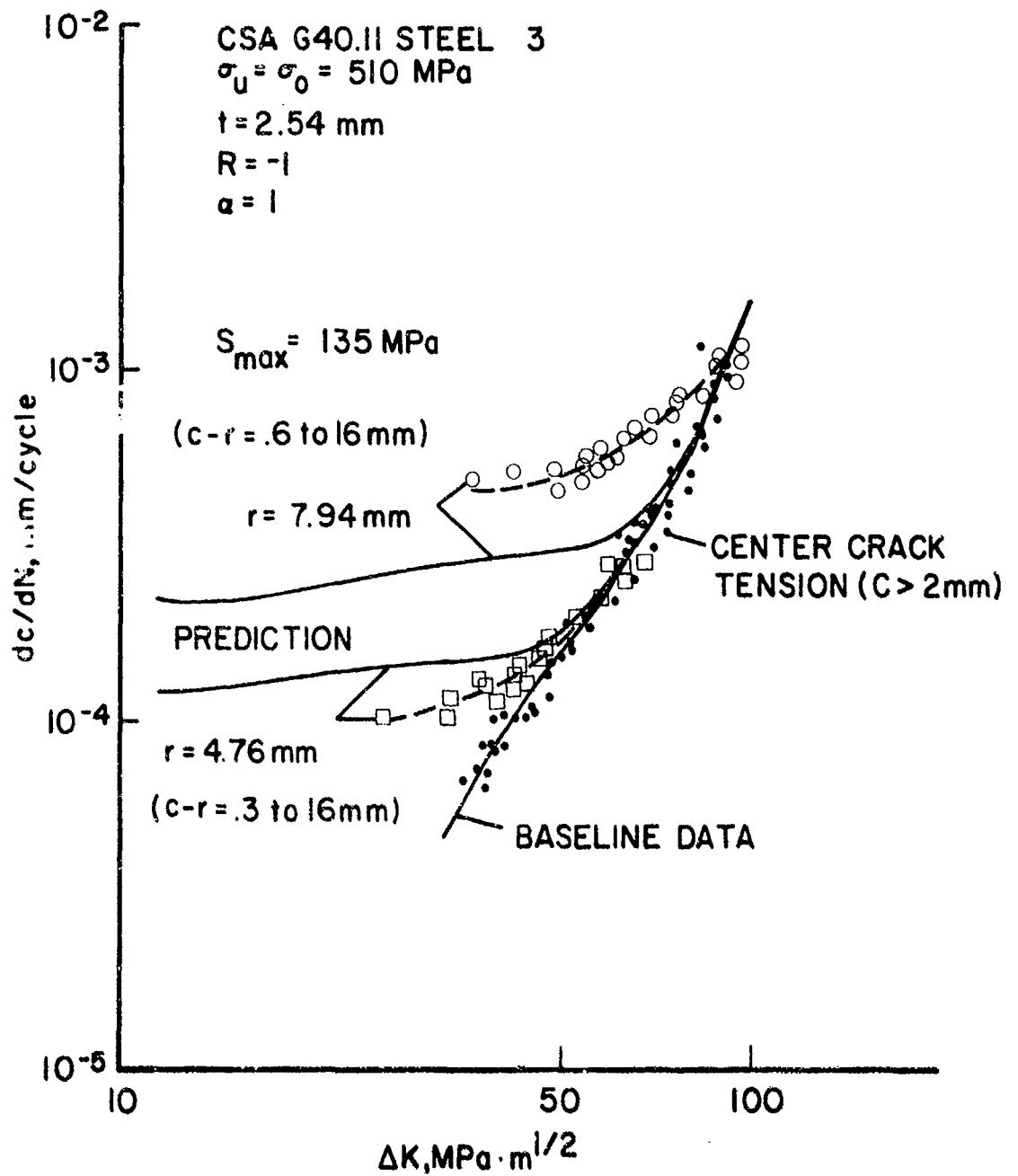


Figure 31. Comparison of Experimental and Predicted Crack Growth Rates for Small Cracks Emanating From a Circular Hole in Steel Specimens [101].

severe. Such a proposal is inconsistent with the observation that a short crack when viewed under a microscope shows a zig-zag path and has a roughness parameter and asperity height (see Figure 11), which is quite large compared to the crack length. Similarly, crack deflection [88] cannot explain the fast growth rates observed in short crack since a short crack deflects significantly quite often. And in all probability, the closure of a short crack may not be negligible. The reason for rapid growth of short cracks becomes even more difficult to explain due to the proposed effects of crack closure, roughness, or crack deflection!

4.4 SURFACE CRACK BEHAVIOUR

Most engineering structures fail in fatigue by the growth of a part-through, thumbnail shaped fatigue crack. The shape of the crack changes as it grows and the growth rate of the crack is not the same along the surface and at the maximum depth point in the interior. At the surface, the state of stress is plane stress whereas at the interior, the constraint to plastic flow is high and the conditions are closer to plane strain. If plasticity induced mechanisms were operative, the closure where the crack meets the surface would be stronger than the closure at the maximum depth point. Even in the case of a through-the-thickness crack, a curved crack front is produced at the mid-thickness of a fracture mechanics specimen. Thus, the basic observation on closure in the case of a thumbnail shaped crack may apply to the closure observed in a specimen with a curved crack front.

Recently, two investigators [65,67] have reported results of closure studies on thumbnail shaped cracks. One of them [65] has measured the closure at the interior using a push-rod gage technique and at the surface using a strain gage technique. It is observed that $U_{\text{interior}}/U_{\text{surface}} \sim 1.13$ where U is defined in Equation (15). Thus, the closure at the surface is stronger than that at the interior. The other investigator [67] estimated $U_{\text{interior}}/U_{\text{surface}}$ from the crack growth rate, the observed variation of aspect ratio of the crack as it grew and the experimentally determined K_{op} at the surface. The agreement between the $U_{\text{interior}}/U_{\text{surface}}$ value obtained by the two investigators is good. In fact, the results obtained have been used to predict the retardation and subsequent growth of a crack following a single cycle overload of the thumbnail shaped crack [65] as reported earlier in Figure 30.

If one assumes that such results are applicable also to the growth of a through-the-thickness crack with a curved front, it has interesting implications. The crack front curvature does not change much during the growth of such cracks and if one were to assume that the closure concept is valid, the implication is that FCGR is faster at the surface than at the interior of a thick specimen. Probably, the difference in the state of stress at the surface and at the interior produces this difference in FCGR.

4.5 EFFECT OF RESIDUAL STRESS

The effect of residual stress on K_{op} and da/dN is important since closure and its effect are manifested in the residual stress it produces.

The nature and origin of the residual stresses produced by closure are briefly discussed at first. Later, the effect of the residual stresses produced by processing and specimen fabrication on K_{op} and da/dN is considered.

The nature of residual stress due to closure of a CCT specimen was experimentally determined [5] by cutting sections across the specimen and measuring forces to reverse displacement. The finite element formulation for the same geometry reports [136] a stress distribution which is given in Figure 5.

On the other hand, the residual stress distribution in the ligament of a CT specimen has not been comprehensively investigated even though this specimen is widely used by many investigators for closure studies. However, one can speculate the stress distribution pattern in a CT specimen by combining the results of the various investigators as discussed below.

The residual stresses near the crack tip of a CT specimen have been determined by X-ray [105]. The X-ray beam size is rather large and X-ray measures the stresses only at the surface. This, naturally, introduces significant uncertainties in the reported stress pattern as it exists across the thickness and very close to the crack tip. However, at high values of overload, the residual stress pattern produced near the crack tip is as reported in Figure 5. The general pattern of residual stresses as measured in the ligament of the CT specimen prepared from a photoelastic material [106] is similar to that shown in Figure 5. Similarly, the residual back face strain value experimentally determined by the back face strain gage

technique [107,108] is compressive as represented in Figure 5. This is further confirmed by the fact that at a given K_{op} value, the magnitude of the residual back face strain increases as crack length increases [107]. Thus, Figure 5 is a fair representation of the contact and the residual stresses in the plane of the crack of a CT specimen.

It has been shown [106] by progressive removal of the plastic wake by machining, that in a photoelastic material, the residual compressive stress originates from the plastic wake and this causes closure. Also, a dislocation model is proposed which agrees with the decrease of such residual stress when the length of the plastic wake was progressively decreased by machining [106]. Such results emphasize the importance of the compressive stresses and the fact that the whole length of the plastic wake plays a role in producing closure.

In addition to the residual stresses originating from closure as discussed above, one must consider the effect of the residual stresses introduced in a material during processing and fabrication such as welding, forging, or extrusion. The fatigue crack growth rate in the specimen prepared from such a material could exhibit acceleration or deceleration of crack growth rates depending upon the pattern of residual stresses present.

One investigator has accounted for the effect of residual stress on da/dN by the modification of the stress intensity factor relationship through suitable formulas [109]. Such a modification changes K_{max} , K_{min} , and R and one can then use suitable empirical relationship to normalize da/dN data. Alternatively, one can account for such effects by considering

the effect the residual stresses have on experimentally determined K_{op} . It has been observed [110] that K_{op} decreases if the residual stress is tensile and K_{op} increases if the residual stress is compressive over the crack faces. Such effects are obviously similar to that produced by the application of compressive load and tensile overloads, respectively.

In view of the above, as well as the point made earlier that closure produces a given pattern of residual stresses, one can expect that the effect of the residual stress on da/dN can be appropriately represented through its effect on K_{op} . In fact, the use of ΔK_{eff} instead of ΔK in the case of a specimen which contains residual stress, has been shown [110] to produce FCGR data which agrees quite well with the FCGR data obtained after the material is stress relieved [110]. This is shown in Figure 32. Unfortunately, such investigations are few.

It has also been noted [110] that residual stresses when present across the thickness with tension at the interior and compression at the surface layers, enhances crack front curvature. This is synonymous with lower K_{op} values at the surface layers and higher values at the interior. Interestingly enough, such results are consistent with the results obtained for a thumbnail shaped surface crack as discussed in Section 4.4.

An examination of the effect the residual stress pattern has on the K_{op} , can help us to examine the validity of the various mechanisms proposed for closure. For as pointed out in Section 2, the residual stress produced by the plasticity induced mechanism is compressive ahead of the crack tip

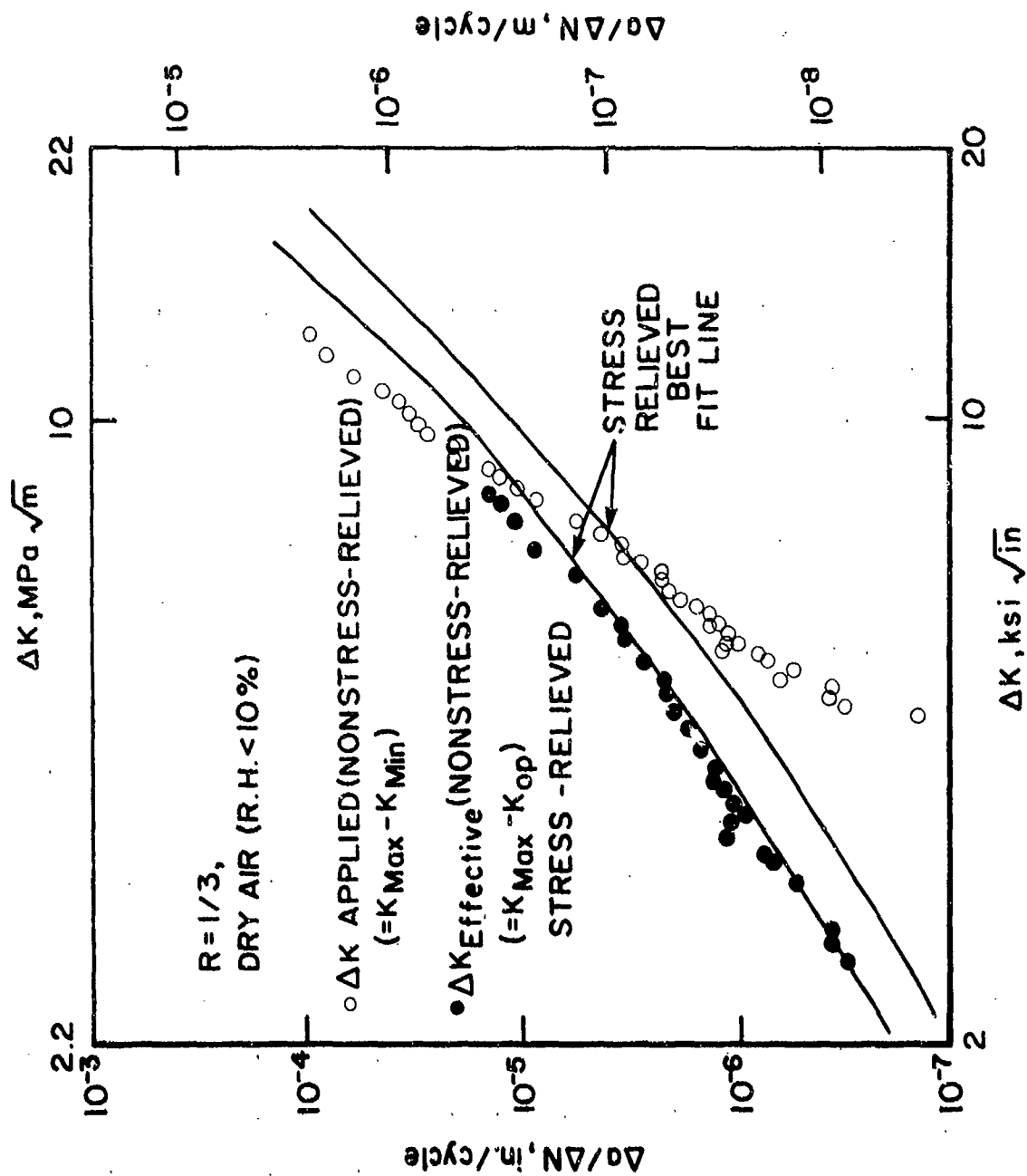


Figure 32. Comparison of da/dN for Non-Stress Relieved and Stress Relieved Materials. The Agreement is Good when ΔK_{eff} is Used for Representing da/dN Data [110].

whereas it is tensile in the case of oxide and asperity induced closure. The asperity and oxide induced closure mechanisms appear inconsistent, when this observation is taken into account with the fact that residual tensile stress decreases K_{op} and thereby increases da/dN .

4.6 ENVIRONMENTAL FACTORS

The effect of the environment on fatigue is very complex and important. It is therefore extensively studied. The environmental effects are examined below in general terms as they concern closure. The effects are different in the near threshold and in the Paris regime.

In the Paris regime, that is, at ΔK values substantially higher than the threshold value, the fatigue crack growth rate in steel is highest in hydrogen sulphide and hydrogen and decreases as the environment is changed successively to moist air, to dry gaseous environment, and to vacuum [23,28, 39,41,111]. A similar trend with regard to the effect of humidity and vacuum environment is also obeyed in the case of aluminum and titanium alloys. These differences have been explained traditionally in terms of hydrogen embrittlement and accordingly, models based on the appropriate anodic or cathodic processes at the crack tip and at the flank of the crack have been proposed. Several mechanisms of hydrogen embrittlement have been advanced to explain the effect of frequency, etc. But the precise mechanism of hydrogen embrittlement is not clearly known. On the other hand, attempts have been made to characterize the observed difference in fatigue crack growth rates in terms of the K_{op} determined in various environments [39]. Unfortunately, such investigations are rather few.

K_{op} of aluminum alloys in the Paris regime, has been determined [39,41] in vacuum, dry oxygen (or nitrogen) and also in air with different percentages of relative humidity. It is observed that K_{op} is highest in vacuum and decreases successively as the environment changes to dry oxygen (or nitrogen), to air with 50% to air with 100%, relative humidity, as shown in Figure 33. Correspondingly, the difference in da/dN is accounted for in terms of closure, since a plot of da/dN versus ΔK_{eff} yields a straight line which is independent of all environments. Contrary to such observations, it has also been reported that in case of titanium alloys, K_{op} does not change even if the environment is changed from vacuum to one atmosphere [4,28]. Thus, the results of attempts to incorporate environmental effects is not conclusive. In fact, it has also been shown that a change from dry to humid environment significantly changes the crack tip strains and crack tip opening displacements in an aluminum alloy [112]. Thus, apart from the K_{op} effects, one should consider local crack tip microplasticity to explain the observed difference in da/dN due to changes in environment.

Regarding the environmental effects in the Paris regime as discussed above, in the threshold and near-threshold regime, the effects are quite different and depend on the R value [13,14,21,22,23]. In the near-threshold regime at low R value, da/dN is highest (and correspondingly, ΔK_{th} is lowest) in all dry environments and is the same for all gases, be it argon or hydrogen. Thus, da/dN in steel decreases as the environment is changed to moist air [13,14,21]. Since hydrogen and argon exhibit identical behaviour, hydrogen embrittlement cannot explain the observed difference [13,14,21]. The more interesting point is that at high R values, dry hydrogen, dry argon,

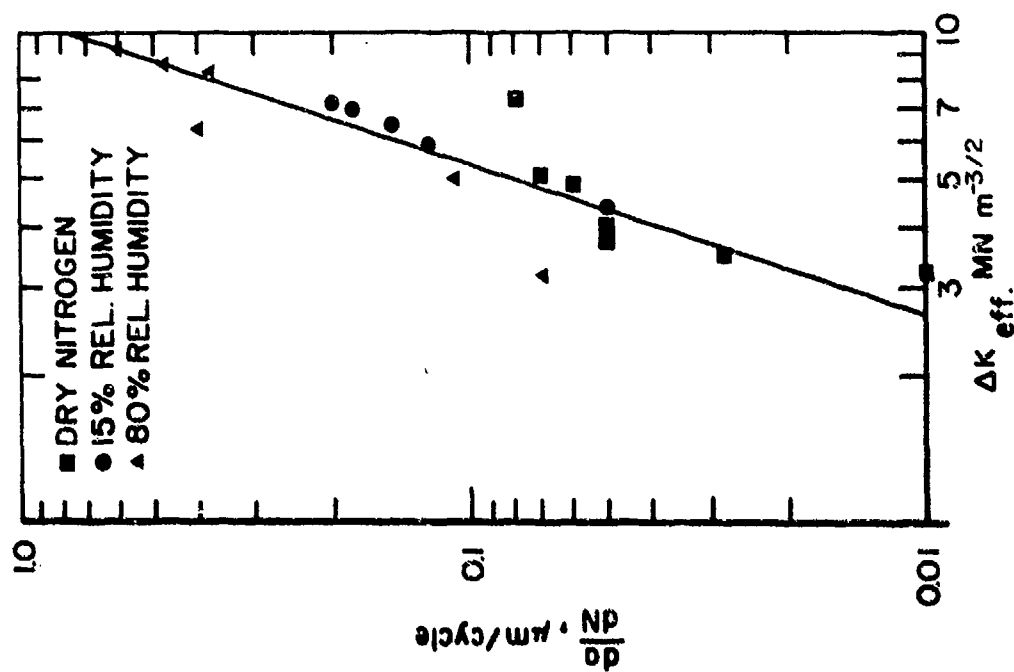
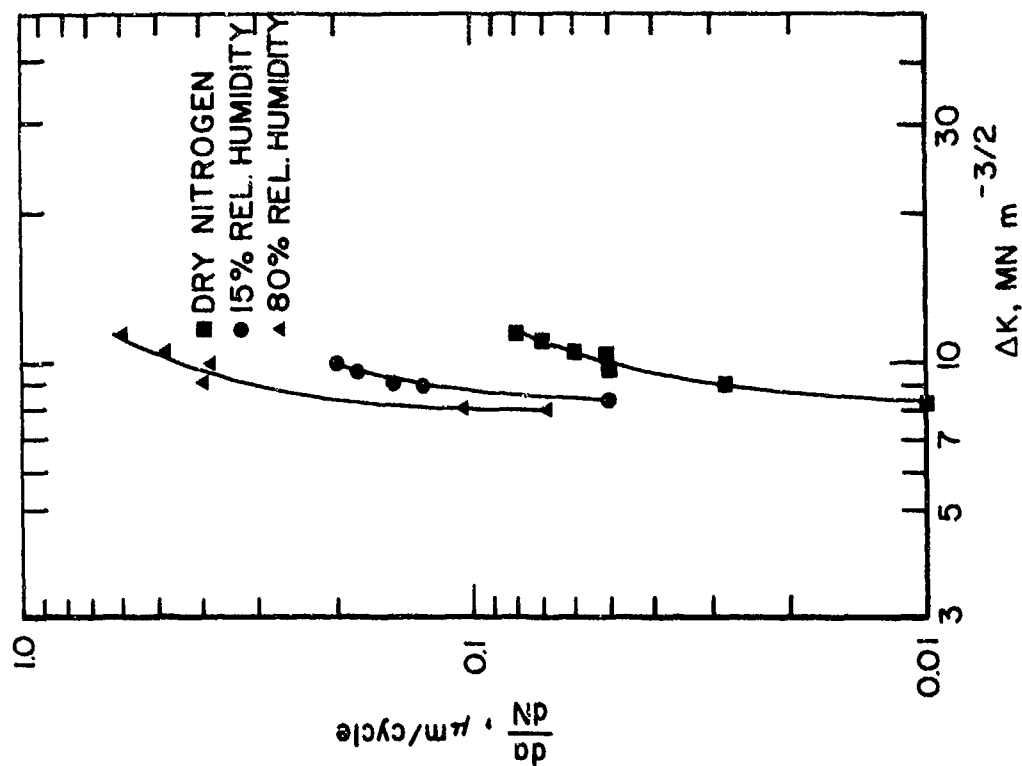


Figure 33. a - Effect of Environment on Crack Propagation Rate in 7075-T651 Al Alloy, 30b
 b - Normalization of the Data Reported in Figure 33a When da/dN is Plotted Against ΔK_{eff} [39].

and moist air all exhibit some da/dN and threshold behaviour. This difference at the high and low R values has been explained through the proposed oxide induced closure mechanism. The limitations of this mechanism have been discussed earlier in Section 2.3. Additionally, there is another important aspect which apparently cannot be explained through this mechanism. For instance, in vacuum, the da/dN is slower than in all other environments, particularly at high R -values [21,22,114], in case of steels and aluminum alloys. Obviously, oxide induced closure cannot explain the observed difference in the da/dN for a vacuum and for a dry hydrogen environment since the difference in the oxidation behaviour in these two environments would be rather small.

The oxide induced closure mechanism has been proposed recently. The mechanism should be verified through K_{op} measurements in the different environments in the threshold regime. In fact, no verification in terms of da/dN versus environmentally modified ΔK_{eff} has been attempted in this regime.

The effect of the environment is much too complex by itself. When one takes closure into account, the observed phenomenon becomes too complex to understand and explain. For a better characterization of the problem, further experimental work is necessary.

4.7 MICROSTRUCTURAL AND FRACTOGRAPHIC FEATURES

In the past, it has been generally contended that microstructure has a small influence on the da/dN in the Paris regime and has a significant

influence on da/dN and ΔK_{th} only in the threshold regime. However, experimental results reported recently show that microstructural features, such as grain size, lamellar spacing, dispersion of phases, solute level, and the inclusion size and shape distribution, can significantly influence da/dN in the Paris regime.

In the Paris regime, the da/dN decreases as the prior austenitic grain size in steel [113,116] or α -grain size or the dispersion of phases in Ti-alloy [117,118] increase or the dispersion of α and α' in dual phase steel [88] changes. In fact, an interesting result on the effect of grain size is $\Delta K_T = 5.5\sigma_Y\sqrt{d}$ where d = prior austenitic grain diameter [113]. Similarly, an increase in interlamellar spacing [115,116] of pearlite in steel increases da/dN and decreases ΔK_{th} . In the threshold regime, microstructural features influence da/dN for all materials. In general, all microstructural features which promote coarse, planar, heterogeneous, and reversible slip with increased slip length decrease da/dN , particularly at low ΔK levels. Conversely, features which promote homogeneous, wavy slip produce increased da/dN .

Fractographic features, in general, originate from the microstructure, and one of the features which decrease da/dN is increased crack branching or crack path deflection producing increased roughness and secondary cracking. The crack deflects since the crack propagates along specific crystallographic planes in the grain and therefore, the larger the grain size, the larger the deflections which in turn produce slower da/dN and higher ΔK_{th} . Such

increased slip planarity could also be produced by changing precipitate morphology [118]. It is contended that K_{op} constitutes the bulk of ΔK_{th} . Thus, the microstructural features which increase ΔK_{th} and decrease da/dN at the threshold regime as discussed above, will correspondingly increase K_{op} .

In fact, K_{op} measured in different Ti-alloys has been shown to relate to the roughness [4]. However, the scales of roughness considered in this investigation are in the range of 200 μm which is three orders larger than the roughness contemplated in the models of roughness induced closure [8,12,60]. As K_{op} increases, the roughness also increases and since such increase has no systematic relationship with yield strengths of the titanium alloys investigated, the plasticity induced mechanism is discounted. However, one should also consider that plasticity depends not only on yield strength, but also on K_{max} . The three titanium alloys which had widely differing ΔK_{th} and therefore, K_{op} in these alloys were determined in different ranges of K_{max} values and, therefore, the three alloys experienced three different loading histories. Thus, K_{op} or roughness could differ even if the σ_y values of these alloys were the same. Thus, the possibility of plasticity induced closure cannot be discounted in these experiments.

Recently, it has been suggested [88] that crack deflection over distances of the order 30-100 μm at angles ranging from 30 to 70° can retard crack growth rate substantially. Such deflection decreases K_I or even the effective K of a branched crack and produces the observed decrease in da/dN . It is shown that a change in microstructure can produce crack deflection

and accordingly cause a decrease in da/dN . Apparently, such a change in microstructure also increases K_{op} . However, according to the author [88], the increased K_{op} can only partly account for the decrease in da/dN ; and part of the decrease in da/dN is accounted for by crack deflection.

Measurement of fractographic features is difficult. For example, a change in striation spacing determined through fractographic observation [77] has been used to identify the closure load. In fact, such confidence in striation spacing measurement is reinforced by a recent investigation where an excellent correspondence between striation spacing and macroscopic crack growth rates was obtained [69]. In fact, these investigators also report a good correlation between striation spacing and ΔK_{eff} ($=K_{max} - K_{op}$) for different R values [69]. However, others report that the observed correspondence between macroscopic growth rate and striation spacing is poor [7,94].

A change in the slope of a da/dN versus ΔK plot often corresponds to a change in micromechanism such as faceted to striated growth or transgranular to intergranular [69]. What is interesting, however, is that a plot of da/dN versus ΔK_{eff} with closure taken into account appears relatively smooth [69]. It is not clear, whether this is the result of K_{op} , appropriately accounting for change of micromechanism or of changed format of data representation.

Microstructural and fractographic features are difficult to quantify and determine. To add to this, the determination of closure has its inherent uncertainties and unanswered questions. Thus, significant phenomenological

study is required before K_{op} can be related to the microstructural and fractographic features. Such studies are important, for they alone can provide the important clues, for instance, to develop materials where K_{op} always equals K_{max} , arresting all fatigue crack growth!

4.8 MATERIAL PROPERTIES

The important properties which may influence K_{op} are young's modulus, uniaxial yield strength, the strain hardening (both monotonic and cyclic), and strain softening (cyclic). It has been observed [125] that K_{op} should be independent of young's modulus. However, this has not been investigated. Similarly, the effect of strain hardening or softening on K_{op} has not been investigated. Since cyclic strain hardening and strain softening has little effect [80] on the pattern of overload retardation - a phenomenon directly related to closure, it is likely that cyclic hardening or softening has only a secondary effect on K_{op} .

In one of the investigations, the effect of σ_y on bulk K_{op} has been studied in a test situation where other factors are identical. The result is reported in Figure 34. It appears that K_{op} decreases as the yield strength increases suggesting obviously that a plasticity induced mechanism is probably operative. One can, of course, argue that the differences in the microstructural features in materials with different yield strengths can produce different fracture surface roughness and, therefore, the corresponding differences in K_{op} [4]. This has been discussed earlier in Section 4.1.

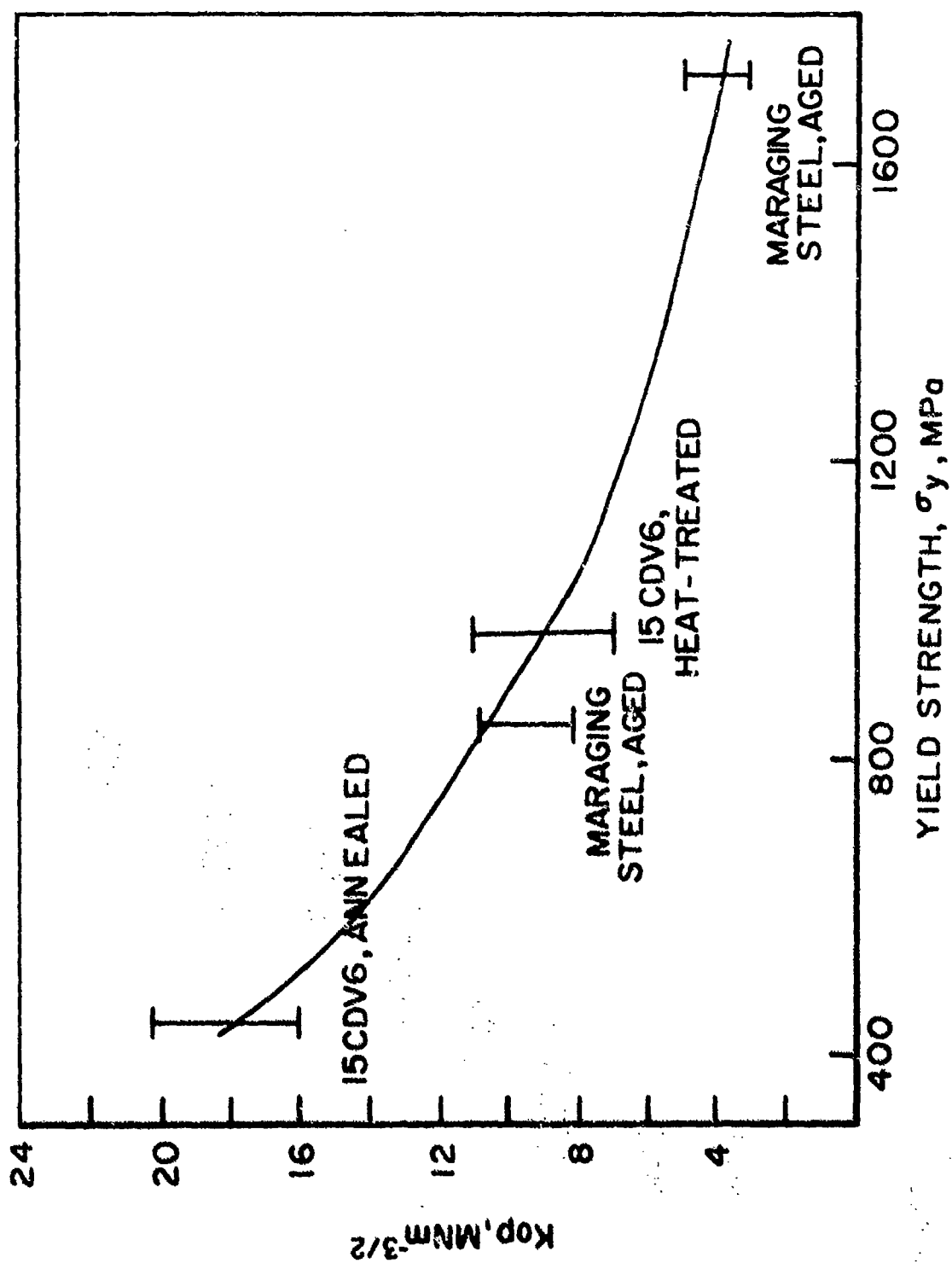


Figure 34. Effect of σ_y on K_{op} in CT Specimens, $B=4$ mm, $W=50$ mm and Varying a/W . Scatter in K_{op} Values Reported is Attributed to Different Pre-cracking History [31,34].

4.9 EFFECT OF SIZE AND GEOMETRY

The effect of size and geometry on K_{op} must be evaluated for reliable life prediction. However, little experimental and only limited numerical work has been carried out for a comprehensive evaluation of the problem.

Size refers to dimensions such as the thickness (dimension along z direction) the crack length and the width (dimensions along x direction) and geometry refers to the shape, in general, and in particular, to the ratio of dimensions along x and y direction, to the loading configuration and also to the nature of the far field stress distribution in the body.

In numerical experiments, Newman [103] has varied the effect of the nature of the far field distribution by considering CCT specimens without a hole but with a crack in one case and with crack emerging from a hole in the other case. With closures calculated numerically and da/dN determined experimentally in both the cases, Newman shows that the difference in closure accounts for the difference in da/dN . Since da/dN in the case of a crack emerging from a hole would be faster, K_{op} , in the case of a specimen with a hole would be lower than K_{op} of the specimen without a hole. However, in order to use such numerical analysis for specimen configurations other than CCT, one requires closed form relationships for K and displacement with a Dugdale plastic zone in the specimen. Unfortunately, such results are not available for all configurations. Besides, such an approach gives results for plane stress or plane strain plasticity only. Since the state of stress

in a precracked body is intermediate, some systematic experimental study would be useful. Experimental investigations of the effect of geometry on K_{op} are scarce. However, there is indirect evidence that K_{op} could depend on the geometry. For instance, the overload retardation behaviour of a CCT specimen is reported to be substantially different from that of CT specimen [82] implying that their K_{op} values of a CCT are higher than that of a CT specimen. And, the fatigue crack growth data when plotted as da/dN versus ΔK often show layering where for a low constraint specimen such as a CCT, da/dN values are higher than that of a CT specimen [120]. Similarly, side-grooving can lower da/dN values. If one takes all these facts into account, it would seem that plots of da/dN versus ΔK_{eff} for CCP and CT specimens may show increased differences and layering. An investigation of the K_{op} value of CT and CCP specimens should be interesting.

Recent investigations [17,121-124,139-147] have shown that the plastic zone, even when it is small, depends systematically on W , a/W , and specimen geometry and that the small scale yielding assumption which has been invoked in the analysis of fatigue and fracture quite freely in the past, should be used with caution. One can thus expect K_{op} to depend on W and a/W to some extent. In fact, even if plasticity were to be independent of W and a/W , and we assume that K_{op} originates from the plastic wake, one can still expect K_{op} to depend on a/W because the wedging action of the plastic wake for instance, in a CT specimen, would have less of an effect at the load-line as the length of the wake increases. It is likely that the increased plasticity at higher a/W probably compensates the decreased effect of a long plastic wake producing negligible effect on closure unless the crack lengths

are much different or the plastic wake is too small. But these speculations require further investigation. The effect of width on K_{op} has not been reported but using similar arguments, one would expect an effect of width on K_{op} . Since plasticity decreases with width [121-124], K_{op} should decrease with increasing W at a given a/W . However, this too is a matter of investigation.

The effect of thickness on K_{op} requires three-dimensional elastic-plastic analysis, for, as pointed out in Section 3, preferential yielding in the surface layer can substantially alter the closure response of a precracked body. The evidences for these are several: progressive removal of surface layers progressively decreases K_{op} [59], overload retardation is less in a thick as compared to a thin specimen [83], the introduction of side grooves dramatically decreases the number of delay cycles [119], machining of surface layers reduces the number of delay cycles [142], and the closure at the interior is less than at the surface [43,65,67]. And even though in most fatigue crack analysis, the crack front is idealized in the manner shown in Figure 6, the actual crack front is very complicated - more complicated than the curved crack front reported in Figure 8. The true nature of three-dimensional crack front is evident from Figure 35 as reported in [63,89]. As a result of such a crack front, some out of plane bending and modes II and III are invariably produced at the crack front in any specimen. To what extent, this has produced the contradictions, anomalies, and the usual scatter observed in fatigue data is hard to say. But, when one takes into account all these observations, the problem of the fatigue crack growth and particularly of the closure, indeed, appears too complex to characterize and formulate. Thus, it seems that the first step in resolution of the problem is to generate FCGR and closure data in experiments where modes II and III are practically negligible.

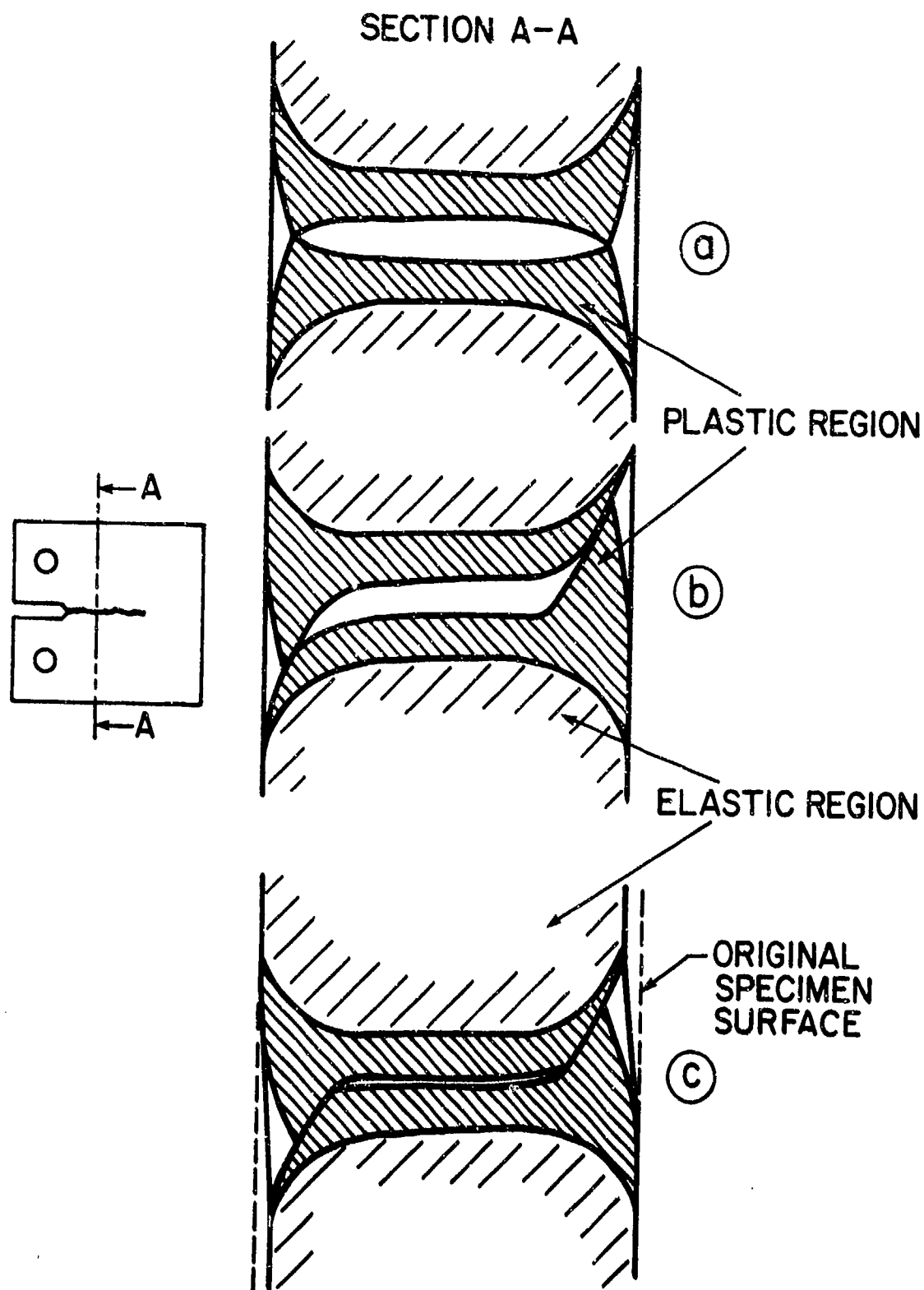
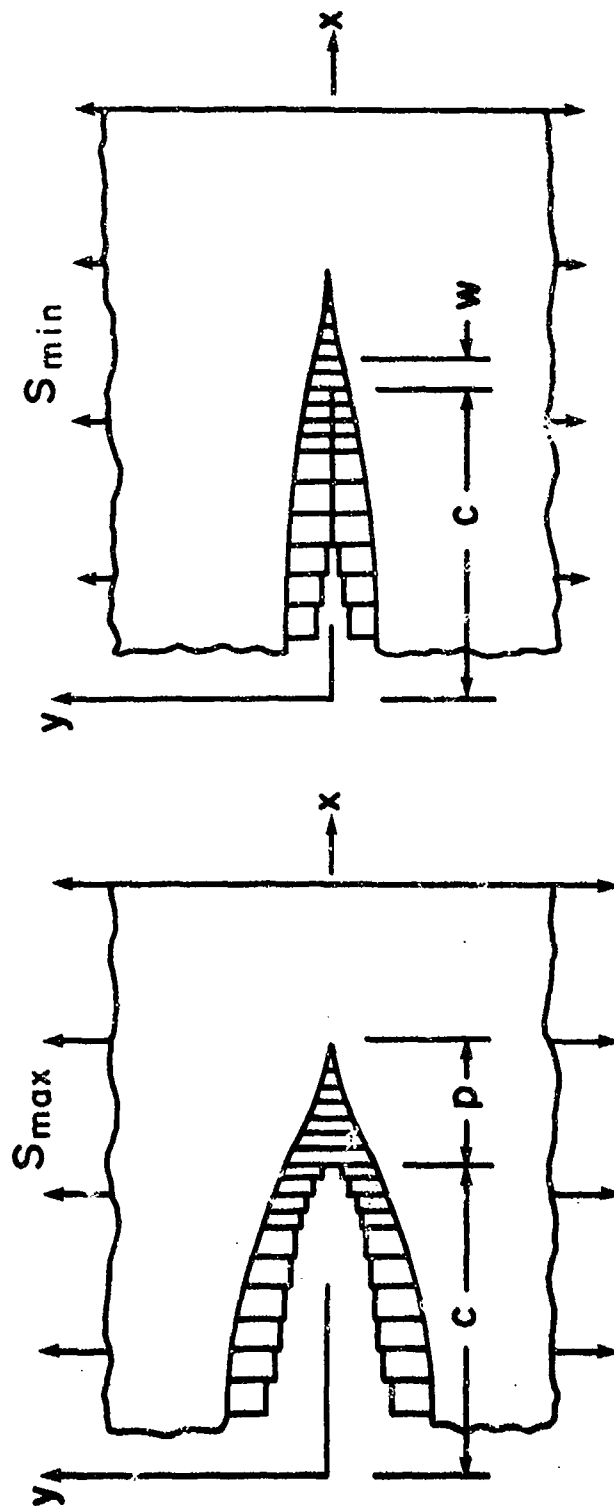
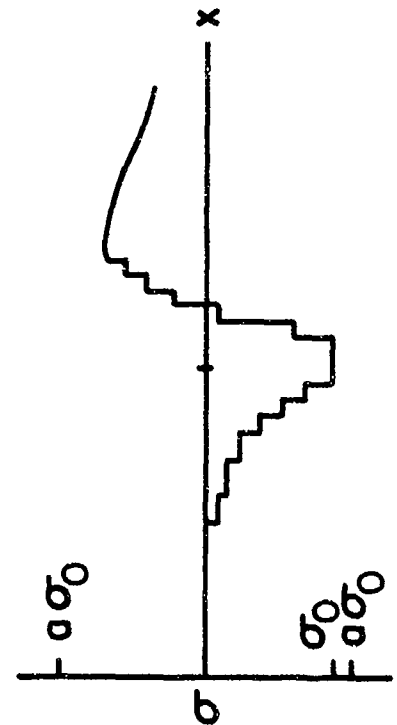


Figure 35. Fracture Surface Profile as Influenced by Specimen Size and Loading (a) Symmetric Profile, (b) Non-Symmetric Profile, and (c) Out of Plane Sliding in Thin Specimens with Non-Symmetric Profile Relaxes Compressive Force [89].



(a) MAXIMUM STRESS



(b) MINIMUM STRESS

The above discussion confirms that closure in practical situations is a three-dimensional problem. And it is interesting that in spite of the complex nature of the problem as discussed above, K_{op} determined from the two-dimensional analysis or from the experiments which are based on two-dimensional considerations can produce such good correlation with da/dN .

4.10 COMMENTS ON THE PHENOMENOLOGICAL STUDY OF CLOSURE

The phenomenological studies concerning closure reveal numerous contradictions, discrepancies, and unexplained facts. However, a few general observations concerning the different aspects of closure as discussed in this section are summarized below.

The basic experimental facts concerning the dependence of K_{op} on K_{max} , K_{min} , and R for a given constant amplitude test situation are not clearly established. Unless this is accomplished, it is difficult to formulate closure phenomena and to interpret the results of closure studies. Most studies make little distinction between 'bulk', 'local', near tip surface, and near tip closure behaviours. One wonders if such distinction is relevant since we do not know which one of these closures really control da/dN . This adds to the general confusion.

In spite of this, the use of ΔK_{eff} instead of ΔK , normalizes da/dN data for wide variations of K_{max} , K_{min} , K , and accounts for the change in the growth rate produced by step overloads, surface crack behaviour, residual stress effects, and the effect of environment in many instances. This is indeed intriguing when one considers (1) the wide divergence that is observed in the results of studies conducted to evaluate the effects of the different

variables, (2) the uncertainties in the determination of K_{op} , and (3) our ignorance as to which K_{op} really controls da/dN . In fact, the nonlinear plots of da/dN versus ΔK in the Paris regime are sometimes curved convex and sometimes concave. If closure were to have a systematic relationship with K_{max} , it is unlikely that use of the closure concept would remove the nonlinearities in all instances.

K_{op} at the interior is less than the K_{op} at the surface of a thumbnail crack. This needs further investigation. The behaviour of short cracks remains unexplained and requires systematic experimental work for its characterization.

A study of the effect of residual stress on K_{op} and da/dN indicates that the residual compressive stresses introduced at the crack tip during closure decrease da/dN . In fact, the introduction of a controlled residual stress pattern and its effect on K_{op} and da/dN can be examined to check the validity of the different mechanisms of closure that have been proposed.

Correlation of microstructural and fractographic features with K_{op} and da/dN is an important area of research, both from the standpoint of developing fatigue resistant materials and in understanding the origin of closure.

The asperity and oxide induced closure mechanisms need to be carefully studied in terms of the residual stress pattern that these mechanisms produce. Such studies can provide a firm physical foundation for a more realistic formulation of the models from which K_{op} can be calculated.

The plasticity induced closure mechanism has some basic discrepancies such as: K_{op} is observed to increase, remain constant, or even decrease with increasing K_{max} in regimes where admittedly, asperity and oxide induced closure is inapplicable. These and other discrepancies probably arise since the history dependence of closure extends over dimensions which are orders of magnitude larger than the plastic zone size. However, if the history dependence is established through experimental work, other questions must be raised about the customary assumptions made in closure and fatigue studies.

Even though the effects of the material properties and the size and geometry on closure are most important, they have not been studied. Careful experimental work needs to be conducted because recent work has shown that the assumption of small scale yielding is inconsistent with experimental observations. In fact, such studies may indicate new directions in the development and application of more reliable and economic life prediction technology.

5. PREDICTION OF CLOSURE

A reliable calculation of closure is key to reliable life prediction. Based on a given mechanism and model of closure, it should be possible to calculate K_{op} in any precracked body of arbitrary size and geometry made from a given material and subjected to a given history of loading. The various mechanisms of closure were discussed in Section 2 and it was pointed out that the asperity and oxide induced mechanisms require further development in order to use them for prediction of closure. In this section, various methods based on the plasticity induced mechanism for the calculation of K_{op} are briefly examined. As pointed out earlier, the residual displacement in the wake and the residual stresses ahead of the crack would modify the state of stress, strain, and displacement at the crack tip. These modifications have to be taken into account to calculate plasticity and closure and also to understand how K_{op} changes ΔK_{eff} and da/dN .

To facilitate subsequent discussion, the methods of the calculation of K_{op} are classified into two broad categories: (1) Finite element based methods, and (2) Analytical procedures not based on finite elements. The analytical procedures give a better physical insight into the closure phenomenon but can be used only for simple geometries. On the other hand, the finite element method can, in principle, be used for complex loading and geometry but the results may depend upon the element mesh chosen. The analytical procedures are discussed at first.

5.1 ANALYTICAL PROCEDURES

Several groups of workers have used analytical procedures to calculate K_{op} . The works of Fuhring and Seeger [125,126], Dill and Saff [127], Budiansky and Hutchinson [128], and Paris and Hermann [32] are discussed very briefly in this section.

Fuhring and Seeger [125] were the first (their work was originally published in German) to use Dugdale's model for the analysis of crack closure which takes into account the stress and displacement variation for every consecutive half-cycle. They examined the details of the residual stress and strain field at the wake of a growing fatigue crack which produce contact stresses and which, in turn, affect the entire state of stress, strain, and displacement in the vicinity of the crack tip. The contact stress calculation is based on the assumption of a trapezoidal distribution of residual displacement along the length of the crack. The contact stresses have a large gradient and this is taken into account in discretization of the crack axis into nodes and line elements. The stresses and displacement are solved from Dugdale's results using an iteration procedure.

The results show that under constant amplitude loading with constant load, K_{op}/K_{max} is almost independent of K_{max} for aspect ratios less than 0.7. The value of U increases with R . The analysis also evaluates the extent of closure and the effect of a reversed cycle ($R < 0$) on closure.

The results obtained by Fuhring and Seeger are for plane stress. Even though the analysis evaluates the effect of aspect ratio and periodic spacing, $2b$, the results apply to a remotely stressed infinite sheet with an array of colinear cracks with length $2a$ and periodic spacing $2b$. The applicability of such results to finite specimens with geometries such as CT or three point bend is yet to be examined.

These workers have used a similar approach to predict crack growth rates under variable amplitude or sequence loading which are presumed to be governed by memory rules [126]. The main trend of the results of Fuhring and Seeger have been verified [84] by displacement measurements in the vicinity of the crack tip using a grid technique.

Dill and Saff [127] have used a simple contact stress model of closure. The approach is similar to the one used by Fuhring and Seeger [125]. They evaluated the stress intensity caused by crack surface contact which, in turn, produces an interference between the mating crack surfaces. The interference is determined from an analysis of the elastic displacement during loading, elastic displacement during unloading, and the permanent deformation left in the wake of a growing crack. A Dugdale model is used to make an integral equation formulation of the closure condition. The interference is treated as a wedge acting behind the crack tip and the contact stresses created by this wedge are calculated by idealizing the wedge as 25 constant stress elements which experience only compressive contact stress which have a maximum value of σ_y . An influence coefficient matrix is developed for the stress-displacement relationship between elements using a weight function

approach. The stresses give contact stress intensity at the minimum load and therefore, the ΔK_{eff} . The results of the model show good agreement with Elber's experimental results as given in Equation (15). The predicted crack growth from this contact stress model compares quite well with the experimentally determined crack growth rates obtained under spectrum loading. It was pointed out in Section 4.1 that Equation (15) does not agree with experimental results of several other investigators. To this extent, the general applicability of the model is doubtful.

The work by Budianisky and Hutchinson [128] calculates crack opening load, crack closing load, and residual plastic stretch at the crack tip by a complex function method under the assumption of small scale yielding according to the ideally-plastic Dugdale-Barenblatt model. The results are reported for a range of load ratios. It is observed that in contrast to the stationary crack which suffers reverse plastic flow over a distance which is $\frac{1}{2}$ the monotonic plastic zone size, the corresponding reverse plastic zone size for a growing fatigue crack is 1/10 of the monotonic plastic zone. The K_{clo}/K_{max} is .48 and $K_{op}/K_{max} = .56$. The analysis provides justification for the adoption of an effective stress intensity range to represent fatigue crack growth rate. However, the analysis is appropriate only for plane stress; on the other hand, the plane strain condition applies over most of the crack tip region. Thus, even though the results given some valuable insight into closure and guidelines for future work, the results reported here are not expected to agree with experiments.

Paris and Hermann [32] have reported an approximate relationship of K_{op} which incorporates some of the features of the closure phenomenon. Using the results of this relationship, they predict the variation of K_{op}/K_{max} following overload which agree very well with the experimentally determined variation of upper closure point. The relationship indicates that K_{op}/K_{max} should be independent of R . Since the nature of this relationship is quadratic, Paris and Hermann have hinted that the transition in K_{op}/K_{max} experimentally observed at $a/W \sim 0.55$ to 0.6 during a constant amplitude test is consistent with the two K_{op}/K_{max} values that would be obtained from such a quadratic equation. However, whether the transition is a phenomenon inherent to closure or is merely a result of the history dependence of K_{op} , is a matter of experimental investigation.

5.2 FINITE ELEMENT BASED METHOD

Finite element based methods of the calculation of K_{op} of three different groups of workers are discussed below: Ogura, Ohji, and Ohkibu [129,130], Nakagaki and Atluri [131], and Newman and his coworkers [132-137].

Ohji, Ogura, and Ohkubo [129] and Ogura and Ohji [130] have used incremental finite element elastic-plastic analysis with a fine constant strain triangle mesh. Results were obtained for a double edged notched specimen which explained the experimentally observed non-propagating fatigue cracks ahead of a notch using the concept of closure. These workers have also investigated the effect of overload on closure and residual stresses. It was observed that the closure stress at first decreases and then increases

to a maximum and then drops again. Such a variation of closure stress obviously can explain the observed variation of crack growth rate following retardation as discussed in Section 4.2. Overload produces residual compressive stresses and the region of such stresses increases as the overload increases. They also show that compressive load just following an overload decreases K_{op} which corresponds to the usually observed increase in the experimental da/dN in such cases. The analysis was done for a double edge notched specimen under plane stress condition. It is not clear as to how the contact stresses generated in the plastic wake were taken into account in their analysis.

Nakagaki and Atluri [131] have used circular-sector shaped hybrid elements centered at the crack tip with the HRR stress and strain singularities embedded in the special elements near the crack tip. The procedure is computationally inexpensive due to (1) the use of such elements which permit adoption of rather coarse mesh and (2) the use of a procedure wherein the elastic part of the structure is isolated and its stiffness remains unchanged during loading. In this analysis, the stresses at opening and closure are determined for a CCP specimen and they agree quite well with each other. ΔK_{eff} is calculated from σ_{cl} obtained for constant amplitude and other sequence loadings. In all cases, ΔK_{eff} is observed to follow a pattern which is commensurate with the observed patterns of da/dN during such load sequencing. The crack surface deformation profiles are different for different load sequencing and this controls the resultant residual stresses and possibly the growth retardation. Obviously, the approach has computational advantages. It also takes into account blunting, which is experimentally observed during overloading. However, it is not clear as to how the contact stresses in the plastic wake are taken into account in their analysis.

The most extensive and comprehensive finite element based analysis of closure has been done by Newman and coworkers [132-137]. First, to investigate closure using finite elements [132], Newman [136,137] has developed and verified a crack closure model that simulates plane stress and plane strain conditions by using a 'constraint factor'. The analysis is based on a Dugdale model which was modified to leave plastically deformed material in the wake of the advancing crack.

A schematic of the crack surface displacement reported in Figure 36 shows a plastic region of length ρ and a residual plastic deformation along the crack surfaces. These regions are composed of rigid perfectly plastic (constant stress) bar elements with a flow stress σ_0 . The bar elements are broken in the region of residual plastic deformation and carry compressive load only. The physical crack is of half length c which on unloading, produces a reverse plastic zone, w . The governing equations for the crack closure model were set up using the stress intensity factor and crack surface displacements for a CCP specimen and then solved for the contact stresses and the stresses in the plastic zone. The opening stress, S_0 , was calculated by equating the stress intensity factor due to an applied stress increment ($S_0 - S_{min}$) to the stress intensity factor due to the contact stresses. The calculations were made both for plane stress and plane strain conditions, that is with varying constraint factor. A constraint factor of 2.3 was chosen for further calculation of life prediction since it gave a good correlation under constant amplitude loading.

The model gives results wherein K_{op}/K_{max} is in the range of .25 to .35 and is independent of crack length. The plane stress values K_{op}/K_{max} were higher, that is in the neighbourhood of 0.5 to 0.6. With increasing stress level, the plane stress K_{op}/K_{max} decreased.

The model was used to correlate crack growth rates under constant amplitude loading and to predict crack growth under aircraft spectrum loading on 2219-T851 aluminum alloy plate material. The predicted crack growth lines agreed well with experimental data obtained from 80 crack growth tests subjected to various load histories. The ratio of predicted to experimental lives ranged from 0.5 to 1.8.

Even though the choice of a constraint factor of 2.3 has no fundamental basis, the predictive capability of the model is quite encouraging. The applicability of this model to other geometries and size needs further investigation.

5.3 COMMENTS ON PREDICTION OF CLOSURE

It is obvious from the discussion above that analysis of closure is not sufficiently developed, to enable prediction of closure in a precracked body of arbitrary size and geometry. Since the plasticity in the surface layers plays an important role in determining fatigue crack growth following overload, the problem is obviously three-dimensional. Thus, even though two-dimensional analysis of various sizes and geometry would help us to achieve a better understanding and characterization of closure, the development

of a satisfactory methodology of prediction of closure would probably await the development of three-dimensional elastic-plastic analysis of precracked body. However, it should be emphasized that a systematic experimental study can produce a better comprehension of the problem and this can eventually help us to simplify the three-dimensional problem to something which is manageable.

6. CONCLUDING REMARKS

1. The asperity and oxide induced closure mechanisms as proposed produce residual tensile stresses near the crack tip whereas the crack tip residual stresses as experimentally observed and as considered in plasticity induced mechanism are compressive. These different residual stress patterns cannot give the same da/dN even though the resultant ΔK 's may be equal. This contradiction can be resolved if the models based on asperity and oxide induced closure mechanisms are reformulated to produce compressive stresses over the whole wake of the crack. The asperity and oxide induced closure mechanisms require further experimental work and development before they can be used for the analysis and prediction of closure.

2. One should distinguish between bulk, near tip surface, near tip interior, and possibly local closure behaviours during the experimental determination of closure. It is necessary to ascertain which of these closures actually controls da/dN in different experimental situations.

3. Crack mouth opening displacement gage, back face strain gage, and Elber clip gage are the most widely used for the experimental determination of bulk K_{op} . The use of the offset procedure either through the use of a differential amplifier or a microprocessor can increase the magnification and sensitivity of closure determination very significantly. However, the advantages gained from such a procedure cannot be realized unless there is a corresponding improvement in minimizing friction, misalignment, and out of

plane bending during loading of the specimen and in the measurement of displacement. In addition, the procedure for identification of the closure load from the $P-\Delta V$ plots needs to be standardized. This may help us to identify the difference between bulk and local K_{op} wherever such a difference exists.

4. The more attractive and reliable methods for the determination of near tip surface closure are the interferometric displacement gage and the replication followed by measurement with a scanning electron microscope.

5. The push rod gage technique appears to be an interesting method of determination of near tip closure at the interior. However, the most certain method of ascertaining the difference in the closure at the interior and surface is to determine closure by offset procedure after progressive removal of the surface layers by machining. An analysis of the closure behaviours so determined on specimens of different initial thickness can provide important insight into the role and origin of closure. Similar investigation of the variation of K_{op} with progressive machining of the plastic wake along the crack plane can help us to distinguish between the different closures and the roles they play in decreasing da/dN .

6. The use of terms such as plane stress and plane strain is confusing since most experimental situations correspond to a state of stress which is intermediate. Besides, the experimental conditions of closure studies which correspond to these two extreme behaviours need to be clearly defined and established.

7. In order to understand and characterize closure, it is necessary to study and report the extent of closure and the residual displacement due to closure in addition to the K_{op} values usually reported in most investigations.

8. The basic experimental facts concerning the dependence of K_{op} on K_{max} , K_{min} , and R are not clearly established. Besides, there are several contradictions and discrepancies. Even then, the use of ΔK_{eff} instead of ΔK accounts for the change in growth rate produced not only by wide variations of K_{max} , K_{min} , and R , but also by the other factors such as step overload, surface crack behaviour, residual stress effects, and the effect of environment. To what extent a log-log plot with a permissible scatter band of two conceals any discrepancies that would have been otherwise observed is hard to say.

9. Residual compressive stresses increase K_{op} and decrease da/dN while the effect of residual tensile stress is the opposite. This should be taken into account in formulating any mechanism of closure.

10. Correlation of microstructural and fractographic features with K_{op} and da/dN is an important area of research both from the standpoint of developing fatigue resistant materials and in understanding the origin of closure.

11. The plasticity induced closure mechanism has some basic discrepancies such as: K_{op} is observed to increase, remain constant, or even decrease with increasing K_{max} in regimes where asperity and oxide closures, as postulated, are inapplicable. These and other discrepancies probably arise since, in most experiments, the effect of the history dependence of closure which could extend over dimensions that are orders of magnitude larger than the plastic zone size is ignored.

12. Systematic experimental investigation is required to evaluate the effect of material properties, size, and geometry on closure. Machining of surface layers after overload application or sidegrooving increases post overload crack growth rates very significantly. Thus, the surface layer and thickness influence K_{op} . Similarly, recent investigations show that plastic zone can depend on W and a/W . These results underline the importance of such an investigation.

13. Analysis of closure is not sufficiently developed to predict closure in a precracked body of arbitrary size and geometry. Satisfactory prediction of the real world problem requires three-dimensional elastic-plastic analysis. However, two-dimensional elastic-plastic analysis and systematic experimental work can produce a better comprehension of the problem and eventually help us to simplify the real world problem to something which is manageable.

REFERENCES

1. P. C. Paris, "Twenty Years of Reflections on Questions Concerning Fatigue Crack Growth, Part I: Historical Observations and Perspectives, Fatigue Threshold," EMAS Publication Ltd, Warley, U.K., pp. 1-10, (1981).
2. J. Schijve, Four Lectures on Fatigue Crack Growth, Engineering Fracture Mechanics, 11, pp. 167-221, (1979).
3. N. A. Fleck, "The Use of Compliance and Electrical Resistance Techniques to Characterize Fatigue Crack Closure," CUED/MATS/TR.89, Jan. (1982), Engineering Department, Cambridge University.
4. J. E. Allison, "The Influence of Slip Character and Microstructure on Fatigue Crack Growth in Alpha and Alpha & Beta Titanium Alloys," Ph.D. Thesis, Carnegie-Mellon University, October (1982).
5. W. Elber, "Fatigue Crack Closure Under Cyclic Tension," Engineering Fracture Mechanics, 2, pp. 37-45, (1970).
6. W. Elber, "Significance of Fatigue Crack Closure, Damage Tolerance in Aircraft Structures," ASTM STP 486, pp. 230-242, (1971).
7. N. Walker and C. J. Beevers, "A Fatigue Crack Closure Mechanism In Titanium," Fatigue of Engineering Materials and Structure, 1, pp. 135-148, (1979).
8. C. J. Beevers, R. L. Carlson, K. Bell, and E. A. Starke, "A Model for Fatigue Crack Closure," Accepted for publication in Engineering Fracture Mechanics.
9. C. J. Beevers, K. Bell, and R. L. Carlson, "Fatigue Crack Closure and the Fatigue Threshold."
10. K. Minakawa and A. J. McEvily, "On Crack Closure in Near-Threshold Region," Scripta Metallurgica, Vol. 15, pp. 633-636, (1981).
11. R. O. Ritchie and S. Suresh, "Some Consideration on Fatigue Crack Closure Induced by Fracture Surface Morphology," Metallurgical Transactions 13A, pp. 937-940, (1982).
12. S. Suresh and R. O. Ritchie, "A Geometric Model for Fatigue Crack Closure Induced by Fracture Surface Morphology," Metallurgical Transactions, 13A, pp. 1627-1631, (1982).
13. R. O. Ritchie, S. Suresh, and C. M. Moss, "Near-Threshold Fatigue Crack Growth in 2 1/2 Cr-Mo Pressure Vessel Steel in Air and Hydrogen," Journal of Engineering and Materials Technology, Transactions ASME, Series H, 102, pp. 293-299, (1980).

14. S. Suresh, G. F. Zamiski, and R. O. Ritchie, "Oxidation and Crack Closure. An Explanation for Near Threshold Corrosion Fatigue Crack Growth Behaviour," Metallurgical Transaction, 12A, pp. 1435-1443, (1981).
15. B. N. Leis, M. F. Kanninen, A. T. Hopper, J. Ahmad, and D. Broek, "A Critical Review of Short Crack Problem in Fatigue," AFWAL-TR-83-4019, AFWAL Materials Laboratory, WPAFB, Ohio, January (1983).
16. P. C. Paris and F. Erdogan, "A Critical Analysis of Crack Propagation Laws," Journal of Basic Engineering, Transaction ASME, 85, pp. 528-534, (1963).
17. S. Banerjee, "Influence of Specimen Size and Configuration on the Plastic Zone Size, Toughness, and Crack Growth," Engineering Fracture Mechanics, 15 (3-4), pp. 343-390, (1981).
18. K. Minakawa and A. J. McEvily, "On Near-Threshold Fatigue Crack Growth in Steels and Aluminum Alloys," Fatigue Threshold, Vol. 1, J. Backlund, A. F. Blom, and C. J. Beevers, EMAS Publication, Westerley, U.K., pp. 373-390, (1981).
19. S. Suresh, "Micromechanism of Fatigue Crack Growth Retardation Following Overloads," Engineering Fracture Mechanics, 18 (3), pp. 577-593, (1983).
20. P. C. Paris, R. J. Bucci, E. T. Wessel, W. G. Clark, and T. R. Mager, "Extensive Study of Low Fatigue Crack Growth Rates in A533 and A508 Steels," Stress Analysis and Crack Growth, ASTM STP 513, pp. 141-176, (1972).
21. A. T. Stewart, "The Influence of Environment and Stress Ratio on Fatigue Crack Growth at Near Threshold Stress Intensities in Low Alloy Steels," Engineering Fracture Mechanics, 13, pp. 463-478, (1980).
22. A. K. Vasudevan and S. Suresh, "Influence of Corrosion Deposits on Near-Threshold Fatigue Crack Growth Behaviour in 2XXX and 7XXX Series Aluminum Alloys," Metallurgical Transactions, 13A, pp. 2271-2280, (1982).
23. P. K. Liaw, S. J. Hudak, and J. Keith Donald, "Influence of Gaseous Environments on Rates of Near Threshold Fatigue Crack Propagation in NiCrMoV Steel," Metallurgical Transaction, 13A, pp. 1633-1645, (1982).
24. C. Robin, S. Dominiak, and G. Pluvinaige, "Variation of Crack Opening-Load Diagram with Fatigue Crack Growth Rate," Materials Science and Engineering, 29, pp. 145-150, (1977).
25. R. D. Brown and J. Weertman, "Effects of Tensile Overloads on Crack Closure and Crack Propagation Rates in 7050 Aluminum," Engineering Fracture Mechanics, 10, pp. 867-878, (1978).

26. Y. Nakai, K. Tanaka, and T. Nakanishi, "The Effects of Stress Ratio and Grain Size on Near-Threshold FCG in Low-Carbon Steel," *Engineering Fracture Mechanics*, 15 (3-4), pp. 291-302, (1981).
27. M. W. Mahoney and N. E. Paton, "Closure: An Explanation for Fatigue Crack Growth Rate Acceleration/Retardation Due to Overloads in Austenetic Stainless Steels," *Fracture 1977*, ICF-4, 2, Waterloo University Press, Waterloo, Canada, pp. 1081-1089, (1977).
28. V. Bachmann and D. Munz, "Fatigue Crack Evaluation with the Potential Method," *Engineering Fracture Mechanics*, 11, pp. 61-71, (1979).
29. R. J. Asaro, L. Hermann, and J. M. Baik, "Transitions in Fatigue Crack Closure in 2048 Aluminum - Communication," *Metallurgical Transactions*, 12A, pp. 1133-1135, (1981).
30. P. E. Irving, J. L. Robinson, and C. J. Beevers, "A Study of the Effects of Mechanical and Environmental Variables on Fatigue Crack Closure," *Engineering Fracture Mechanics*, 7, pp. 619-630, (1975).
31. R. Srikanth, "Plastic Energy Dissipation and Crack Closure Studies in Fatigue," M-Tech Dissertation, Indian Institute of Technology, Bombay, India, (1983).
32. P. C. Paris and L. Hermann, "Twenty Years of Reflection on Questions Involving Fatigue Crack Growth, Part II: Some Observations of Crack Closure," *Fatigue Threshold*, EMAS Publications, Warely, U.K., pp. 11-32, (1981).
33. R. A. Schimdt and P. C. Paris, "Threshold for Fatigue Crack Propagation and the Effects of Load Ratio and Frequency," *ASTM STP 536*, pp. 79-94, (1973).
34. M. Ghate, "Crack Closure Measurements in Fatigue," B. Tech Project Report, Indian Institute of Technology, Bombay, India, (1983).
35. S. Kawa, "The Effect of Stress Ratio on FCG in a 3% NaCl Solution," *Engineering Fracture Mechanics*, 16, 6, pp. 857-870, (1982).
36. D. Gan and J. Weertman, "Crack Closure and Crack Propagation Rates in 7050 Al," *Engineering Fracture Mechanics*, 15 (1-2), pp. 87-106, (1981).
37. W. D. Dover and F. E. W. Charlesworth, "The Use of the Plastic Crack Tip Opening Displacement to Correlate Fatigue Crack Growth Data for a Structural Steel," *Advances in Fracture Research*, ICF-5, 2, D. Francois ed., Pergamon Press, pp. 933-941, (1981).
38. O. Buck, C. L. Ho, and H. L. Marcus, "Plasticity Effects in Crack Propagation," *Engineering Fracture Mechanics*, 5, pp. 23-34, (1973).

39. O. Buck, J. Frandsen, and H. L. Marcus, "Crack Tip Plasticity and Environmental Crack Propagation," *Engineering Fracture Mechanics*, 7, pp. 167-171, (1975).
40. J. D. Frandsen, R. V. Inman, and O. Buck, "A Comparison of Acoustic and Strain Gauge Techniques for Crack Closure," *International Journal of Fracture*, 11, pp. 345-348, (1975).
41. D. S. Mahulikar and H. L. Marcus, "Fatigue Crack Closure and Residual Displacement Results in Al Alloys," *Engineering Fracture Mechanics*, 3, pp. 257-264, (1981).
42. M. D. Halliday, "Low Rates of Fatigue Crack Growth in Beta Heat Treated Titanium Alloy," *Advances in Fracture Research*, ICF-5, D. Fracais ed., Pergamon Press, pp. 953-961, (1981).
43. N. A. Fleck and R. A. Smith, "Crack Closure - Is it Just a Surface Phenomenon?," *International Journal of Fatigue*, pp. 157-160, July (1982).
44. T. T. Shih and R. P. Wei, "A Study of Crack Closure in Fatigue," *Engineering Fracture Mechanics*, 6, pp. 19-32, (1974).
45. K. D. Unangst, T. T. Shih, and R. P. Wei, "Crack Closure in 2219-T851 Aluminum Alloy," *Engineering Fracture Mechanics*, 9, pp. 725-734, (1977).
46. V. Bachman and D. Munz, "Crack Closure in Fatigue Crack Propagation," *Fatigue Testing and Design*, Society of Environmental Engineers, 2, pp. 351-352, (1976).
47. R. Sunder and P. K. Dash, "Measurement of Fatigue Crack Closure Through Electron Microscopy," *International Journal of Fatigue*, 4, pp. 97-105, (1982).
48. J. K. Masuva and J. C. Radon, "Fatigue Crack Growth at Low Stress Intensities," *Proceedings of Fatigue*, 81, U.K., pp. 106-116, March (1981).
49. W. N. Sharpe, Jr., "Interferometric Surface Strain Measurement," *International Journal of Non-Destructive Testing*, 3, pp. 57-76, (1971).
50. D. E. Macha, W. N. Sharpe, Jr., and A. F. Grandt, Jr., "A Laser Interferometry Method for Experimental Stress Intensity Factor Calibration," *Cracks and Fracture*, ASTM STP 601, pp. 490-505, (1976).
51. W. N. Sharpe, Jr., "A Minicomputer-Controlled Laser-Interferometric Technique for Crack Tip Opening Displacement," *Acta Imeko*, pp. 499-506, (1979).
52. D. E. Macha, D. M. Corbly, and J. W. Jones, "On the Variation of Fatigue-Crack-Opening Load with Measurement Location," *Experimental Mechanics*, 19 (6), pp. 207-213, (1979).

53. J. W. Jones, "The Interferometric Measurement of Near Crack Tip Displacement in a Nickel Base Superalloy at Ambient and Elevated Temperatures," AFWAL Materials Laboratory, Technical Report, AFML-TR-78-159, WPAFB, Ohio, March (1979).
54. J. W. Jones, D. E. Macha, and D. M. Corbly, "Observations on Fatigue Crack Opening Load Determination," International Journal of Fracture, 14, pp. R25-R30. (1978).
55. J. Lankford and D. L. Davidson, "The Effects of Overloads Upon Fatigue Crack Tip Opening Displacement and Crack Tip Opening/Closing Loads in Aluminum Alloys," Advances in Fracture Research, ICF-5, 2, D. Fracais Ed., Pergamon Press, pp. 899-906, (1981).
56. H. Sehitoglu, "Characterization of Crack Closure," Paper Presented at 16th ASTM Symposium on Fracture Mechanics, Battelle Columbus Laboratories, Columbus, Ohio, 15-17 August (1983).
57. H. Nisitani and M. Kage, "Observation of Crack Closure Phenomenon at the Tip of a Fatigue Crack by Electron Microscopy," Fracture 1977, 2, ICF-4, Waterloo, Canada, 19-24 June (1977).
58. F. J. Pitoniak, A. F. Grandt, L. T. Montulli, and P. F. Packman, "Fatigue Crack Retardation and Closure in Polymethylmethacrylate," Engineering Fracture Mechanics.
59. T. C. Lindley and C. E. Richards, "The Relevance of Crack Closure to Fatigue Crack Propagation," Materials Science and Engineering, 14, pp. 281-293, (1974).
60. I. C. Mayes and T. J. Baker, "An Understanding of Fatigue Threshold Through the Influence of Non-Metallic Inclusions in Steel," Fatigue of Engineering Materials and Structures, 4 (1), pp. 79-96, (1981).
61. M. D. Halliday and C. J. Beevers, "Some Aspects of Fatigue Crack Closure in Two Contrasting Aluminum Alloys," JTEVA, 9 (4), pp. 195-201.
62. W. J. D. Shaw and I. LeMay, "Crack Closure During Fatigue Crack Propagation," Fracture Mechanics, ASTM STP 677, pp. 233-246, (1979).
63. G. Marci, "Effect of Active Plastic Zone on Fatigue Crack Growth Rates," Fracture Mechanics, ASTM STP 677, pp. 168-186, (1979).
64. C. Q. Bowles, "An Experimental Technique for the Vacuum Infiltrating of Cracks with Plastic and Subsequent Study in the SEM," Technical Report LR-249, Delft University of Technology, Department of Aeronautic Engineering, June (1977).
65. N. A. Fleck, I. F. C. Smith, and R. A. Smith, "Closure Behaviour of Surface Cracks," Fatigue of Engineering Materials and Structures, 6 (3), pp. 325-239, (1983).

66. J. A. Vazquez, A. Morrore, and J. C. Gasco, "A Comparative Experimental Study on Fatigue Crack Closure Behaviour Under Cyclic Loading for Steels and Al Alloys," ASTM STP 677, pp. 187-197, (1979).
67. M. Jolles, "Constraint Effects on the Prediction of Fatigue Life Surface Flaws," Journal of Engineering Materials and Technology, 105, pp. 215-218, (1983).
68. R. J. Stofanak, R. W. Hertzberg, G. Miller, R. Jaccard, and K. Donald, "On the Cyclic Behaviour of Cast and Extruded Aluminum Alloys, Part A: Fatigue Crack Propagation," Engineering Fracture Mechanics, 17 (6), pp. 541-554, (1983).
69. R. J. Stofanak, R. W. Hertzberg, J. Leupp, and R. Jaccard, "On the Cyclic Behaviour of Cast and Extruded Aluminum Alloys, Part B: Fractography," Engineering Fracture Mechanics, 17 (6), pp. 541-544, (1983).
70. M. Katchner and M. Kaplan, "Effect of R-Factor and Crack Closure on Fatigue Crack Growth Rate for Aluminum and Titanium Alloy," Fracture Toughness and Slow Stable Cracking, ASTM STP 559, pp. 264-282, (1974).
71. K. Minakawa, Y. Matsuo, and A. J. McEvily, "The Influence of a Duplex Microstructure in Steels on FCG in Near-Threshold Region," Metallurgical Transactions, 13A, pp. 439-445, (1982).
72. J. Tirosh and A. Ludelski, "Note on Residual Stresses Induced by Fatigue Cracking," Engineering Fracture Mechanics, 13, pp. 453-461, (1980).
73. S. Chand and S. B. L. Garg, "Crack Closure Studies Under Constant Amplitude Loading," Engineering Fracture Mechanics, 18 (2), pp. 333-347, (1983).
74. N. J. Adams, "Fatigue Crack Closure at Positive Stresses, Engineering Fracture Mechanics, 4, pp. 543-554, (1972).
75. Y. F. Cheng and H. Brunner, "Photoelastic Research in Progress on Fatigue Crack Closure," International Journal of Fracture, 6, pp. 431-434, (1970).
76. J. C. Radon, "Fatigue Crack Growth in the Threshold Region," Fatigue Thresholds, Vol. 1, Ed. J. Backlund, A. Blom, and C. J. Beevers, EMAS Publication, U.K., (1981).
77. R. M. Pelloux, M. Farall, and W. M. McGee, "Assessment of Crack Tip Closure in an Aluminum Alloy by Electronfractography," Fatigue of Engineering Materials and Structures, 1, pp. 21-35, (1979).

78. R. G. Foreman, V. E. Kearney, and R. M. Engle, "Numerical Analysis of Crack Propagation in Cyclically-Loaded Structures," *Journal of Basic Engineering*, Transaction ASME, D, 89, pp. 459-464, (1967).
79. E. K. Walker, "The Effect of Stress Ratio During Crack Propagation and Fatigue for 2024-T3 and 7075-T6 Aluminum," *Effects of Environment and Complex Load History on Fatigue Life*, ASTM STP 462, pp. 1-14, (1970).
80. W. J. Mills, R. W. Hertzberg, and R. Roberts, "Load Interaction Effects on Fatigue Crack Growth in A514F Steel Alloy," *Cyclic Stress-Strain and Plastic Deformation Aspect of Fatigue Crack Growth*, ASTM STP 637, pp. 192-208, (1977).
81. S. Matsuoka and K. Tanaka, "Delayed Retardation Phenomenon of Fatigue Crack Growth Resulting From a Single Application of Overload," *Engineering Fracture Mechanics*, 10, pp. 515-525, (1973).
82. K. Tanaka, S. Matsuoka, V. Schimdt, and M. Kuna, "Influence of Specimen Geometry on Delayed Retardation Phenomenon of Fatigue Crack Growth in HY80 Steel and A5083 Aluminum Alloy," *Proceedings of the 5th International Conference on Advances in Fracture*, Cannes, France, pp. 1789-1798, (1981).
83. R. P. Wei, N. E. Fenelli, K. D. Unangst, and T. T. Shih, "Fatigue Crack Growth Response Following a High Load Excursion in 2219-T851 Aluminum Alloy," *J. Engineering Materials and Technology*, Transaction ASME, 102, pp. 280-292, (1980).
84. H. Nowack, K. H. Trautmann, K. H. Schultz, and G. Lutjering, "Sequence Effects on Fatigue Crack Propagation: Mechanical and Microstructural Contributions," *ASTM STP 677*, pp. 36-53, (1979).
85. V. W. Trebules, Jr., R. Roberts, and R. W. Hertzberg, "Effect of Multiple Overloads on Fatigue Crack Propagation in 2024-T3 Aluminum Alloy," *Progress in Flaw Growth and Fracture Toughness Testing*, ASTM STP 536, pp. 115-146, (1973).
86. D. M. Corbly and P. F. Packman, "On the Influence of Single and Multiple Peak Overloads on Fatigue Crack Propagation in 7075-T6511 Aluminum," *Engineering Fracture Mechanics*, Vol. 5, pp. 479-497, (1973).
87. H. Kitagawa, R. Yuuki, and T. Ohira, "Crack Morphological Aspect in Fracture Mechanics," *Engineering Fracture Mechanics*, 7, pp. 515-529, (1975).
88. S. Suresh, "Crack Deflection: Implications for the Growth of Long and Short Fatigue Cracks," *Metallurgical Transactions*, 14A, pp. 2315-2385, (1983).
89. G. Marci and P. F. Packman, "The Effect of Plastic Wake Zone on the Conditions for Fatigue Crack Propagation," *International Journal of Fracture*, 16, pp. 282-295, (1980).

90. D. Gan and J. Weertman, "Fatigue Crack Closure After Overload," *Engineering Fracture Mechanics*, 18 (1), pp. 155-160, (1983).
91. J. Lankford and D. L. Davidson, "The Effect of Overloads Upon Fatigue Crack Tip Opening Displacement and Crack Tip Opening/Closing Loads in Aluminum Alloys," *Advances in Fracture Research, Fifth International Conference on Fracture*, Ed. D. Francois et al., pp. 899-906, (1980).
92. S. J. Hudak, D. L. Davidson, and K. S. Chan, "Measurement and Analysis of Crack Tip Processes Associated with Variable Amplitude Fatigue Crack Growth," *NASA Contractor Report 172228, NASA-Langley Research Center, Hampton, Virginia, September (1983)*.
93. F. J. Bernard, T. C. Lindley, and C. E. Richards, "The Effect of Single Overloads on Fatigue Crack Propagation in Steels," *Metals Science*, pp. 390-398, (1977).
94. E. F. J. von Euw, R. W. Hertzberg, and R. Roberts, "Delay Effects in Fatigue Crack Propagation, Stress Analysis, and Growth of Cracks," *ASTM STP 513*, pp. 230-259, (1972).
95. J. D. Willenborg, R. M. Engle, and H. A. Wood, "A Crack Growth Retardation Model Using an Effective Stress Concept," *AFFDL-TM-71-1-FBR, Air Force Flight Dynamics Laboratory*, (1970).
96. O. E. Wheeler, *Transactions, American Society of Mechanical Engineering, Journal of Basic Engineering*, 94, pp. 181-186, (1972).
97. B. J. Habibie, "On the Integration Method of Crack Propagation in Elasto-Plastic Material Under Operational Loads and Plane Stresses," *3rd International Conference on Fracture, München, April (1973)*.
98. T. D. Gray and J. P. Gallagher, "Mechanics of Crack Growth," *ASTM STP 590*, pp. 331-344, (1976).
99. R. E. Jones, "Fatigue Crack Growth Retardation After Single Cycle Peak Overload in Ti-6Al-4V Titanium Alloy," *Engineering Fracture Mechanics*, 5, pp. 585-604, (1973).
100. J. F. Knott and A. C. Pickard, "Effects of Overloads on Fatigue Crack Propagation: Aluminum Alloys," *Metal Science*, 11, pp. 399-404, (1977).
101. J. C. Newman, Jr., "A Nonlinear Fracture Mechanics Approach to the Growth of Short Cracks," *AGARD Specialists Meeting on Behaviour of Short Cracks, Toronto, Canada, 20-21 September (1982)*.
102. J. C. Newman, Jr., "A Crack Closure Model for Predicting Fatigue Crack Growth Under Aircraft Spectrum Loading," *ASTM STP 748*, pp. 53-84, (1981).

103. J. C. Newman, Jr., "A Non-Linear Fracture Mechanics Approach to the Growth of Short Cracks," AGARD Specialist Meeting on Behaviour of Short Cracks, Toronto, Canada, 20-21 September (1982).
104. B. N. Leis, J. Ahmad, A. T. Hopper, and M. F. Kanninen, "Growth of Short Cracks in IN718," Paper presented at the 16th National Symposium on Fracture Mechanics, Battelle Columbus Laboratories, Columbus, Ohio, 15-17 August (1983).
105. J. E. Allison, "Measurement of Crack-Tip Stress Distributions by X-Ray Diffraction," Fracture Mechanics, Ed. C. W. Smith, ASTM STP 677, pp. 550-562, (1979).
106. J. Tirosh and A. Ladelski, "Note on Residual Stresses Induced by Fatigue Cracking," Engineering Fracture Mechanics, 13, pp. 453-461, (1980).
107. I. C. Mayes and T. J. Baker, "An Understanding of Fatigue Thresholds Through the Influence of Non-Metallic Inclusions in Steel," Fatigue of Engineering Materials and Structures, Vol. 4 (1), pp. 79-96, (1981).
108. I. C. Mayes and T. J. Baker, "Load Transference Across Crack Faces During FCG at Positive Values of R in Low Growth Rate Regime," Metal Science, 15, pp. 320-322, (1981).
109. G. Glinka, "Effect of Residual Stresses on Fatigue Crack Growth in Steel Weldments Under Constant and Variable Amplitude Loads," Fracture Mechanics, Ed. C. W. Smith, ASTM STP 677, pp. 198-214, (1979).
110. R. J. Bucci, "Effect of Residual Stress on Fatigue Crack Growth Measurement," Fracture Mechanics, Ed. R. Roberts, ASTM STP 743, pp. 28-47, (1981).
111. M. C. Lafarie-Frenot, J. Petit, and C. Gasc, "A Contribution to the Study of Fatigue Crack Closure in Vacuum," Fatigue of Engineering Materials and Structures, Vol. 1, pp. 431-438, (1979).
112. D. L. Davidson and J. Lankford, "The Effect of Water Vapour on Fatigue Crack Tip Mechanics in 7075-T651 Aluminum Alloy," Fatigue of Engineering Materials and Structures, 6 (3), pp. 241-256, (1983).
113. G. R. Yoder, L. A. Cooley, and T. W. Crooker, "A Critical Analysis of Grain Size and Yield Strength Dependence of Near Threshold Fatigue Crack Growth in Steels," Fracture Mechanics, Ed. J. C. Lewis and G. Sines, Fourteenth Symposium, ASTM STP 791, Vol. I. pp. 348-365, (1981).
114. C. J. Beevers, "Some Aspects of the Influence of Microstructures and Environment on ΔK Thresholds," Fatigue Thresholds, Ed. Backlund, Blom, and Beevers, EMAS Publications, U.K., pp. 257-275, (1981).

115. Po-we Kao and J. G. Byrne, "Microstructural Influence on Fatigue Crack Propagation in Pearlitic Steels," Fatigue Thresholds, Ed. Backlund, Blom, and Beevers, EMAS Publications Ltd, U.K., pp. 313-327, (1981).
116. G. T. Gray, III, A. W. Thompson, J. C. Williams, and D. H. Stone, "Influence of Microstructure on Fatigue Crack Growth Behaviour in Fully Pearlitic Steels," Fatigue Thresholds, Ed. Backlund, Blom, and Beevers, EMAS Publications Ltd, U.K., pp. 345-361, (1981).
117. C. W. Brown and G. C. Smith, "The Effect of Microstructure and Texture on the Fatigue Crack Growth Thresholds," Fatigue Thresholds, Ed. Backlund, Blom, and Beevers, EMAS Publications Ltd, pp. 329-343, (1981).
118. G. R. Yoder, L. A. Cooley, and T. W. Crooker, "50-Fold Difference in Region II FCP Resistance of Titanium Alloys: Grain Size Effect," Journal of Engineering Materials and Technology, Transaction ASME, Series H, 101, pp. 86-90, (1979).
119. J. P. Hess, A. F. Grandt, Jr., and A. Dumanis, "Effect of Side-Grooves on Fatigue Crack Retardation," Fatigue of Engineering Materials and Structures, 6 (2), pp. 189-199, (1983).
120. D. Rhodes and J. C. Radon, "Effect of Some Secondary Test Variables on Fatigue Crack Growth," Fracture Mechanics: Fourteenth Symposium - Vol. II, ASTM STP 791, pp. 33-46, (1982).
121. H. Terada, "Elastic and Elasto-Plastic Stress Analysis of the Standard Compact Tension Specimen," Submitted to ASME Journal of Pressure Vessel Technology, (1982).
122. S. Mall and J. C. Newman, Jr., "The Dugdale Model for the Compact Tension Specimen," Paper presented at the 16th National Symposium on Fracture Mechanics, sponsored by ASTM E-24 Committee, Columbus, Ohio, 15-17 August (1983).
123. S. K. Putatunda and S. Banerjee, "Effect of Size on Plasticity and Fracture Toughness," To be shortly published in Engineering Fracture Mechanics.
124. K. A. Gupte and S. Banerjee, "Fracture of Round Bars Loaded in Mode III and a Procedure for K_{IIIc} Determination," To be shortly published in Engineering Fracture Mechanics.
125. H. Fuhring and T. Seeger, "Dugdale Crack Closure Analysis of Fatigue Cracks Under Constant Amplitude Loading," Engineering Fracture Mechanics, 11, pp. 99-122, (1979).
126. H. Fuhring and T. Seeger, "Structural Memory of Cracked Components Under Irregular Loading, ASTM STP 677, pp. 144-167, (1979).

127. H. D. Dill and C. R. Saff, "Spectrum Crack Growth Prediction Method Based on Crack Surface Displacement and Contact Analyses," *Fatigue Crack Growths Under Spectrum Loads*, ASTM STP 595, pp. 306-319, (1976).
128. B. Budiansky and J. W. Hutchinson, "Analysis of Closure in Fatigue Crack Growth," *Journal of Applied Mechanics*, 45, pp. 267-276, (1978).
129. K. Ohji, K. Ogura, and Y. Ohkoku, "Cyclic Analysis of a Propagating Crack and its Correlation with Fatigue Crack Growth," *Engineering Fracture Mechanics*, 7, pp. 457-464, (1975).
130. K. Ogura and K. Ohji, "FEM Analysis of Crack Closure and Delay Effects in Fatigue Crack Growth Under Variable Amplitude Loading," *Engineering Fracture Mechanics*, 9, pp. 471-480, (1977).
131. M. Nakagaki and S. N. Atluri, "Elastic-Plastic Analysis of FC Closure in Modes I and II," *AIAA Journal*, 18, pp. 1110-1117, (1980).
132. J. C. Newman, Jr., "Finite Element Analysis of Fatigue Crack Propagation - Including the Effects of Crack Closure," Ph.D. Thesis, Virginia Polytechnic Institute and State University, (1974).
133. J. C. Newman, Jr. and H. Armen, Jr., "Elastic-Plastic Analysis of a Propagating Crack Under Cyclic Loading, *AIAA Journal*, 13 (8), pp. 1017-1023, (1975).
134. J. C. Newman, Jr., "A Finite Element Analysis of Fatigue Crack Closure," *Mechanics of Crack Growth*, ASTM STP 590, pp. 280-301, (1976).
135. J. C. Newman, Jr., "Finite Element Analysis of Crack Growth Under Monotonic and Cyclic Loading," *Cyclic Stress-Strain and Plastic Deformation Aspects of Fatigue Crack Growth*, ASTM STP 637, pp. 56-80, (1977).
136. J. C. Newman, Jr., "A Crack Closure Model for Predicting Fatigue Crack Growth Under Aircraft Spectrum Loading," *Methods and Models for Predicting Fatigue Crack Growth Under Random Loading*, Ed. J. B. Chang and C. M. Hudson, ASTM STP 748, pp. 53-84, (1981).
137. J. C. Newman, Jr., "Prediction of Fatigue Crack Growth Under Variable-Amplitude and Spectrum Loading Using a Closure Model," *Design of Fatigue and Fracture Resistant Structures*, Ed. P. R. Abelkis and C. M. Hudson, ASTM STP 761, pp. 255-277, (1982).
138. H. Fuhring, "Practical Application of a Model for Fatigue Damage with Irregular Cyclic Loading," *Advances in Fracture Research*, ICF-5, 4, pp. 1823-1832, (1981).
139. L. N. McCartney, "A Note on Closure During FCG," *International Journal of Fracture*, Vol. 15, pp. R21-R24, (1979).

140. T. C. Lindley and L. N. McCartney, "Mechanics and Mechanisms of FCG in Developments in Fracture Mechanics," Vol. 2, G. G. Chell ed., Applied Science Publications, London, pp. 247-322, (1981).
141. R. L. Hewitt, "Accuracy and Precision of Crack Length Measurements Using a Compliance Technique," Journal of Testing and Evaluation, JTEVA, 11 (2), pp. 150-155, (1983).
142. A. J. McEvily, "Current Aspects of Fatigue, Appendix: Overload Experiments," Fatigue 1977 Conference, University of Cambridge, 28-30 March (1977).
143. W. N. Sharpe, Jr., D. M. Corbly, and A. F. Grandt, Jr., "Effects of Rest Time on Fatigue Crack Retardation and Observations of Crack Closure," Fatigue Crack Growths Under Spectrum Loads, ASTM STP 595, pp. 61-77, (1976).
144. G. R. Chanani, Discussion, Fatigue Crack Growth Under Spectrum Loads, ASTM STP 595, p. 75, (1976).
145. P. T. Heald, G. M. Spink, and P. J. Worthington, Materials Science and Engineering, 10, pp. 129-138, (1972).
146. G. G. Chell, "Developments in Fracture Mechanics - I," G. G. Chell ed., Applied Science Publishers, London, pp. 67-105, (1979).
147. R. deWit, "A Review of Generalized Failure Criteria Based on the Plastic Strip Yield Model," Fracture Mechanics: Fourteenth Symposium - Volume I: Theory and Analysis, J. G. Lewis and G. Sines Eds., ASTM STP 791, pp. 1-24-I-50, (1983).